

CHAPTER ONE

General Introduction

1.1 Introduction

Three phase Induction Motor (IM) have extensive applications in electrical machines, about half of the electrical energy generated in a developed country is ultimately consumed by electric motors, of which over 90 % are induction motors. For a comparatively long period, Induction Motors (IMs) have mainly been deployed in constant-speed motor drives for general purpose applications [1]. In the large number of applications, like, conveyors, pumps, centrifugal machines, machine tools, presses, elevators, and packaging equipment etc. AC motors are more popular with their integration. The major benefits of utilizing AC motor in a system are improved reliability, higher efficiency, better performance, easy scalability and feasibility of speed and torque control by different techniques [2].

By utilizing frequency converters are the most speed control methods of economical IM are realized [3]. In a large number of power applications, the Inverters are used. The function of an inverter is to convert DC power to AC, these are offered to as Voltage Source Inverters (VSI). A voltage source inverter (VSI) is one that takes in a fixed voltage from a device, such as a DC power supply, and converts it to a variable-frequency AC supply [4].

The introduction of high power VSI is relatively ease due to suitable properties of IGBT such that high power remediation capability. In spite of this usefulness of IGBT, the switching losses are the main issue and it causes the low current distortion and harmonic losses. To minimize the above problem is

using one of the interesting solutions high performance PWM. The inverter is operated with PWM strategy under the closed loop control to realize the desired output waveform with reduced harmonics. Harmonic contents are the main parameter responsible for the diluting the sinusoidal AC output so the control of the inverter switching is important to minimize the harmonic content of the output voltage [5].

Extensively in the past decades, Pulse width modulation has been studied. Many different PWM methods have been developed to achieve the following roles: linear modulation range is wide, switching loss is less, switching waveform is less Total Harmonic Distortion (THD) in the spectrum, less computation and time easy implementation [6].

With the evolution of microprocessors, Space Vector Pulse Width Modulation(SVPWM) has be one of the most important PWM methods for three phase converters. It utilizes the space vector concept to calculate the duty cycle of the switches, simply the digital implementation of PWM modulators and wide linear modulation range for output line-to-line voltages are the notable features of SVPWM was originally developed as vector approach to PWM for three phase inverters. It is a more sophisticated technique for generating sine wave that provides a higher voltage to the motor with lower total harmonic distortion. The main aim of any modulation technique is to obtain variable output having a maximum fundamental component with minimum harmonics. SVPWM method is an advanced: computation intensive PWM method and possibly the best techniques for variable frequency drive application [7].

For electrical drives good dynamic performance is mandatory so as to respond to the changes in command speed and torques. The performance of the vector control is affected by the modulation strategy used for the inverter and the vector control techniques present faster response of the drive and ensures improved performance by decoupled control of the machine flux and torque that is comparable with the characteristics of a separately excited dc motor [8].

The Field-Oriented Control (FOC) in particular, has become very popular since it delivers superior dynamic and static performance. Field oriented control (FOC) draws support from the initiative of decoupling torque and flux by means of nonlinear coordinate transformation and manipulating these variables by exploiting the direct and quadrature current vector components by means of unit vector ($\sin\theta_e$ and $\cos\theta_e$). Ultimately, the reference stator voltage vector is provided by current regulators. FOC consists of two techniques: (1) direct or feedback vector control and (2) indirect or feed-forward vector control [9].

The Indirect Field Oriented Vector Controlled (IFOC) induction motor drive is gaining much attention because of its less calculation complexity and reduced machine parameter dependence [8].

Over the years, the conventional control such as the proportional-integral (PI), and proportional-integral-derivative (PID) controllers have been utilized together with vector control methods to better control for the speed of induction motors. However, it must be pointed out that conventional controllers have major disadvantages such as performance sensitivity to variations in system's parameters, and the fact that when using fixed gains, the controller may not provide the required speed performance under variations in the parameters and operating conditions of the motor [7,10].

Fuzzy Logic Controller FLC is sometimes seen as the ultimate solution for high-performance drives of the next generation. Such a prediction of future trends is based on comparison of the drive response under PI and FLC speed control, which has been compared on a number of occasions [11]. Fuzzy control was found particularly useful to solve nonlinear control problems or when the plant model is unknown or difficult to build [12].

Fuzzy Logic Control (FLC) has being emerged as an attractive area for research in the control application of fuzzy set theory. The structure

of the FLC (the number of rules, the rules themselves, number and shape of membership functions etc.) is achieved through an essentially manual tuning process which, although time consuming is generally faster and less problematic than the corresponding procedures for conventional PI controllers. The design of conventional controllers relies on the availability of explicit mathematical models (differential and algebraic equations), together with their associated data (parameter values). Such models example in the form of input-output data or expert knowledge, to represent the system behavior [13].

1.2 General Review of Five Legs Inverter (FLI)

In recent year the advancement of variable speed Ac drives using a voltage source inverters(VSI) has been growing with both high performance and advanced technology. However, the most of inverters are used to control just only single inverter to single motor [14].

The five phase voltage source inverter (VSI) fed drives have many advantages over the three phase system. The increased number of phases directly results in an output voltage waveform with relatively less Total Harmonic Distortion [THD]. The five phase VSI fed induction motor has reduced amplitude of torque pulsations and increased frequency of torque pulsations compared to the three phase induction motor. For the constant power output of the machine, the stator current per phase is also reduced and higher average torque per rms current can be achieved for the same size of an equivalent three phase machine. Thus, it leads to the quiet operation of the five phase machine. Even in the absence of one or more phases, the five phase motor effectively drives the load with minimum speed fluctuation [15].

Reference [16] discussed about how to adapt two sets of the three-leg inverter for two induction motors to the Five-Leg Inverter FLI which it still independently controls two sets of a three phase induction motor. After the number of switches are reduced from 12switches to 10 switches. The system can be effort to reduce the switching losses and also to reduce production cost when reduced the number of

switches, driver circuits and capacitor by using the same DC bus [17,18]. In modern electric drives the modulation of switching is carried out to achieve the required AC wave shape. This is met by incorporating the duration of 'ON' & 'OFF' periods. The techniques to get the duration of ON interval for a particular switch depend upon the control logic or PWM technique to be adopted. In a PWM scheme the output voltage and frequency can be controlled with the help of the switching inside the inverter. The switch may be IGBT, MOSFET, etc. with diodes antiparallel are connected.

1.3 General Review of Modulation of Five Legs Inverter (FLI)

Different PWM schemes such as sinusoidal PWM compares a high frequency triangular carrier with five sinusoidal reference signals, known as the modulating signals, to generate the gating signals for the inverter switches but having a disadvantage that it contains third harmonic in output. To the cancellation of the third harmonic components and better utilization of the DC supply, the third harmonic injection PWM scheme is preferred in five phase applications. Space vector modulation technique has advantage of an optimal output and also reduces harmonic content of the output voltage/current. SVPWM has the advantages of lower harmonics and a higher modulation index in addition to the features of complete digital implementation by a single chip microprocessor, because of its flexibility of manipulation, so SVPWM has increasing application in power converters and motor control [19,20]. The SVPWM is more preferable over the traditional sine pulse width modulation (SPWM) in a five phase VSI [15]. Currently, the multi-machine drive systems are available in two different configurations. The first one comprises N three-phase VSIs feeding N three-phase motors individually while the second one is a system with N parallel-connected three-phase motors fed from a single three-phase VSI [21].

Five-Leg Inverter is utilized to supply two three-phase induction machines. The same leg of the five-leg inverter is shared by one phase of

each motor while the remaining inverter legs are connected to the phases of one motor only. In this thesis, a PWM technique for a Five-Leg VSI supplying a two-motor drive is developed, which utilizes standard three-phase modulators to generate modulation signals for all legs of a Five-Leg VSI. The solution enables any portion of the DC bus voltage to be allocated to any of the two machines. In contrast to the existing PWM techniques. It produces a symmetrical switching pattern, with identical switching frequency in all five inverter legs, and all of the 32 available inverter switching states are utilized [18].

Many types of modulation techniques are used with FLI.

1.3.1 Dual Voltage Modulation (DVM)

Simply utilizes two consecutive switching periods to generate the required voltages for the two machines in an alternating manner. During the first switching period the first machine receives required voltage, while the second machine is effectively short-circuited by means of the zero space vector application. During the second switching period the situation is reversed. Hence, a dual voltage modulation is implemented in each two consecutive switching periods. This technique has the major drawback that DC bus voltage availability is automatically restricted to half of the DC bus voltage for each machine, regardless of the operating conditions of the other machine [22].

1.3.2 Modulation Block Method (MBM)

The available DC bus voltage is subdivided between the two motors according to their voltage references via a so-called modulation block. The modulation block consists of 10 consecutive switching periods. The number of switching periods assigned to any of the two motors during a modulation block determines the percentage allocation of the available DC bus voltage to that motor. This PWM technique is difficult to implement, since it requires preliminary knowledge of the

voltage profile of each motor, and it results in increased current and torque ripples [23,24].

1.3.3 Inversion Table Method (IVM)

The two PWM techniques considered so far utilize only 14 of the 32 available switching states of the five-leg inverter. A different PWM method which automatically allocates the DC bus voltage according to the requirements of each machine (provided the total voltage requirement is within the capability of the DC bus), utilizes 31 inverter switching states (out of the available 32), since zero-vector that short-circuits the load to the negative rail of the DC bus is not used. Figure (1.1) illustrates this PWM scheme. Line voltage references are first calculated and scaled with the measured DC bus voltage. The scaled line voltage references are then compared with a triangular carrier, resulting in so-called modulation functions (m_i). The modulation functions are three-level signals (-1,0,1) and so there are a total of 81 possibilities ($m_{states}=3^4$). However, there are only 32 possible switching states for a five-leg inverter ($s_{states}=2^5$). Therefore, a so-called inversion table (look-up table), which locks the inverter into the previous switching state whenever an unrealizable modulation function is generated. Although aimed at fast practical implementation, this PWM method is not easy to implement in standard DSPs and requires a large look-up table [22].

1.3.4 Double Zero-Sequence Injection Method (DZM)

In contrast to such a situation in the existing PWM scheme, the available DC bus voltage is now automatically divided between the two motors according to their requirements (of course, the total voltage available to two machines is restricted by available DC bus voltage). Since the inverter has five legs, there are 32 possible states and all of these are utilized. The implementation is based on the use of standard three-phase space vector modulators and is therefore easily realized in a DSP. The detail this method will have discussed in chapter three [23].

1.4 General Review of control methods

In transportation systems and industrial applications is Implemented of coordination control of multiple induction motor is very important. There are two categories in coordination control of multiple induction motor.

- 1- Multiple induction motors derived single inverter.
- 2- Multiple induction motors driving multiple inverter.

The increasing in number of IGBTs makes the second control is complex. The single inverter driving multiple induction motor find more advantages because of light weight, low cost, less IGBTs and compact structure. The single inverter drive system may be further classified as follows

- 1- Multiple-leg inverter control.
- 2- Vector control.

Multiple leg inverter control found to have its own disadvantages because of increased in use of IGBTs, in vector control of multiple induction motor, some strategies were proposed to control multiple motor fed by the single inverter [25].

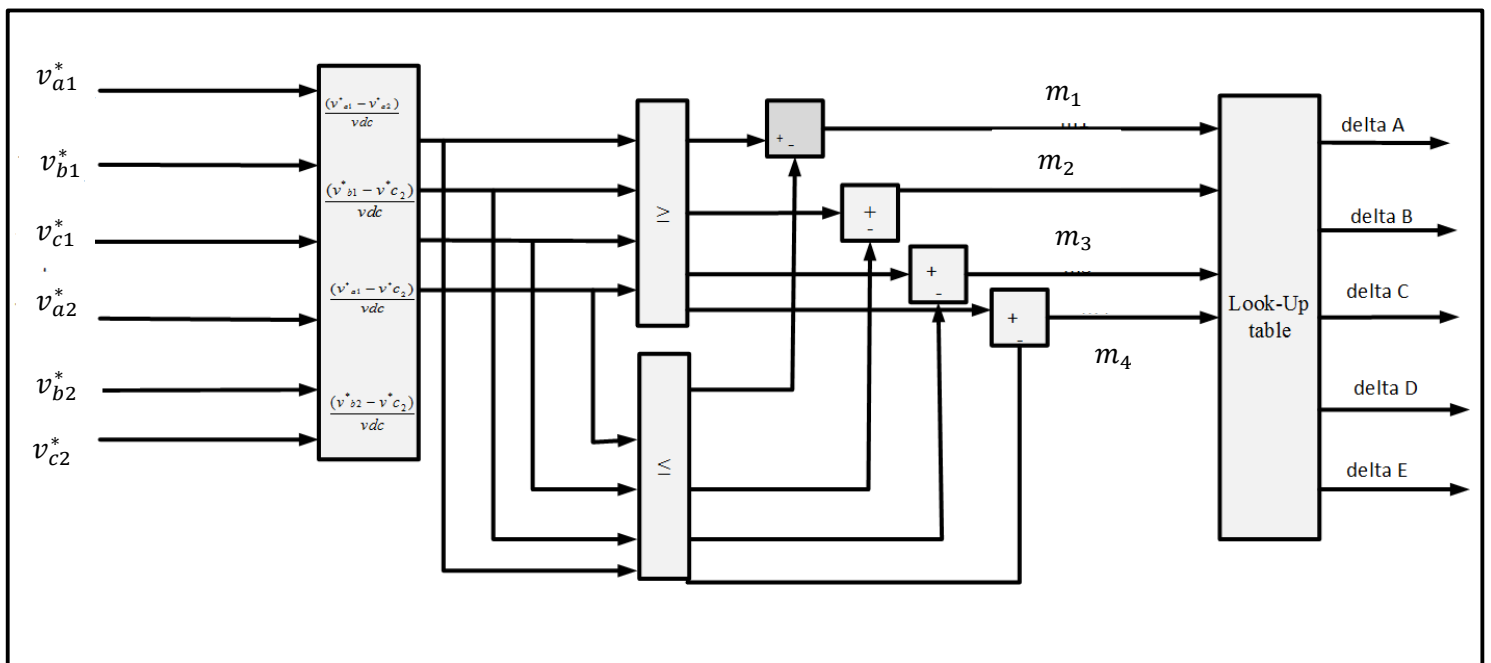


Figure (1-1) Block diagram of Inversion Table Method

1.4 Literature Review

This section discussed the historical survey of related works to this thesis in two tracks as follows

Track 1: Modulation and vector control based PI and Fuzzy Logic Controller

In 2010, Atif. I. et al. used many number of pulse width modulation for getting variable voltage and frequency from inverter, the most widely utilized PWM for a three-phase VSI are carrier-based sinusoidal PWM and SVPWM, SVPWM is better in DC bus utilization, discussed on step by step development of Matlab/Simulink model of SVPWM followed by them experimental implementation [26].

Ghadeer.A.A and Hisham.M.T ,in 2014, focused on step by step development SVPWM implemented on an Induction motor. The model of a three-phase a VSI is discussed depend on space vector theory. By using Matlab/Simulink the simulation results are obtained [28].

K. Sravanthi. et al. in 2015 proposes the implementation of a different SVPWM technique applied to the IFOC of IM drive involves decoupling of the stator current into torque and flux producing components of an IM then Indirect vector controlled induction motor drive using different SVPWM techniques are implemented in Matlab/Simulink program the corresponding harmonic spectrum is determined according to various SVPWM techniques [29].

Benudhar.S. et.al. In 2010 presented feedforward vector controlled induction motor drive, the simulation results obtained under varying operating conditions like step change in torque command step change in speed command. Then FLC is used for controlling the speed. The performance of FLC has been investigated and compared with the conventional PI controller based drive. The simulation results showed that fuzzy controller is superior to conventional PI controller under dynamic condition [30].

Biranchi.N,K.et.al. In 2011[31] and 2012[32] present a FLC of speed based on fuzzy logic approach for an indirect vector controlled induction motor drive for high performance. The analysis, design and simulation of the FLC for IFOC induction motor are carried out based on fuzzy set theory. The proposed fuzzy controller is compared with PI controller with no load and various load condition. The result proves the robustness and effectiveness of the proposed fuzzy controller for high performance of IM drive system.

Pradeep.B.J.et.al. In 2013 confers the effectiveness and efficacy of the vector controlled IM drive computed by the stability of performance in terms of the peak overshoot, settling time (time taken to arrive the required speed and torque), and the steady state error. Showing that IFOC technique performs peripherally better than the other two techniques when the steady state error is considered. The projected work concludes that, depend up on the overall evaluation of performance, the three vector control techniques prove identical control performance [9].

Priya C. and Virali P. Shah, in 2014 presented FLC for a PWM VSI fed induction motor based on IFOC after that replacement of PI controller by FLC based on fuzzy set theory. The performance of the intelligent controller FLC has been investigated through digital simulation utilizing Matlab-Simulink program for various operating conditions such as sudden change in reference speed and load torque. The simulation results prove that the performance of the FLC is better than that of the classical PI controller [33].

Tejas H .Pal.et.al. In 2015 discussed the speed control is observed in closed loop IFOC with different PWM technique such as Hysteresis band controller, Sine-PWM (SPWM), Space Vector Pulse Width Modulation (SVPWM). The speed regulation is achieved with a PI controller which converts the command speed into the command torque and therefore the speed of the drive. Results of

simulation are suitable with analyzed theory, and indicate that the model is practicable and accurate [34].

M.Ankarao and M.Vijaya. K, in 2015, discussed IFOC of IM with conventional PI controller is developed and replaced it with FLC to overcome the problem of overshoot occurred in PI controller, obtained quick steady state response and better speed control, ANN technique is proposed and implemented using Matlab/Simulink program. Where found the stator voltage, speed, and torque responses with conventional PI controller, FLC and proposed artificial neural network based controller are compared and found that the proposed ANN based controller showed increased dynamic performance [35].

Track 2: Modulation and characteristic of two motor drive fed by FLI

Ryuji.O. al.et,in 2006 presented an improved method of voltage utility factor from 50% to 86.6% for a FLI when two IMs are driven in vector control and in a condition. Also many modulation methods for the FLI have been proposed, but voltage utility factor is 50% in these methods. The voltage utility factor of the five-leg inverter is lower than one of the three leg inverter because of maximum voltage utility factor of the three leg inverter is 100%, [36].

M.Jones. al.et. In 2007 discussed analyses applicability of a five-leg VSI for the two-motor center-driven winder system. It is shown that in this type of application it is possible to use the five-leg VSI for the independent control of the two machines. Since the perceived without any significant penalties. Application requires appropriate allocation of the DC link voltage to the two machines, PWM method that ill sited [37].

Slobodan N. al .et., at 2008 [22] and Martin J.al. et., at 2008[24] comprised two three-phase IMs supplied by a five-leg voltage source inverter (VSI). With only five legs available to supply two three-phase motors one inverter leg is connected to both motors and the drive is controlled in such a way that both machines can operate independently. A drive system has recently been developed number of PWM methods. The comparesition, by simulation, four of the available

techniques and shows that the PWM method termed as ‘double zero-sequence injection’ is by far the best. It is the only method which enables an arbitrary distribution of the available DC link voltage between the two machines, while still being able to operate with equal and constant switching frequency in all five inverter legs. Experimental results, which illustrate operation with double zero sequence injection PWM and thus verify the theoretical findings, are demonstrated.

Yusuke O.al.et., in 2009 presented the experimental test results of the independent drive characteristics of two three-phase induction motors (IMs) fed by FLI, with the two-arm modulation technique [38].

Atsushi H.al.et., in 2011 presented the methodology and experimental results of the independent speed control of two three-phase induction motors (IMs) fed by a five-leg inverter FLI with SVPWM. It is found that the proposed method is useful on the term of decreasing gate signals regardless of the same performance characteristic as Two-arm modulation [39].

Tsutomu T .al.et., in 2012 presented the methodology and the experimental results of the independent vector control of two three IMs fed by a five-leg inverter (FLI) with SVPWM. The experimental results are proved that FLI with SVM can drive two IMs independently [40].

Masaya .al.et., in 2013 proposed a method for speed control of two IMs fed sampling time by single (FLI) SVPWM. A SVPWM strategy by separating the for control of two motors using FLI is presented. The experimental results and novelty of proposed controller are presented. The advantages of FLI are reduced number of devices, reduced size, increased efficiency due to total lower losses and volume. The SVPWM strategy that has been used for controlling the IM using three phase VSI cannot be used for controlling the FLI for independent control of two motors [41].

Md Hairul.N.T.al.et., in 2014 presents the implementation of two-arm modulation (TAM) technique for the independent control of a dual IM drive fed

by a FLI. A carrier-based SVPWM technique for TAM is proposed to generate switching signals for FLI. Two independent three-phase space vector modulators are utilized to control two IM motors. The motor drive system applies two outputs separate indirect field-oriented control methods. The stationary voltage from the vector control are synthesized in the three-phase space vector modulator to generate switching signals for FLI. The performance of the independent control of the motors and the voltage utilization factor are likewise analyzed. Simulation and experimental results verify the effectiveness of the proposed method for the independent control of the two IM motor drive system. The proposed technique is successfully validated by dSPACE DS1103 experimental work [42].

Hephzibah Jose Queen.J and Jenifer Rosney Queen.J at 2012 [25] and 2013 [43] introduced comparative study is made between the PI controller and fuzzy controller demonstrating the speed control of dual induction motor using fuzzy logic controller under unbalanced conditions. The control of two induction motor is made by weighed vector value and the process of finding the value of weighed vector is presented. The Matlab platform is using to represent simulation to study the effectiveness of the controls.

S.Lekhchine .al.et., in 2015 the doubly fed IMs, present of estimable advantages at variable speed drive. From that, the analyze of performances of speed FLC is presented because the performances of conventional speed controllers PI are sensitive to parameter variations of the motor. The simulation results showed that the FLC ensure the best dynamic response [44].

1.6 Aim of the Thesis

The aim of this work is to describe modelling and simulation of independent two induction motor fed by five leg inverter FLI. These are done by implementing Simulink models for

1. Three-phase induction motor
2. SVPWM three-phase inverter driving the induction motor.
3. IFOC drive using the above two models.
4. FLI modulation method DZS.
5. IFOC of dual induction motor fed by FLI.
6. FLC of induction motor for SVPWM three phase inverter based on IFOC.
7. FLC of dual induction motor fed by FLI based on IFOC.

1.7 Thesis Organization

The work presented in this thesis is organized in five main chapters including general introduction in chapter one. The chapters are structured as follows.

Chapter two: It introduces are two stages, one stage a mathematical model of the three-phase induction motor complete. The two stage present derived model of SVPWM inverter fed three phase induction motor, the two model is implemented and tested in Matlab/Simulink environment.

Chapter three: In this chapter introduce are third stage, one stage analysis model and modulation of five leg inverter (FLI), second stage present complete model of the indirect field oriented control with SVPWM VSI fed induction motor and using three conventional PI controller, third stage is introducing modelling and control of dual induction motor drive fed by FLI under different operation condition.

Chapter four: This chapter introduces are also two stages, one improved the performance of induction motor drive with IFOC by using fuzzy logic controller FLC and two stage the model of dual IFOC for two three phase induction motor fed by FLI. These is implemented and tested in Matlab/Simulink environment.

Chapter five: In this chapter all the results are summarized and appropriate conclusion has been drawn and future works was suggested.

CHAPTER TWO

ANAIYSIS AND SIMULATION OF THREE PHASE INDUCTION MOTOR (IM)

2.1 Introduction

The induction motor is the most widely used in the industry, has been favored owing to, its simple and rugged structure, good self-starting capability, low cost and reliability [45-46]. Dynamic modeling of induction motor drives is of great prominence to both industry applications and academia due to the prevalence of these motor drives in various industrial steads and pre-testing of motor drive system [47]. To achieved the efficiency, modeling of the motor is very important to represent the behavior of motor, verified and well-recognized engineering strategy to represent the behavior of the system [48].

The dynamic simulation is one of the main steps in the crediting of the designing process for the motor-drive system, by eliminating of the designing mistakes and the resulting errors in the construction prototype and testing [49].

The dynamic model of the induction motor in direct, quadrature, and zero-sequence axes can be derived from fundamental equations of transformation [49]. By using frequency converters, the most economical induction motor speed control methods are realized [3].

Three-phase voltage source inverters VSI are widely used in variable speed AC motor drives applications since they provide high variable frequency and variable voltage supply [26].

A number of pulse width modulation techniques have been presented to obtain variable voltage and frequency supply, more popular among these are carrier-based sinusoidal PWM and space vector pulse width modulation. The major disadvantage of SPWM is lower dc bus voltage utilization, and maximum output voltage from voltage source inverter VSI is limited to $0.5V_{dc}$ (peak) or $0.353 V_{rms}$. Space vector PWM improves dc bus utilization by 15.15%, therefore the digital implementation of SVPWM is easier. The SVPWM is specified as an alternative method to determine the switching pulse width and their position, and there is for a switching cycle a degree of freedom of space vector placement [6].

In SVPWM methods, the voltage reference is provided using a revolving reference vector. In this case magnitude and frequency of the fundamental component in the line side are controlled by the magnitude and frequency, of the reference voltage vector. Space vector modulation utilizes dc bus voltage more efficiently and generates less harmonic distortion in a three phase voltage source inverter [6].

The main role of this chapter is to simulate the mathematical model of three phase induction motor and the SVPWM technique for three phase VSI fed the IM in Matlab/Simulink and study the stator current, torque and speed of motor performance characteristics.

2.2 Simulink Model of Three Phase Induction Motor

The objective of the Matlab/Simulink simulation of a three phase IM is to inspect the dynamic response of the motor during starting and running, and then examine the ability of the motor to synchronize with various values of mechanical load.

The parameters of the motor are listed in appendix A. The base power (S_b) is the rated KVA of the machine. The base voltage (V_b) is the rated line voltage[45].

$$V_b = \sqrt{3}V_{LN} \quad \text{V} \quad \dots\dots (2.1)$$

The base current(I_b) is the rated value of the current

$$I_b = I_L \quad \text{A} \quad \dots\dots (2.2)$$

Base impedance and base electrical speed are given by

$$Z_b = \frac{V_b}{I_b} \quad \Omega \quad \dots\dots (2.3)$$

$$\omega_b = 2\pi f \quad \text{rad/sec} \quad \dots\dots (2.4)$$

2.2.1 Simulink model of Stator Voltage Transformation

The voltage of the stator winding must be transferred to the $qd0$ stationary reference frame. The transformation from abc stator voltages to $qd0$ stationary are performed in as following [45,50].

$$v_{qs}^s = \frac{2}{3}v_{as} - \frac{1}{3}v_{bs} - \frac{1}{3}v_{cs} = \frac{2}{3}v_{ag} - \frac{1}{3}v_{bg} - \frac{1}{3}v_{cg} - v_{sg} \quad \dots\dots (2.5)$$

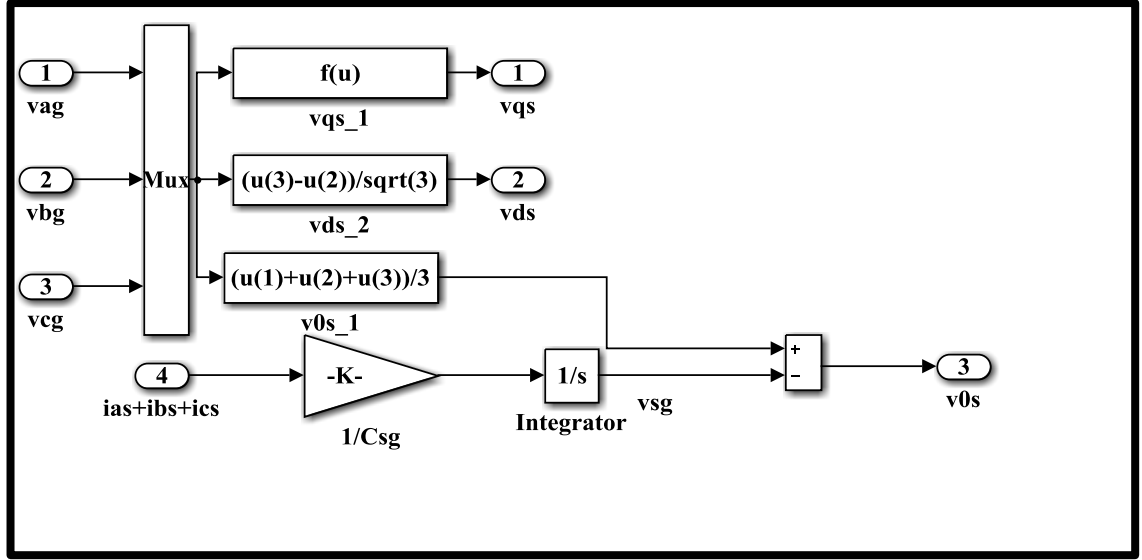
$$v_{ds}^s = \frac{1}{\sqrt{3}}(v_{sc} - v_{bs}) = \frac{1}{\sqrt{3}}(v_{cg} - v_{bg}) \quad \dots\dots (2.6)$$

$$v_{0s} = \frac{1}{3}(v_{as} + v_{bs} + v_{cs}) = \frac{1}{3}(v_{ag} + v_{bg} + v_{cg}) \quad \dots\dots (2.7)$$

Where

v_{ag}, v_{bg} and v_{cg} are the three applied voltage to the terminal of stator.

v_{as}, v_{bs} and v_{cs} are the three voltage of stator. The simulation of the transformation the stator voltage to dq0 stationary voltage is shown in Figure (2-1).



Figure(2-1) Simulink model of the transformation stator phase voltage to qd0 stationary voltage.

2.2.2 Simulink Model for i_q and i_d Determination

The stator qd0 voltage equations with other inputs can be used to solve the flux linkages as follows [45,50]:

$$\psi_{qs}^s = \omega_b \int \left\{ v_{qs}^s + \frac{r_s}{x_{ls}} (\psi_{mq}^s - \psi_{mq}^s) \right\} dt \quad \dots (2.8)$$

$$\psi_{ds}^s = \omega_b \int \left\{ v_{ds}^s + \frac{r_s}{x_{ls}} (\psi_{mq}^s - \psi_{md}^s) \right\} dt. \quad \dots (2.9)$$

$$\psi'_{qr}{}^s = \omega_b \int \left\{ v'_{qr}{}^s + \frac{\omega_r}{\omega_b} \psi'_{dr}{}^s + \frac{r'_r}{x'_{lr}} (\psi_{mq}^s - \psi'_{qr}{}^s) \right\} dt \quad \dots (2.10)$$

$$\psi'_{dr}{}^s = \omega_b \int \left\{ v'_{dr}{}^s + \frac{\omega_r}{\omega_b} \psi'_{qr}{}^s + \frac{r'_r}{x'_{lr}} (\psi_{md}^s - \psi'_{dr}{}^s) \right\} dt \quad \dots (2.11)$$

The mutual linkages flux in term of total linkages flux of the windings can be expressed as follows.

$$\psi_{mq}^s = X_M \left(\frac{\psi_{qs}^s}{x_{ls}} + \frac{\psi'_{qr}{}^s}{x'_{lr}} \right) \quad \dots (2.12)$$

$$\psi_{md}^s = X_M \left(\frac{\psi_{ds}^s}{x_{ls}} + \frac{\psi_{dr}^s}{x'_{lr}} \right) \quad \dots\dots (2.13)$$

where

$$\frac{1}{X_M} = \frac{1}{X_m} + \frac{1}{X_{ls}} + \frac{1}{x'_{lr}} \quad \dots\dots (2.14)$$

x_{ls} and x'_{lr} is the stator and rotor windings leakage reactance.

From the values of the linkages flux of the windings and the values of the mutual flux linkages, the qd current can be determined.

$$i_{qs}^s = \frac{\psi_{qs}^s - \psi_{qm}^s}{X_{ls}} \quad \dots\dots (2.15)$$

$$i'_{qr}{}^s = \frac{\psi'_{qr}{}^s - \psi_{qm}^s}{X'_{lr}} \quad \dots\dots (2.16)$$

Figure (2-2) shows the Simulink model of q-axis i_q induction motor model by using Eq. (2.15) and (2.16).

And also i_d can be determined

$$i_{ds}^s = \frac{\psi_{ds}^s - \psi_{dm}^s}{X_{ls}} \quad \dots\dots (2.17)$$

$$i'_{dr}{}^s = \frac{\psi'_{dr}{}^s - \psi_{dm}^s}{X'_{lr}} \quad \dots\dots (2.18)$$

The simulation of the d-axis i_d induction motor model by using Eq. (2.17) and (2.18) showing in Fig. (2-3).

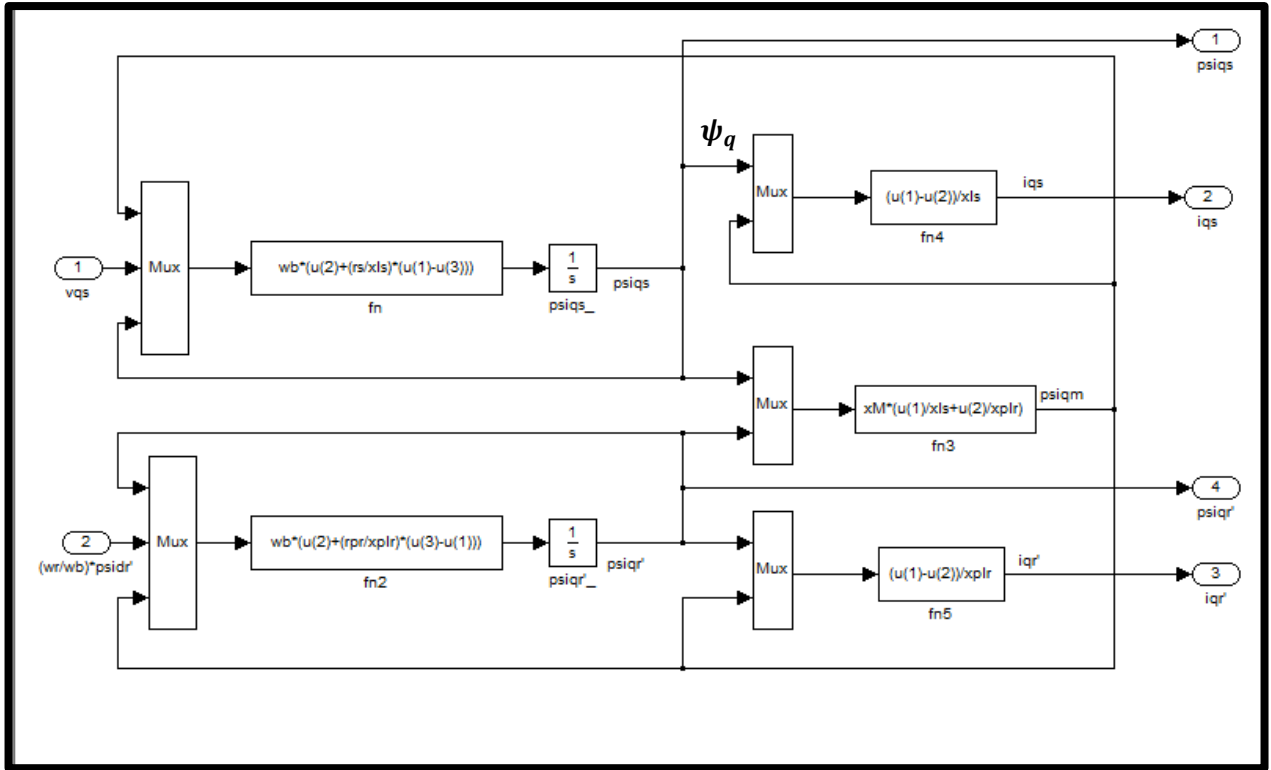


Figure (2-2) Simulink model of q-axis i_q induction motor model.

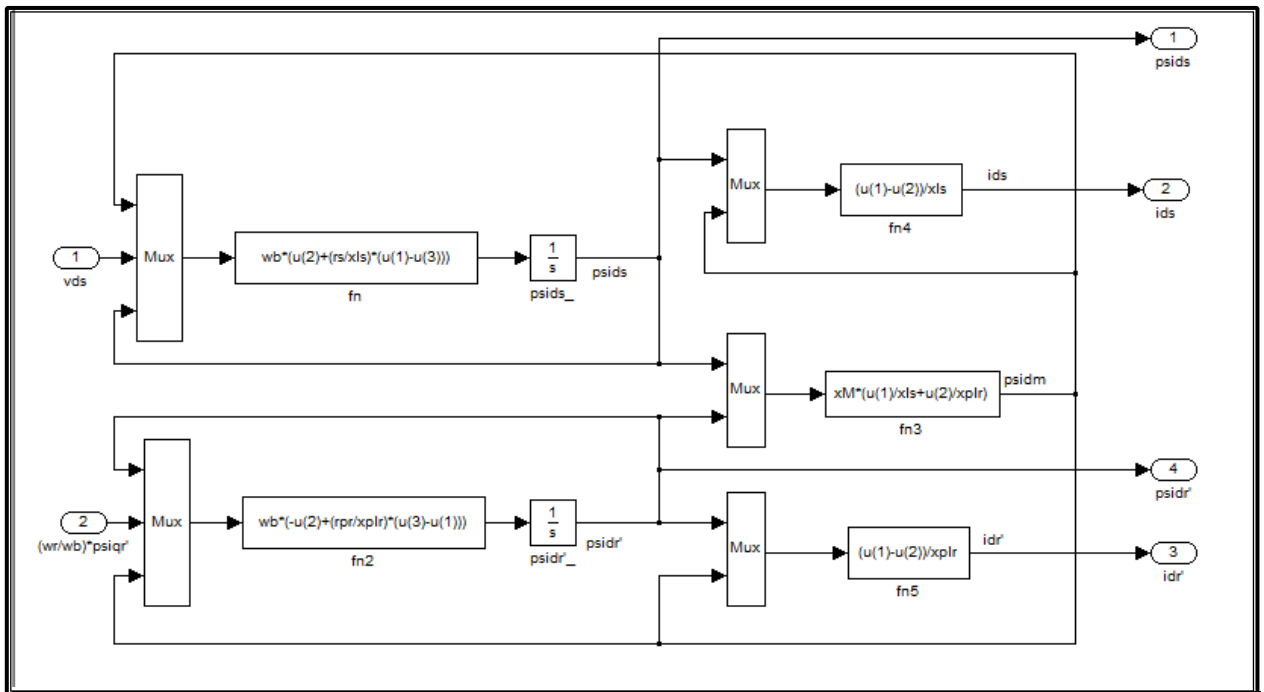


Figure (2-3) Simulink model of d-axis i_d induction motor model.

2.2.3 Simulink Model for Motor Torque and Rotor Motion Equations

The base mechanical angular frequency, ω_{bm} , is $2\omega_b/p$, where ω_b is the base electrical angular frequency and p is the number of pairs.

The electromagnetic torque is [50].

$$T_{em} = \frac{3}{2} \frac{P}{2\omega_b} (\psi_{ds}^s i_{qs}^s - \psi_{qs}^s i_{ds}^s) \quad \dots\dots (2.19)$$

Express equation for rotor motion in per unit as

$$T_{em} + T_{mech} - T_{damp} = J \frac{d\omega_{rm}}{dt} \quad \dots\dots (2.20)$$

$$\text{inertia constant is } H = \frac{1}{2} \frac{J\omega_{bm}^2}{S_b} \quad \dots\dots (2.21)$$

$$T_{em} + T_{mech} - T_{damp} = 2H \frac{d(\omega_r/\omega_b)}{dt} \quad \dots\dots (2.22)$$

Using Eq.'s (2.20), (2.21) and (2.22), the rotor motion simulation of the three phase induction motor can be implemented in Matlab as shown in Figure (2-4)

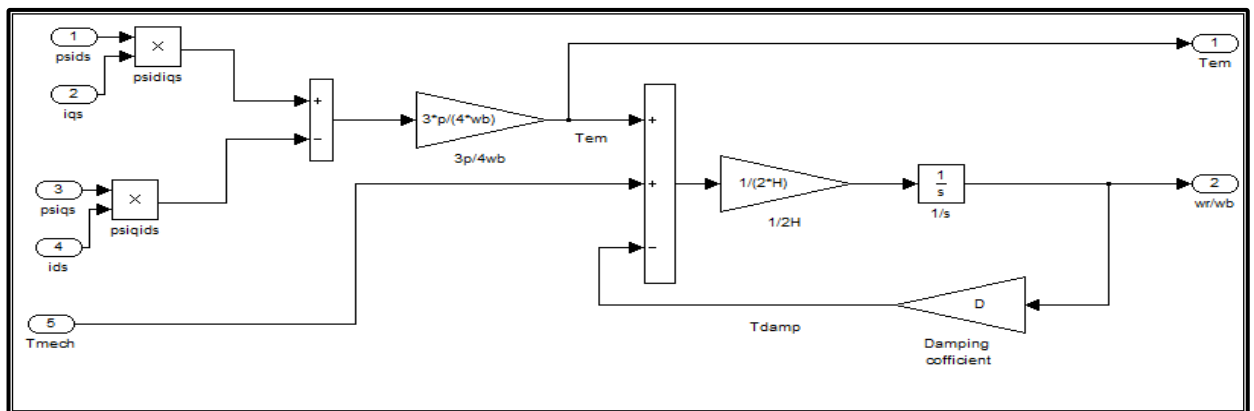


Figure (2-4) Simulink model for torque and rotor motion of IM.

2.2.4 Simulink Model of Stator Winding Currents

The stator winding currents in stationary $qd0$ reference frame are transformed to abc winding current, the currents in the stationary qd reference frame transferred to abc stator currents as following[50].

$$i_{as} = i_{qs}^s + i_{0s} \quad \dots (2.24)$$

$$i_{bs} = \frac{1}{2}i_{qs}^s - \frac{\sqrt{3}}{2}i_{ds}^s + i_{0s} \quad \dots (2.25)$$

$$i_{cs} = -\frac{1}{2}i_{qs}^s + \frac{\sqrt{3}}{2}i_{ds}^s + i_{0s} \quad \dots (2.26)$$

The Simulink model to determine the stator current of the IM is showing in Fig. (2-5).

The motor used in this thesis is 220 V, 374 KW, 60-Hz, three phase induction motor where the Simulink model for the IM is shown in Figure (2-6), and its parameters are given in Appendix A

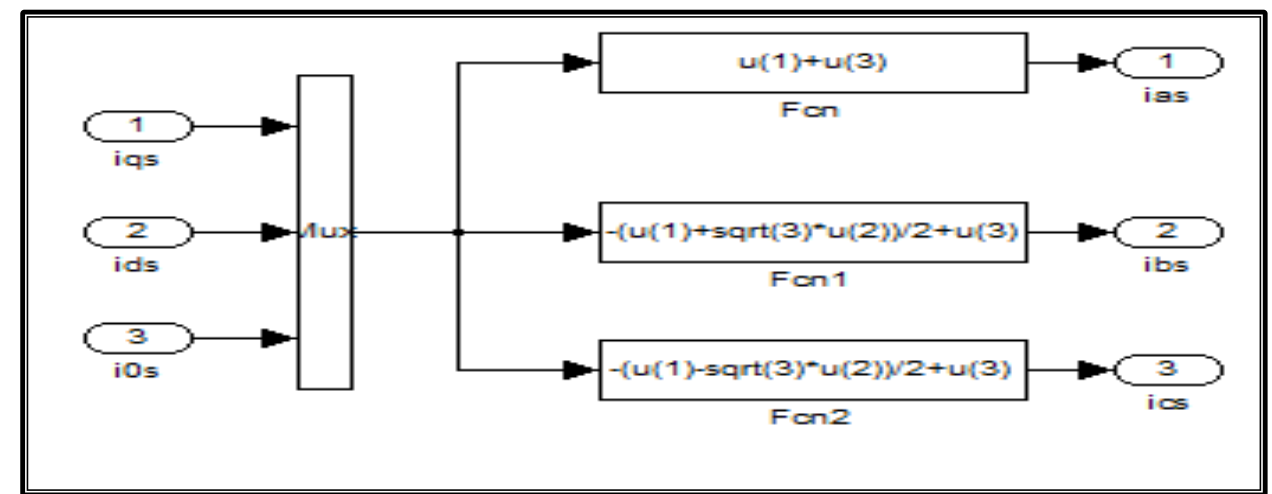


Figure (2-5) Simulink model for transformation from $qd0$ to abc. of IM.

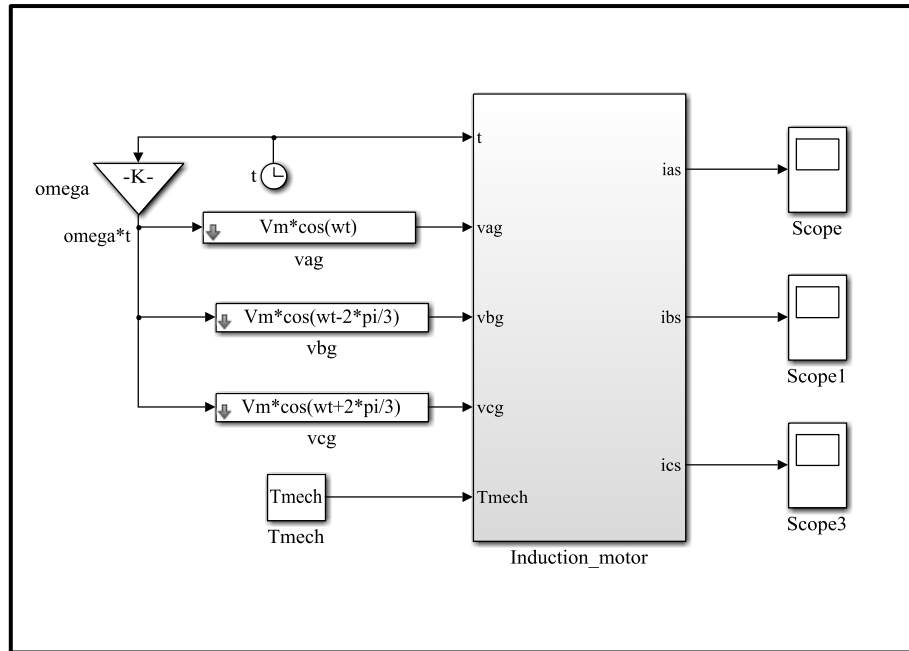
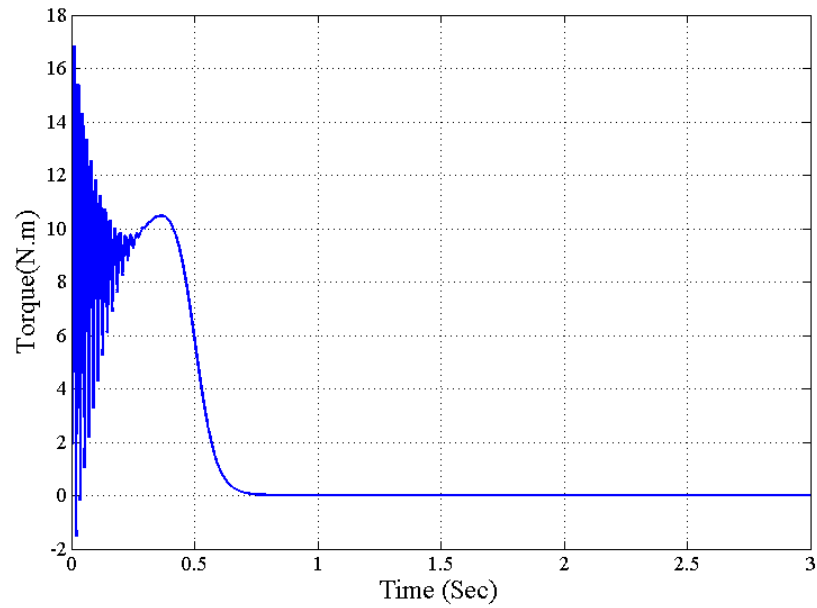


Figure (2-6) Simulink model of three phase IM.

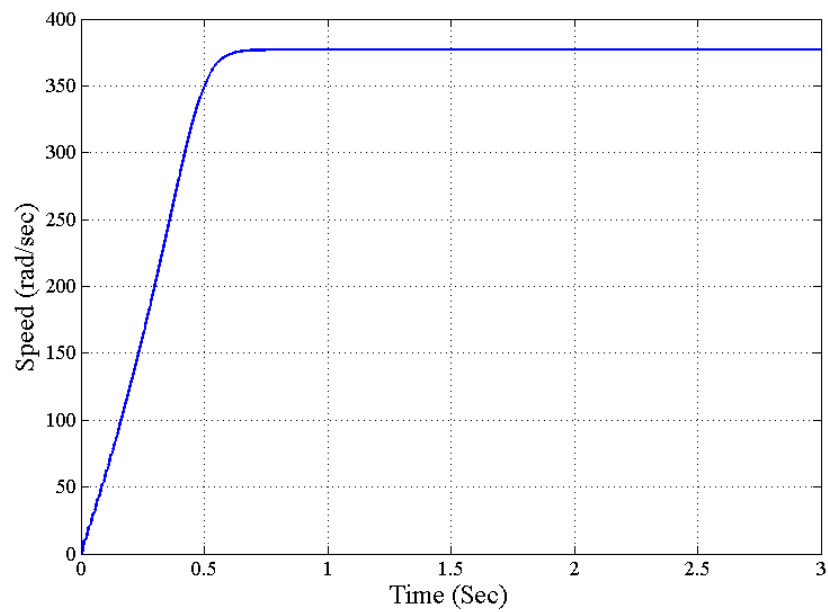
2.3 Simulation Results

To show the possibilities of the proposed model of the 3-phase induction motor (whose parameters are given in Appendix A), the model is simulated using MATLAB/Simulink software package. The no load characteristics are plotted in Figures (2-7-a-e), which show the electromagnetic torque, speed, stator phase current, stator q-axis current component, rotor d-axis current component and torque-speed characteristics speed.

In Figs (2-8-a-e) a load of 2 N.m is applied on the motor for about 1.5 second. The torque, speed, stator phase current, stator d-axis current component is plotted against time. It can be seen that when the load is applied the speed drops down and when it is removed the speed builds up again to its rated value.

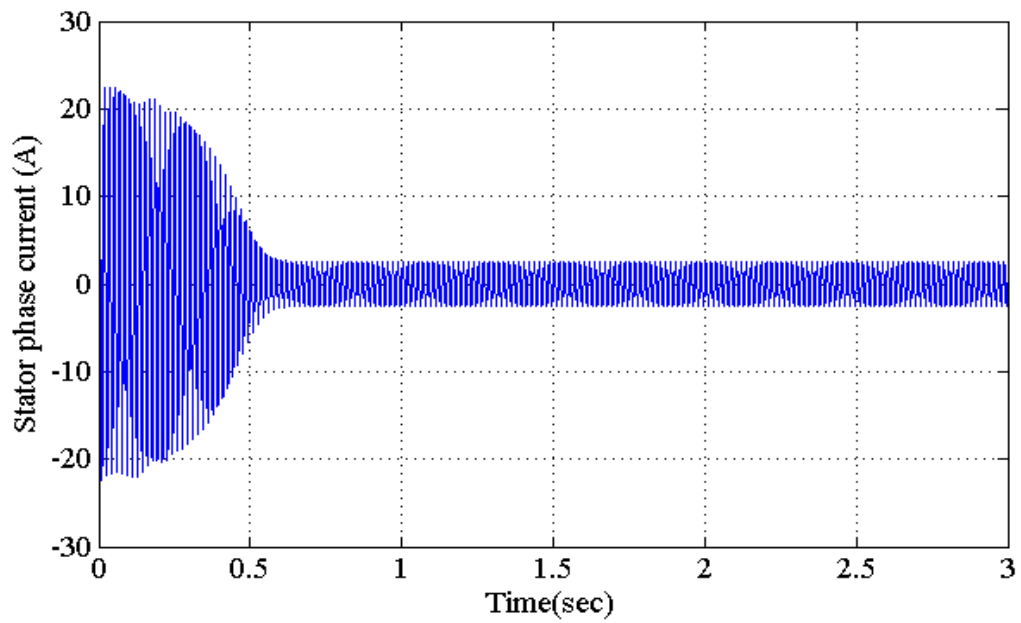


(a)

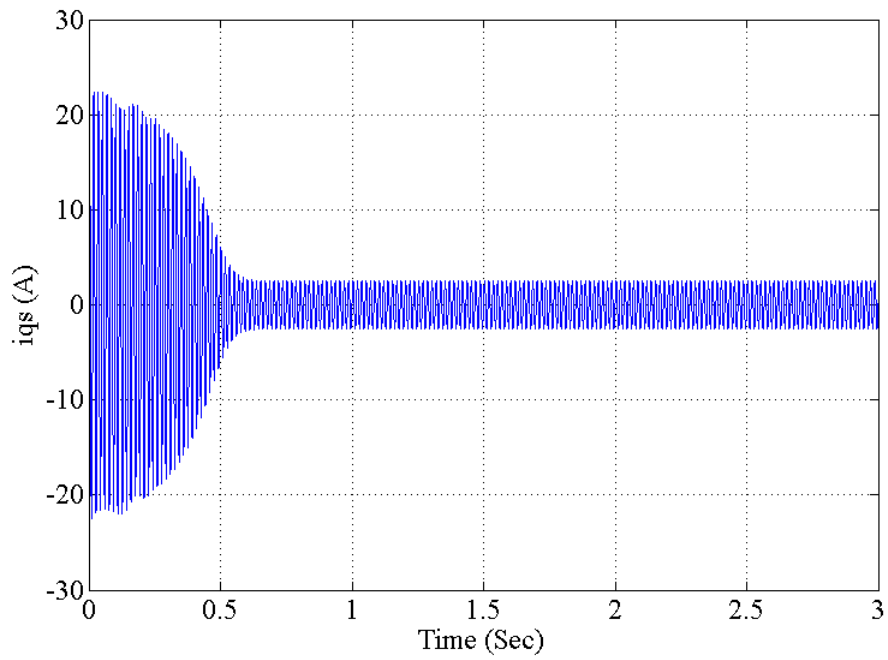


(b)

Figure (2-7) Dynamic response of IM, (a) Torque, (b) Speed, (c) Stator Phase Current, (d) Stator Quarducture Axis Current , (e) i_{ds} .

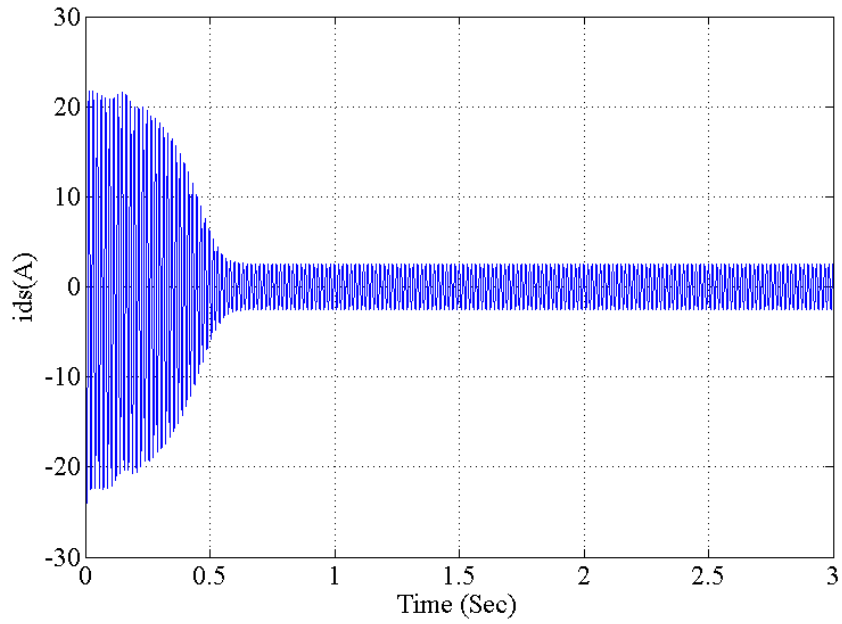


(c)



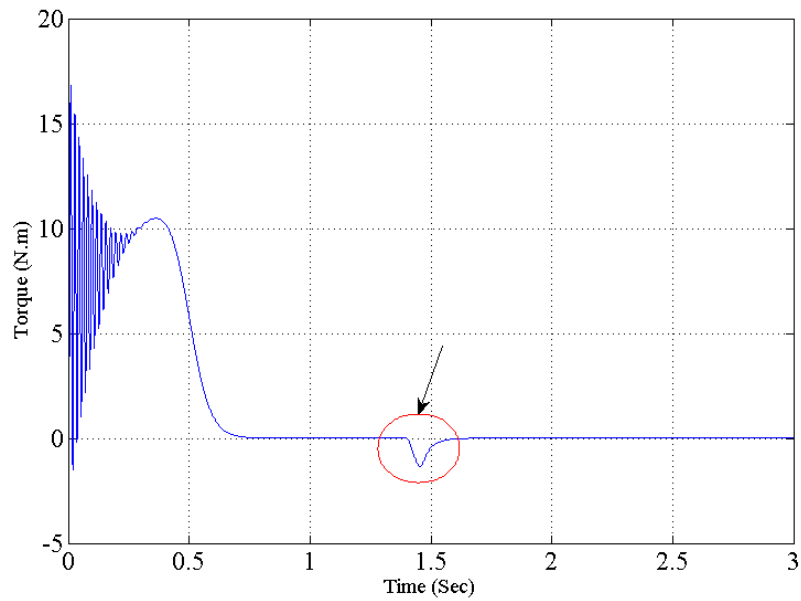
(d)

Figure (2-7) Continued.



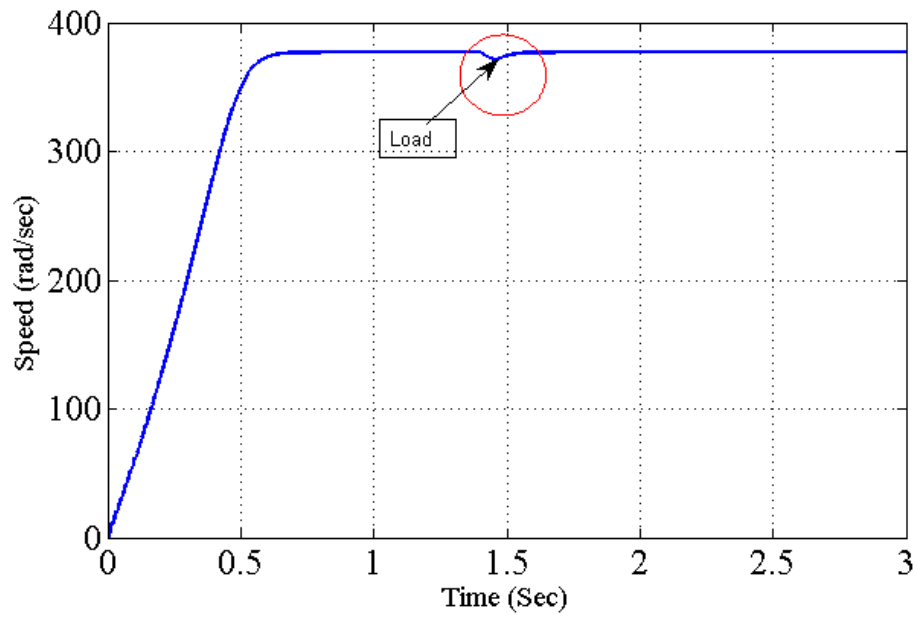
(e)

Figure (2-7) Continued.

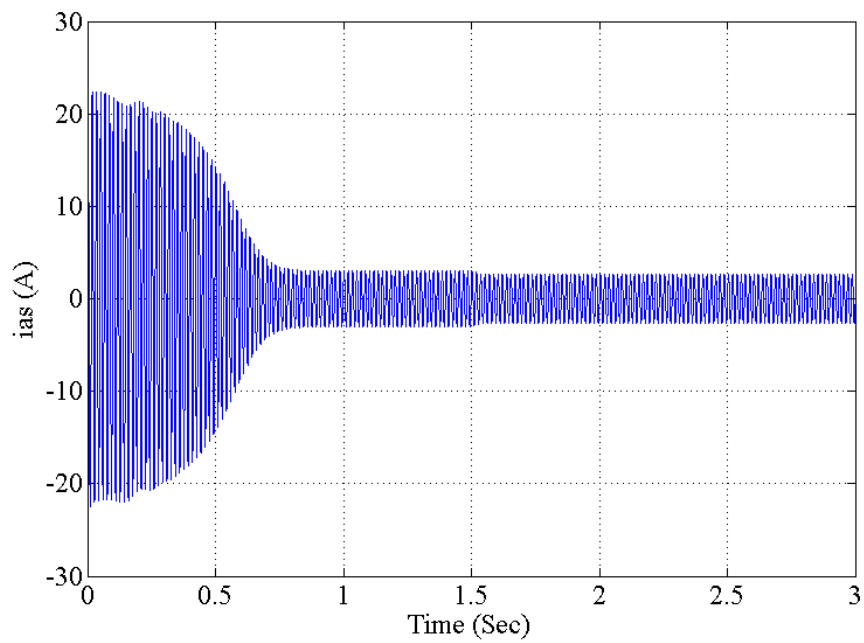


(a)

Figure (2-8) Dynamic response of IM with 2N.m load, (a) Torque, (b) Speed, (c) Stator Phase Current, (d) Stator Quadrature Axis Current, (e) i_{ds} .

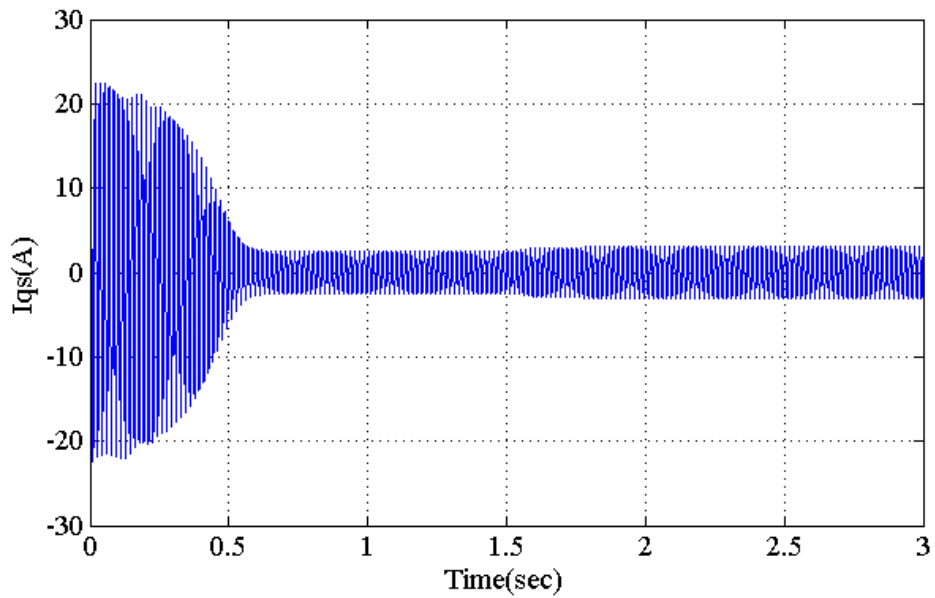


(b)

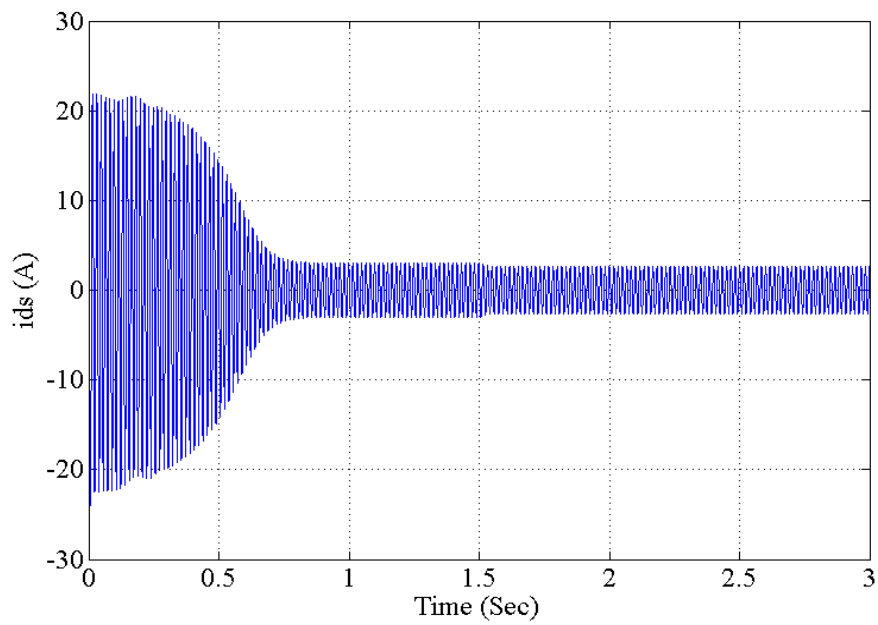


(c)

Figure (2-8) continued.



(d)



(e)

Figure (2-8) Continued.

2.4 Three phase Voltage Source Inverter (VSI)

The structure of a typical three – phase power inverter is shown in Fig. (2.9), where v_a , v_b , v_c are the voltages with frequency and the amplitude can be controlled which is applied to drive the three phase induction motor, and v_{dc} is DC bus of continuous inverter input voltage. The Pulse Width Modulation (PWM) is the standard control strategy used to operate the inverter switches for generating the output voltages with required high quality. The VSI that controlled using PWM techniques with a DC voltage source given to the inverter and the output AC voltage from inverter are controlled by adjusting the ON and OFF periods of the inverter power semiconductors, in which the output voltage is shaped by using six power switches those are classified (S_1 to S_6), and the signals which are generated by the SPWM technique or the SVPWM technique are fired to these switches. Because of the inverter can be operated at higher frequencies, the power semiconductors used in its are the MOSFET. Also power diode utilized with the MOSFET as a freewheeling diode [51].

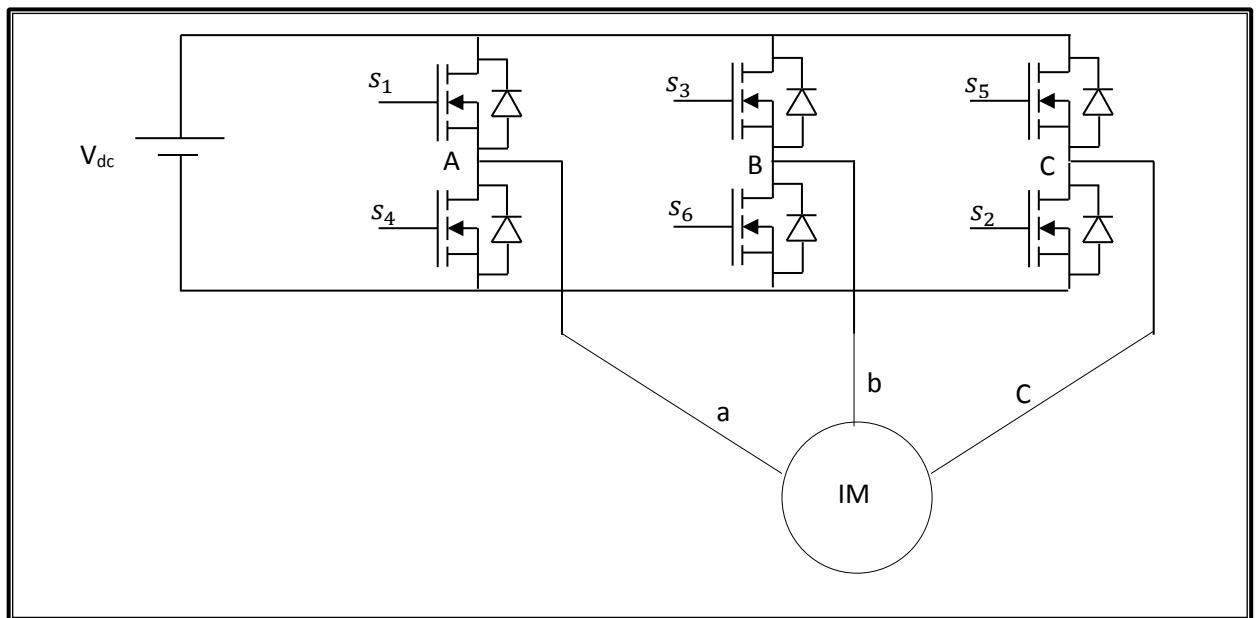


Figure (2-9) Three-phase voltage source.

2.5 Space Vector Pulse Width Modulation Technique

The SVPWM is a technique to obtain pulse width modulated signals that trigger the switches of a three phase voltage source inverter, where it gives pulse signals of variable width with constant switching frequency, and give better DC bus utilization than all other conventional modulation technique because It utilized to generate less harmonic distortion in the output voltages and/or currents applied to the phases of a power system (AC motor) and more efficient use of supply voltage [52].

2.5.1 SVPWM Technique of Three Phase VSI

The 3-phase VSI is controlled by utilizing the switching signals generated by the SVPWM technique. The states of the upper switches are used to determine the output voltage of the inverter, because at any time when the upper switch is switched ON, the lower switch of the same leg is switched OFF [53]. The voltage waveform of the inverter legs is shown in Figure (2-10). One leg of inverter is change its state and remains constant for 60° after one cycle (360°). Therefore for each one cycle (360°), there are six discrete values of leg voltages [19,20]. There are eight switching states of the inverter legs where needed for code the states of the upper arm switches to three bits in binary. Table (2-1) shows the switching states, line voltages, and phase voltages, where the switch is OFF denoting by bit (0) and bit (1) denotes the switch is ON [54].

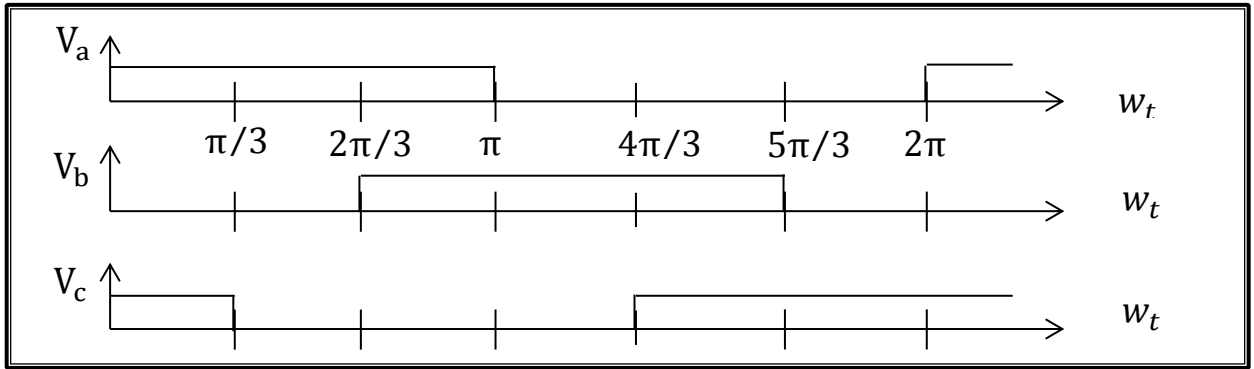


Figure (2-10) Legs voltages waveform of the three-phase .VSI.

Table (2-1) The switching table and output voltages of the VSI.

Voltage vectors	Switching vectors			Phase voltages (P.u)			Line Voltages (P.u)		
	A	B	C	V_{an}	V_{bn}	V_{cn}	V_{ab}	V_{bc}	V_{ca}
v_0	0	0	0	0	0	0	0	0	0
v_1	1	0	0	$2/3$	$-1/3$	$-1/3$	1	0	-1
v_2	1	1	0	$1/3$	$1/3$	$-2/3$	0	1	-1
v_3	0	1	0	$-1/3$	$2/3$	$-1/3$	-1	1	0
v_4	0	1	1	$-2/3$	$1/3$	$1/3$	-1	0	1
v_5	0	0	1	$-1/3$	$-1/3$	$2/3$	0	-1	1
v_6	1	0	1	$1/3$	$-2/3$	$1/3$	1	-1	0
v_7	1	1	1	0	0	0	0	0	0

2.5.2 The Principle of SVPWM Technique

Table (2-1) shows the space vectors which represent the eight switching state of VSI, six non-zero vectors (V_1 to V_6) is divided the complex plane into six sectors of a hexagonal and the center of a hexagonal is located by two zero vectors (null vector), the angle equals to 60° between any two adjacent non-zero vectors as shown in Figure (2-11). In the SVPWM technique, the reference voltage

vector (V_{ref}) is generated by switching between one zero vector and two nearest active space vectors, which is represent the 3-phase AC voltage. By controlling the magnitude and frequency of the V_{ref} the output voltage of VSI may be controlled.

The SVPWM based on the voltages in the stationary $\alpha\beta$ reference frame, are determined by transforming the three phase voltages in the abc reference frame to their equivalent $\alpha\beta$ reference frame in stationary reference frame using Clark's transformation. The maximum amplitude of the output voltage which can be obtained by the SVPWM technique represents the radius of the largest circle which is forms by inside the hexagon [6, 55-56].

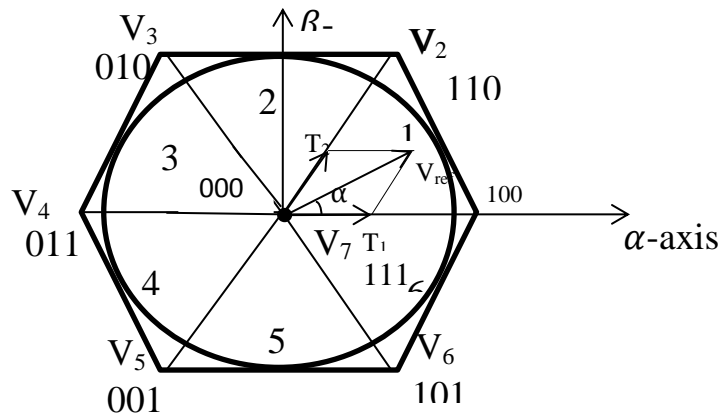


Figure (2-11) Switching vectors and voltage sectors.

2.5.3 Implementation of SVPWM

The concept of space vector is same to rotating magnetic field of the IM's [26]. Three-phase quantities can be converted into two-phase quantities (stationary or rotating reference frame). Then from two-phase quantities will get magnitude and angle of reference space vector, from the angle can find sector number in which reference vector is present. All that can generate modulating signals for VSI and by comparing these modulating signals with carrier wave signal we will get gating signals for VSI [57].

To implement the SVPWM, three steps have to be applied [58].

- 1- Calculate V_{ref} , V_α , V_β , and angle α .
- 2- Calculate the time durations T_0 , T_1 , and T_2 .
- 3- Calculate switching time for each switching device of the voltage source inverter.

Step-1 Determination V_α , and V_β by utilizing Clark's transformation as follows.

$$\begin{bmatrix} V_\alpha \\ V_\beta \end{bmatrix} = \frac{2}{3} \begin{bmatrix} 1 & -1/2 & -1/2 \\ 0 & \sqrt{3}/2 & -\sqrt{3}/2 \end{bmatrix} \begin{bmatrix} V_a \\ V_b \\ V_c \end{bmatrix} \quad \dots\dots (2.27)$$

And then determine $|\bar{V}_{ref}|$, and α from Figure (2-12) as follows

$$|\bar{V}_{ref}| = \sqrt{V_\alpha^2 + V_\beta^2} \quad \dots\dots (2.28)$$

$$\alpha = \tan^{-1} \left(\frac{V_\beta}{V_\alpha} \right) = 2\pi ft \quad \dots\dots (2.29)$$

where: (f) is the fundamental frequency.

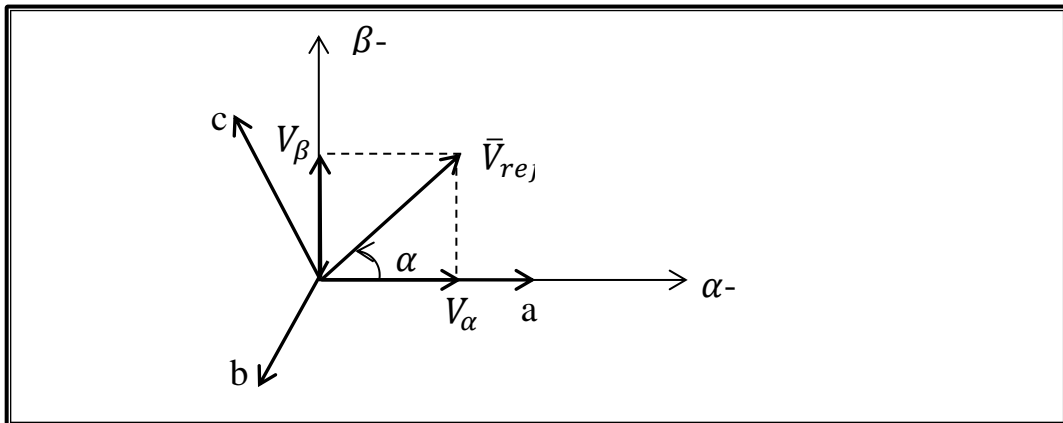


Figure (2-12) Reference voltage vector.

Step-2: From sector-1 of the hexagon shown in Figure (2-11), the time duration T_1 , T_2 , and T_0 can be calculated as following:

$$\int_0^{T_z} \bar{V}_{ref} dt = \int_0^{T_1} \bar{V}_1 dt + \int_{T_1}^{T_1+T_2} \bar{V}_2 dt + \int_{T_1+T_2}^{T_z} \bar{V}_0 dt \quad \dots (2.30)$$

$$T_z \bar{V}_{ref} = T_1 \bar{V}_1 + T_2 \bar{V}_2 \quad \dots (2.31)$$

$$T_z |\bar{V}_{ref}| \begin{bmatrix} \cos \alpha \\ \sin \alpha \end{bmatrix} = T_1 \frac{2}{3} V_{dc} \begin{bmatrix} 1 \\ 0 \end{bmatrix} + T_2 \frac{2}{3} V_{dc} \quad \dots (2.32)$$

$$T_1 = \frac{\sqrt{3} T_z |\bar{V}_{ref}|}{V_{dc}} \sin \left(\frac{\pi}{3} - \alpha \right) \quad \dots (2.33)$$

$$T_2 = \frac{\sqrt{3} T_z |\bar{V}_{ref}|}{V_{dc}} \sin(\alpha) \quad \dots (2.34)$$

$$T_0 = T_z - (T_1 + T_2) \quad \dots (2.35)$$

The switching time during any sectors is

$$T_1 = \frac{\sqrt{3} T_z |\bar{V}_{ref}|}{V_{dc}} \sin \left(\frac{k}{3} \pi - \alpha \right) \quad \dots (2.36)$$

$$T_2 = \frac{\sqrt{3} T_z |\bar{V}_{ref}|}{V_{dc}} \sin \left(\alpha - \frac{k-1}{3} \pi \right) \quad \dots (2.37)$$

$$T_0 = T_z - (T_1 + T_2) \quad \dots (2.38)$$

where:

k is the number of sectors (from 1 to 6), $0 \leq \alpha \leq 60^\circ$

T_z is the switching time ($T_z = 1/f_z$).

Step-3 In the third step the switching time of each switching device is determined. As shown in Figure (2-13) the total switching period T_z is divided in to seven parts, applying zero state vector in the first part for $1/4^{\text{th}}$ of the total zero state vector

time, in the second and third parts applying active state vectors for $1/2^{\text{th}}$ of the total time of their vectors, then applied zero state vector again for $1/4^{\text{th}}$ of the total zero state vector time. This sequence is repeated in the second half of the switching period [51].

2.5.4 Simulink Model of IM Derived by SVPWM Inverter

The Simulink model of voltage control of SVM inverter fed three phase induction motor drive is shown in Figure (2-14), where reference voltage generation block which is shown in Figure (2-15) used to generate the reference voltage from the rotating qd reference frame (v_q , and v_d) which is used to generate the gate signals for the voltage source inverter shown in Figure (2-14)

A flowchart of the Matlab function shown in Figure (2-16) is specified the number of sector and utilized to determine the switching time signals according step -3 for each switching device of the 3-phase space vector pulse width modulation. In the VSI is 163 V used as the the DC bus voltage as shown in Figure (2-17). In Fig. (2-18) F(u)1 and F(u)2 blocks are used to determine the sector number (k) through Eq. (2-28) and the angle .F(u)3 and F(u)4 blocks are used to determine time duration T_1 and T_2 according to Equation(2-36.2-37), $F_z=10$ kHz Switching frequency.

2.6 Simulation Results of IM Fed by SVPWM Inverter

To obtain the dynamic response of the Three-Phase IM with SVPWM inverter which shown in Fig (2-14), the characteristic of Electromagnetic Torque, Rotor speed, Stator Phase Current, Stator quadrature axis component, Line voltage at no load is shown in Fig. (2-19a.e) and the response at step load change is shown in Fig (2-20a-e).

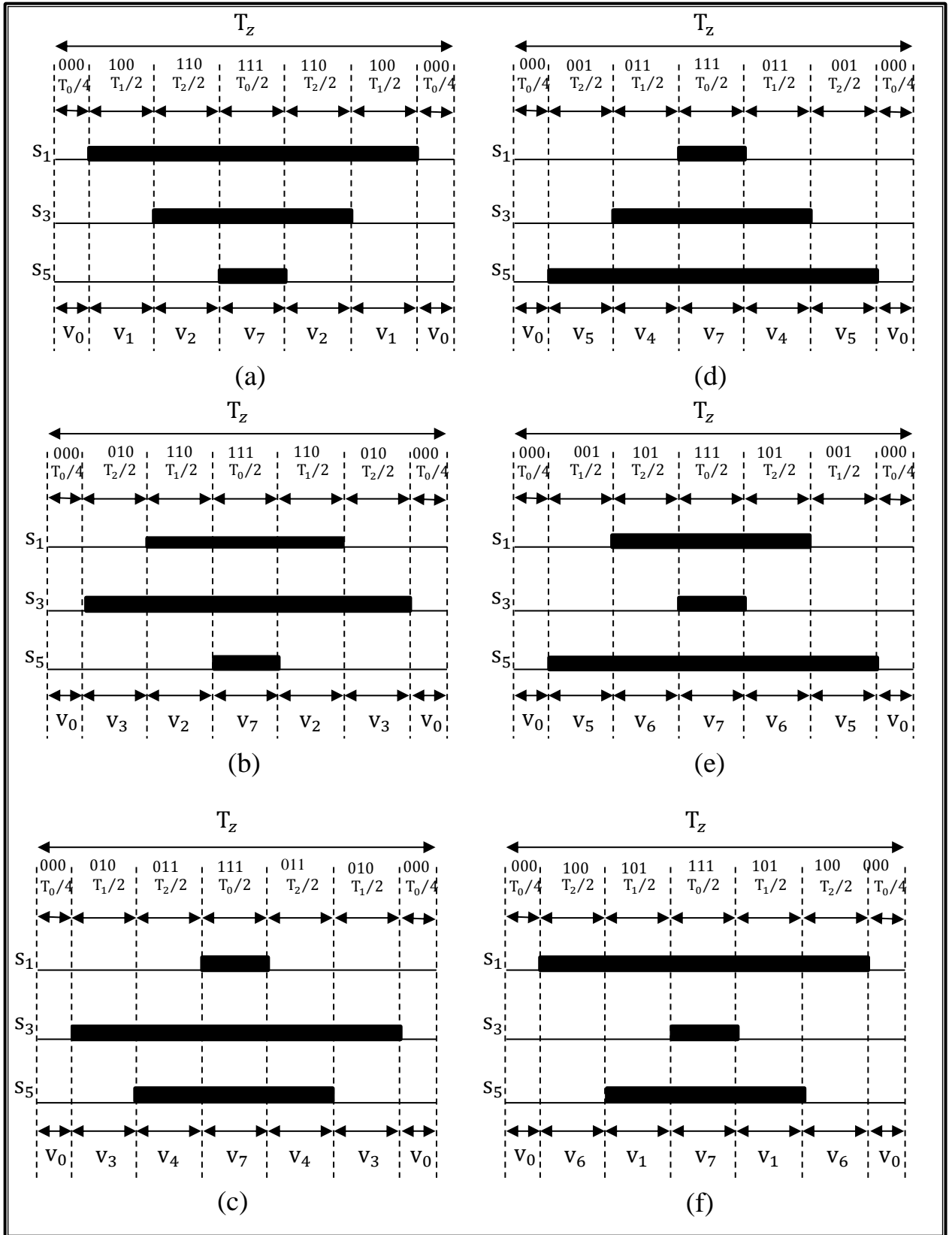


Figure (2-13) switching time duration for six sectors, (a) sector-1, (b) sector-2, (c) sector-3, (d) sector-4, (e) sector-5, (f) sector-6.

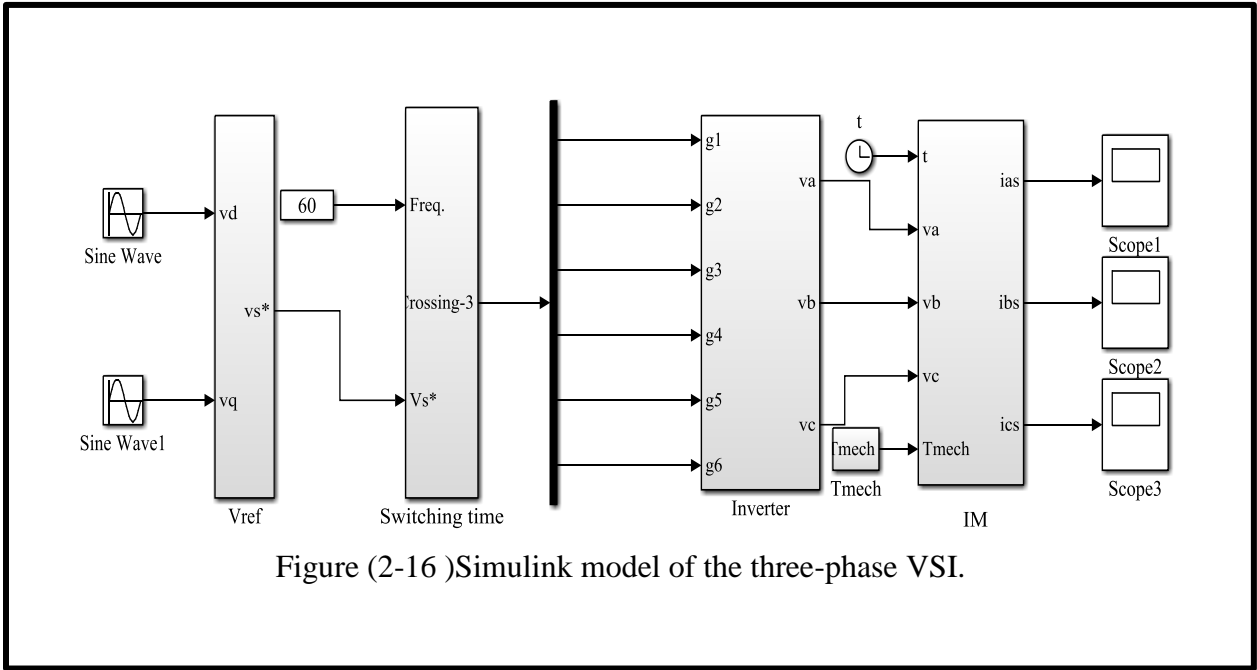


Figure (2-16) Simulink model of the three-phase VSI.

Figure (2-14) Simulink model of SVPWM with IM

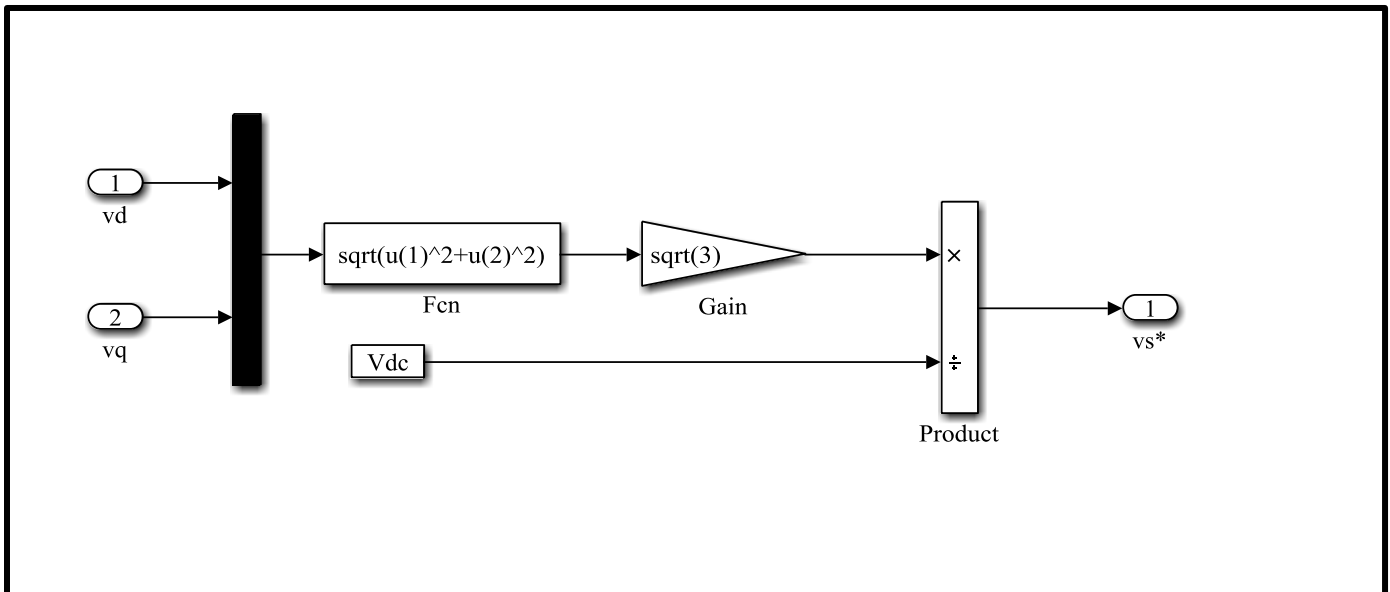


Figure (2-15) Simulink model of Voltage Reference.

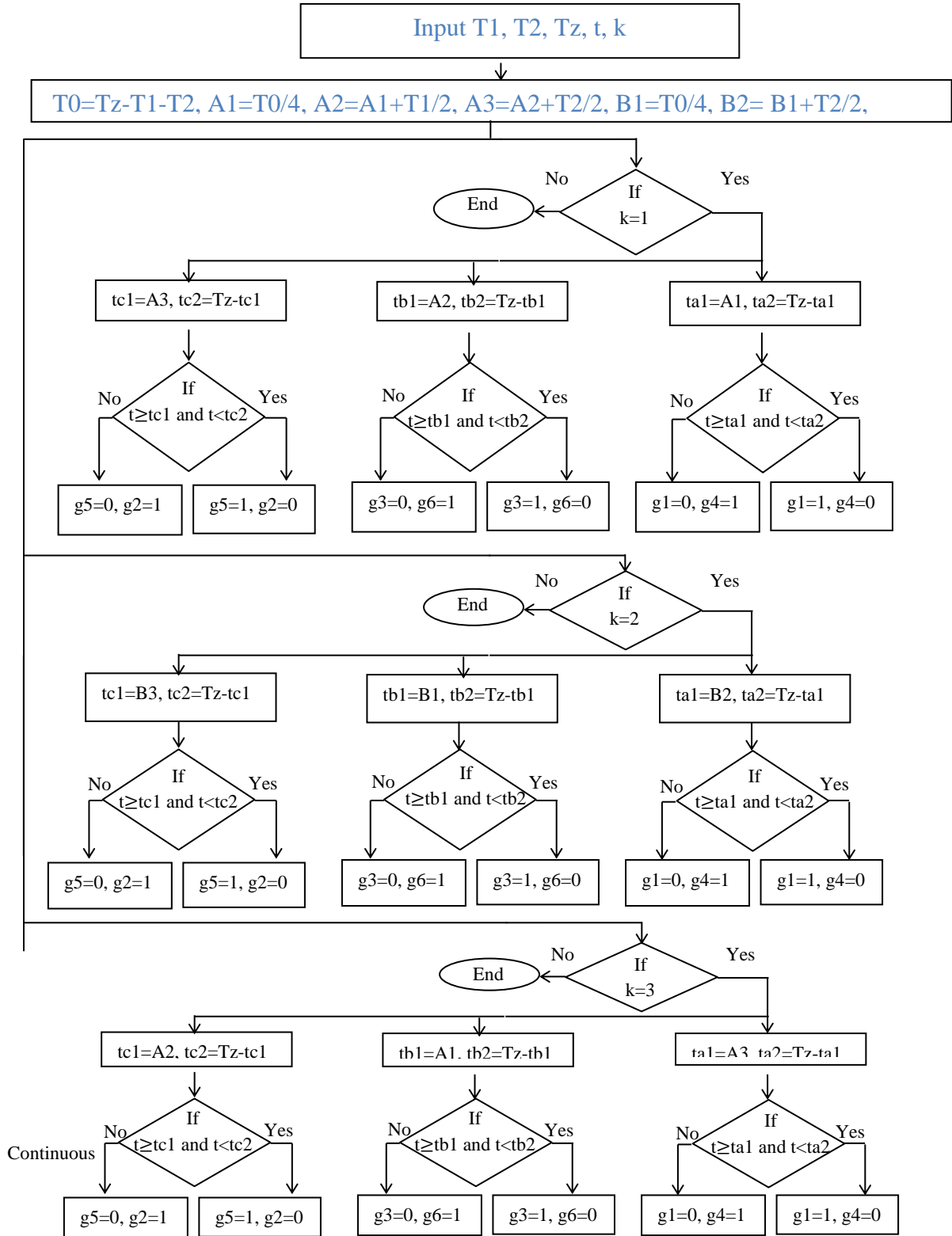


Figure (2-16) Flowchart of mat lab function to determined step-3 .

Continued

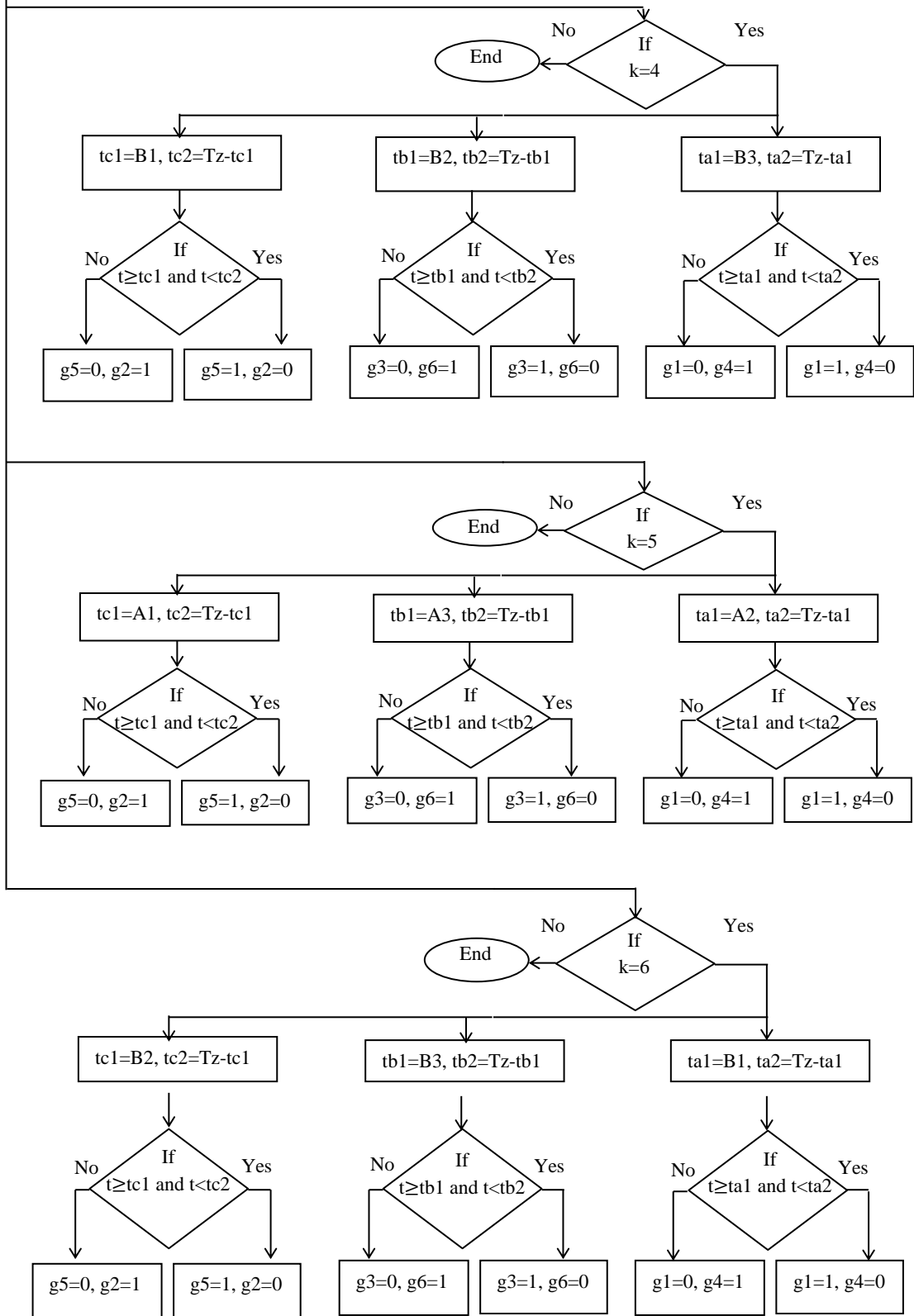


Figure (2-16) Continued.

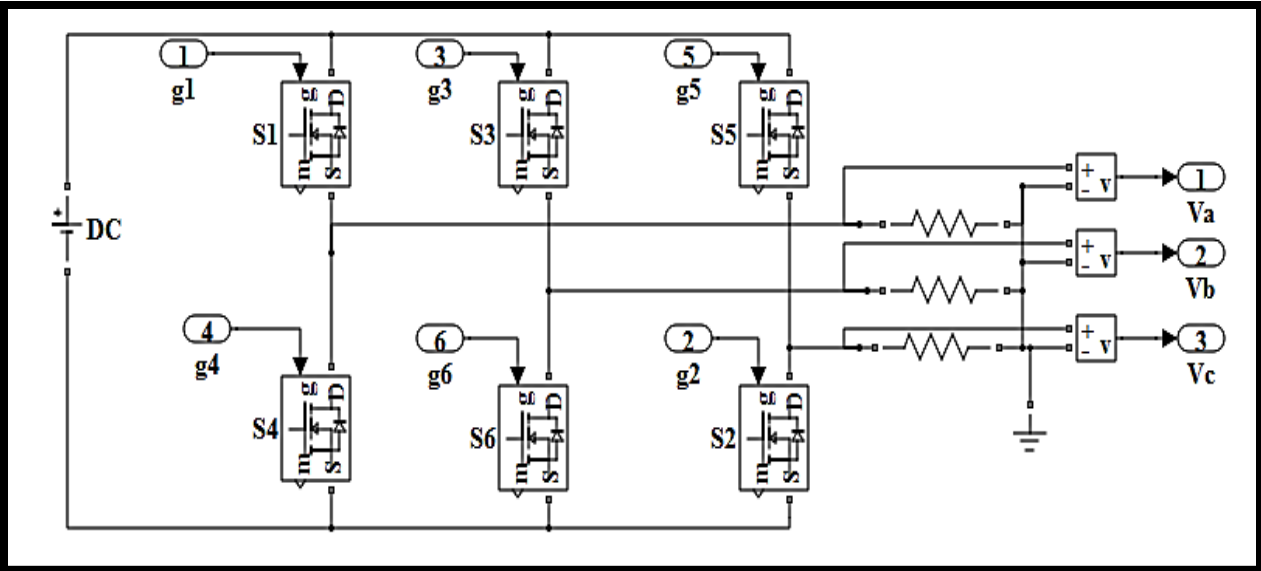


Figure (2-17) Simulink mode of Three-Phase VSI.

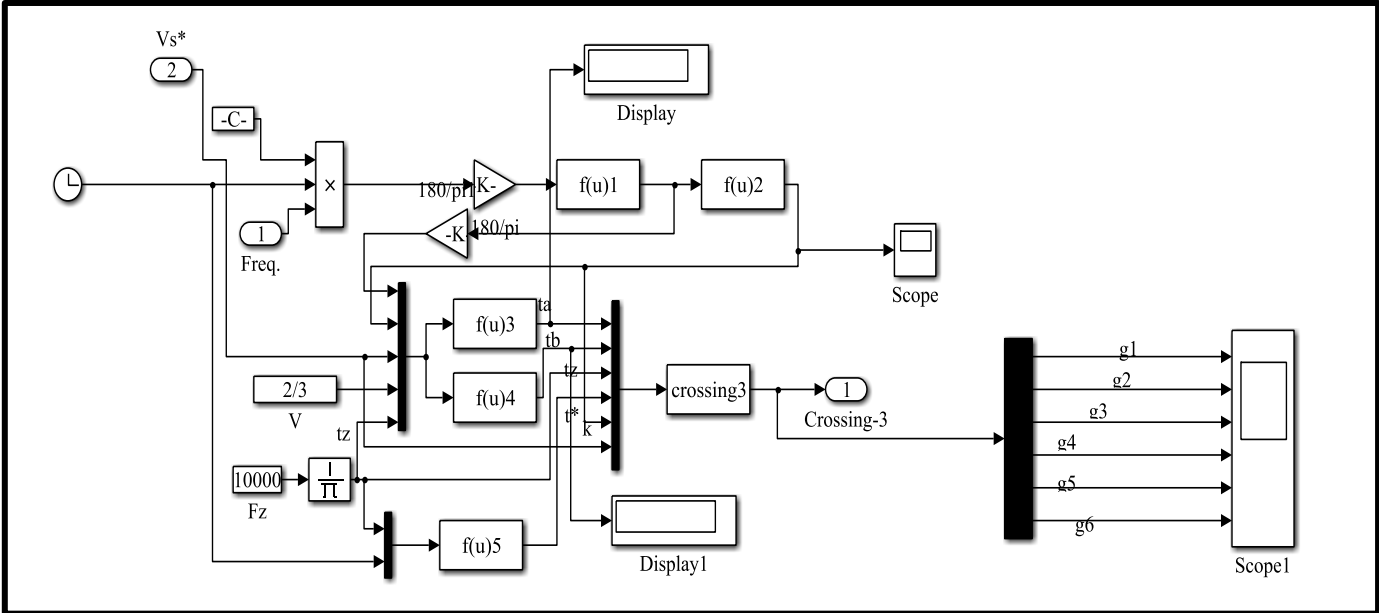
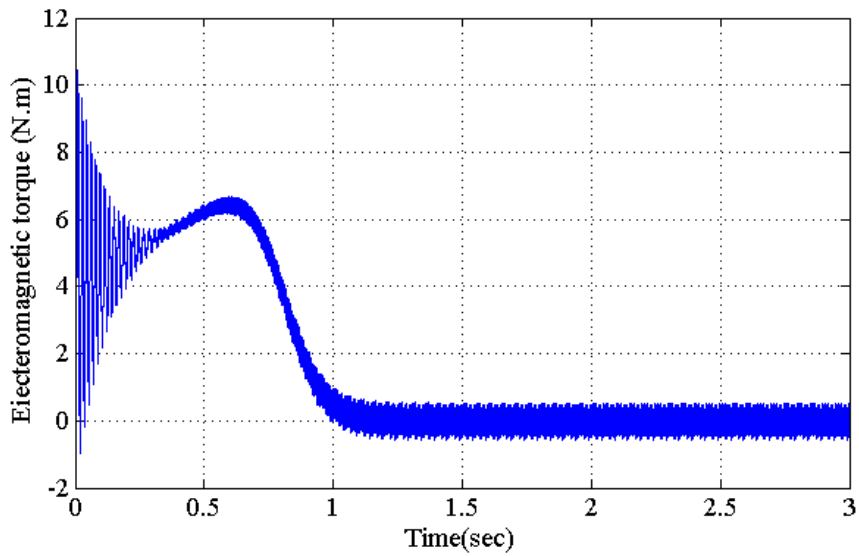
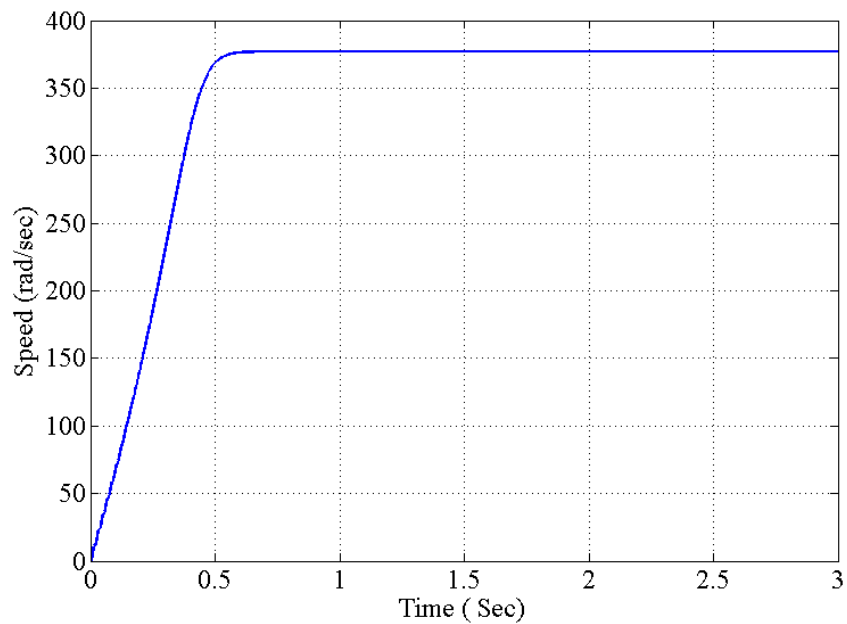


Figure (2-18) Simulink model of time duration block.

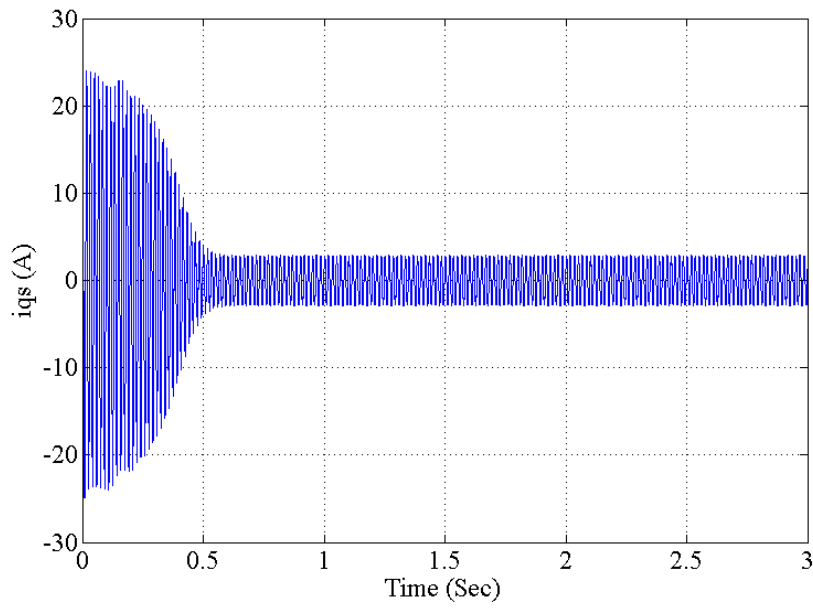


(a)

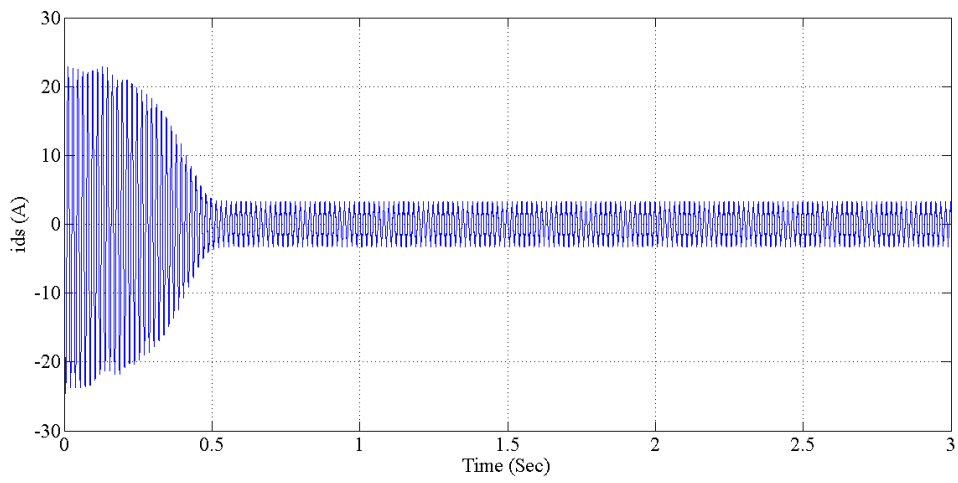


(b)

Figure (2-19) Dynamic response of IM fed by SVPWM Inverter, (a) Electromagnetic torque, (b) Speed, (c) stator quadrature axis current, (e) line voltage ab.

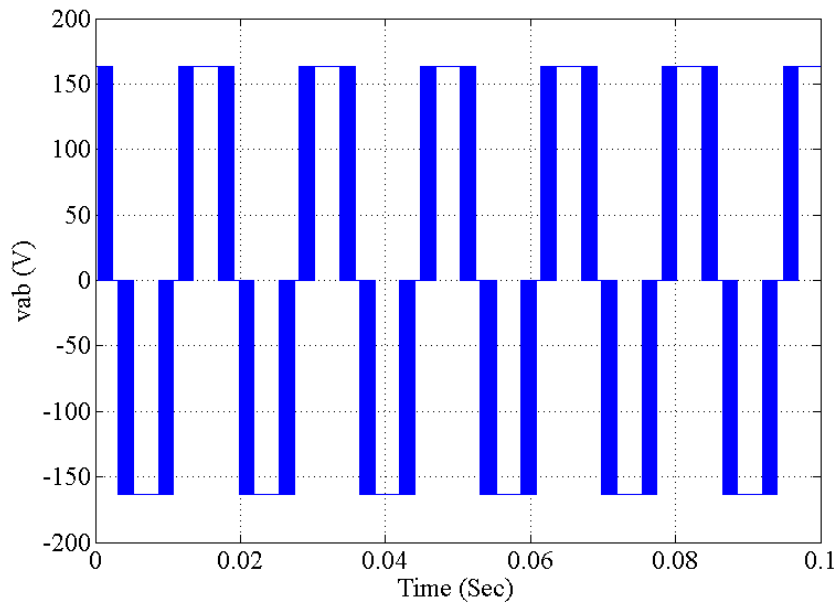


(c)



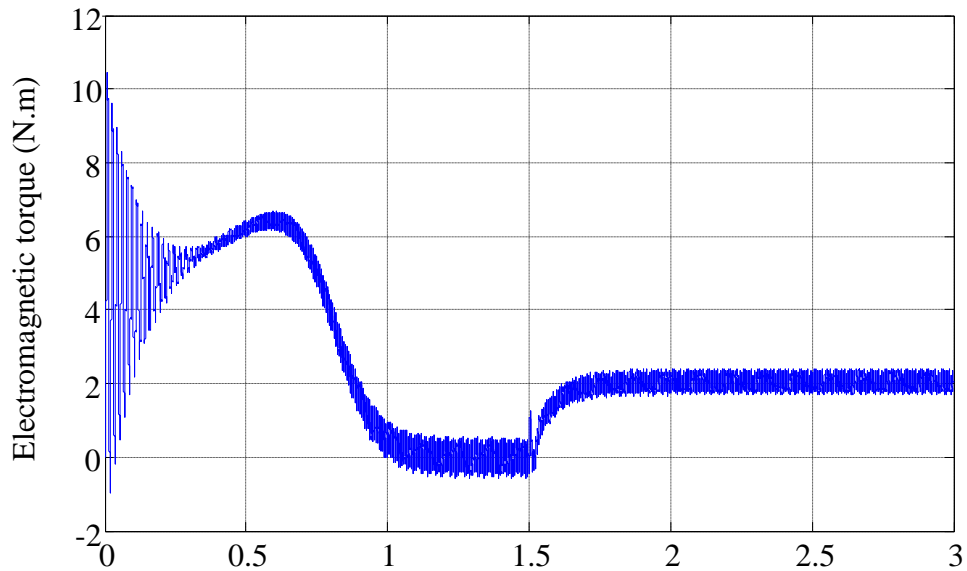
(d)

Figure (2-19) Continued.



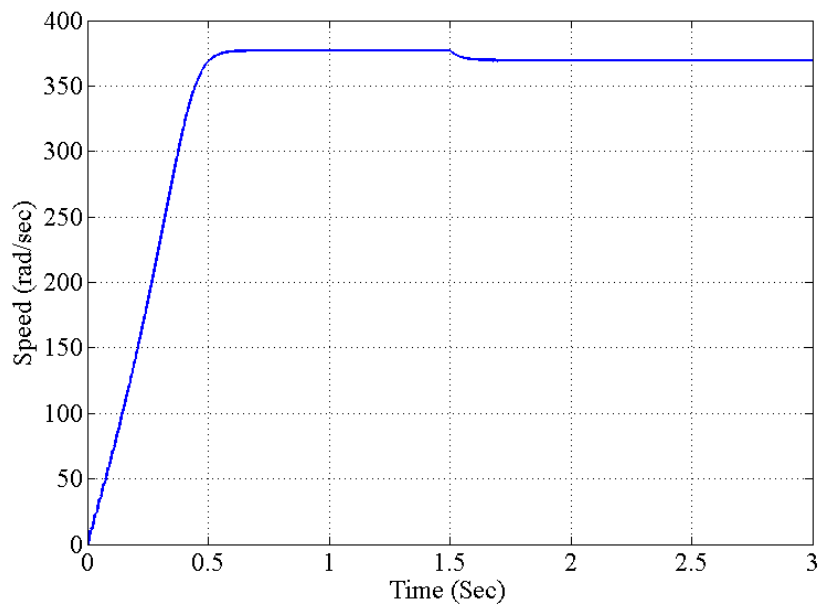
(e)

Figure (2-19) Continued.

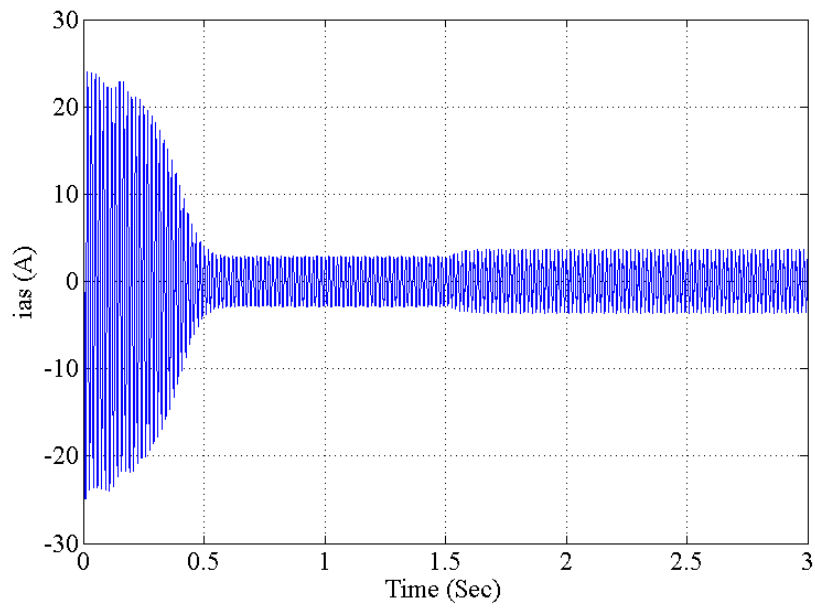


(a)

Figure (2-20) Dynamic response of IM fed by SVPWM Inverter with step load 2N, (a) Electromagnetic torque, (b) Speed, (c) Stator phase current, (d) Stator quadrature axis current, (e) i_{ds} .

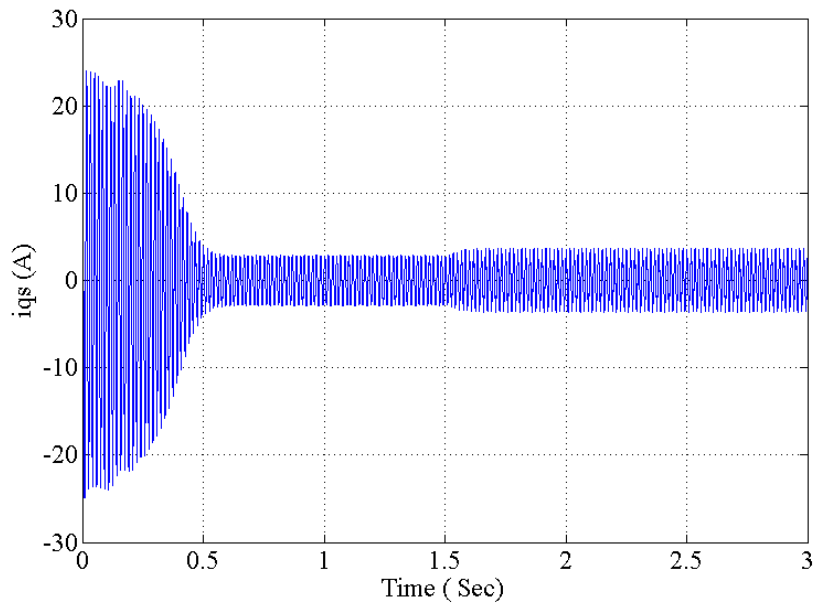


(b)

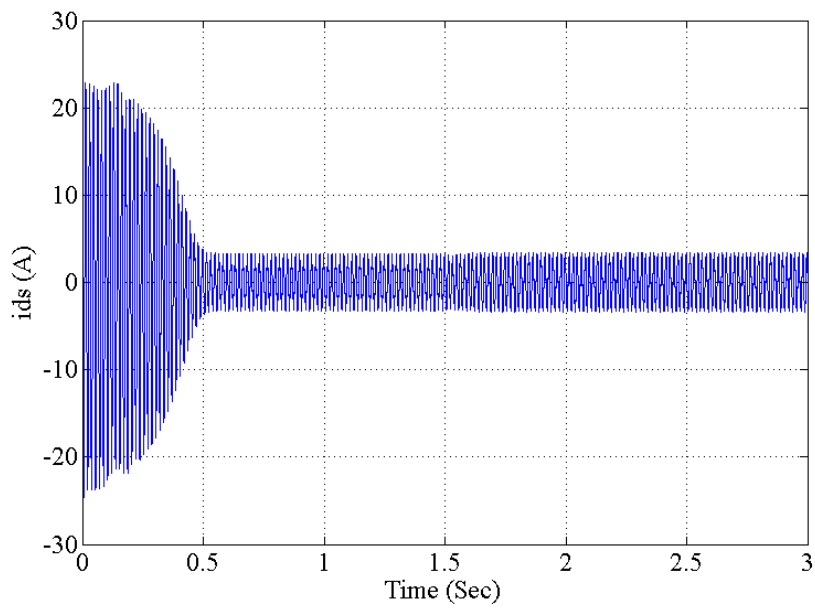


(c)

Figure (2-20) continued.



(d)



(e)

Figure (2-20) continued.

2.7 Conclusion

In this chapter, a Simulink model of three-phase induction motor is implemented using Matlab/Simulink to obtain the dynamic response of the motor, where given a satisfactory response for speed and torque characteristics, and this machine may be used as subsystem at any type of control method and with inverter. SVPWM technique is used to control the VSI. The simulation results show that the SVPWM technique is better because the total harmonic distortion (THD) is less than other modulation technique, and achieve better DC bus voltage utilization compared with other conventional modulation. From characteristics of motor that fed by SVPWM inverter the rotor speed increased, also the time of setting is less and the regulate is more suitable.

Chapter Three

CHARACTERISTIC OF DUAL INDIRECT FIELD ORIENTED VECTOR CONTROL OF TWO THREE PHASE INDUCTION MOTORS FED BY FLI

3.1 Introduction

Recently, the power demand for AC drive is increasing. The performance of machine drives is enhancing by decreasing the cost and size of the drives. Multi-machine System (MMS) is one solution for that [59]. In many manufacturing fields such as electric trains, textile, paper making and mining, multiple motor drive systems (MMS) are demanded, in which two motors may be operate in parallel [60-64]. Generally, this system is required a lot of power switches and high performance control for the number of converter. As a result, will needed a large number of power electronic switches (IGBTs) which is lead to complex of structure and high cost, for reducing this cost is utilized a common DC bus while each motor has its three phase inverter [24].

Probably, frequently, analyzed and reduced switch count topology for two-motor drives employing the five-leg (ten-switch) VSI. One phase of each motor is connected to the common leg of the five-leg VSI, while the remaining two phases of each machine are supplied independently, from the two pairs of inverter legs [22,37].

Five phase inverter fed drives are highly suitable for standalone applications like electric hybrid vehicles, aerospace applications and ship propulsion that require high levels of reliability and efficiency. The third harmonic in a five phase system can be used to effectively reduce the torque pulsations in the steady state operation and the

percentage of the third harmonic included along with the fundamental can be altered by the switching algorithm itself [15].

In this chapter the independent control of a dual induction motor drive system fed by a five-leg inverter is researching to make a good use of the five-leg inverter. In most, each induction motor is adopted indirect field oriented vector control, and using space vector pulse width modulation (SVPWM) for decreasing the switching count compared with the conventional PWM methods for the five-leg inverter(FLI) [65]. However, the structure of control is composed of four PI regulators for current loops and two PI regulators for speed, which is complex in the tuning of all regulators for optimizing performance of system. In addition, the common leg of inverter is shared by two induction motors and two inverter stages are modulated by SVPWM. The principle independent control of two three phase induction motor drive by five leg voltage source inverter is investigated [66-67].

3.2 Five-Phase Voltage Source Inverter

Single-phase VSIs cover low-range power applications, three-phase VSIs cover the medium- to high-power applications and five-phase VSIs cover above the three-phase power applications. The major purpose to these topologies is providing a five-phase voltage source, the frequency, amplitude and phase, of these voltages must be always controllable. As in Single-Leg of VSIs, to avoided a shorting circuit of DC voltage supply any two switches cannot be switched ON at a same time (S_{11} and S_{41}), (S_{31} and S_{61}), (S_{51} and S_{21}), (S_{32} and S_{62}) or (S_{12} and S_{42}) as seen in Fig. (3-1), Similarly, avoiding the undefined states, and thus undefined ac line voltages of output, the switches of any leg of these cannot be switched OFF simultaneously. The topology of five-phase VSI is shown in Fig. (3-1), there are five leg, each leg has two switches with antiparallel diodes across each switch. The load may be considered as (inductive or resistive or a motor load). The five gating signal of VLIs should be

delayed by 72° . According to each other to predicated a balanced of five phase voltages and not balanced if they are not perfectly balanced in phases and magnitudes. Ten diodes and ten transistors can be used [68-69]. Table (3-1) representing the step of switching conducting [70].

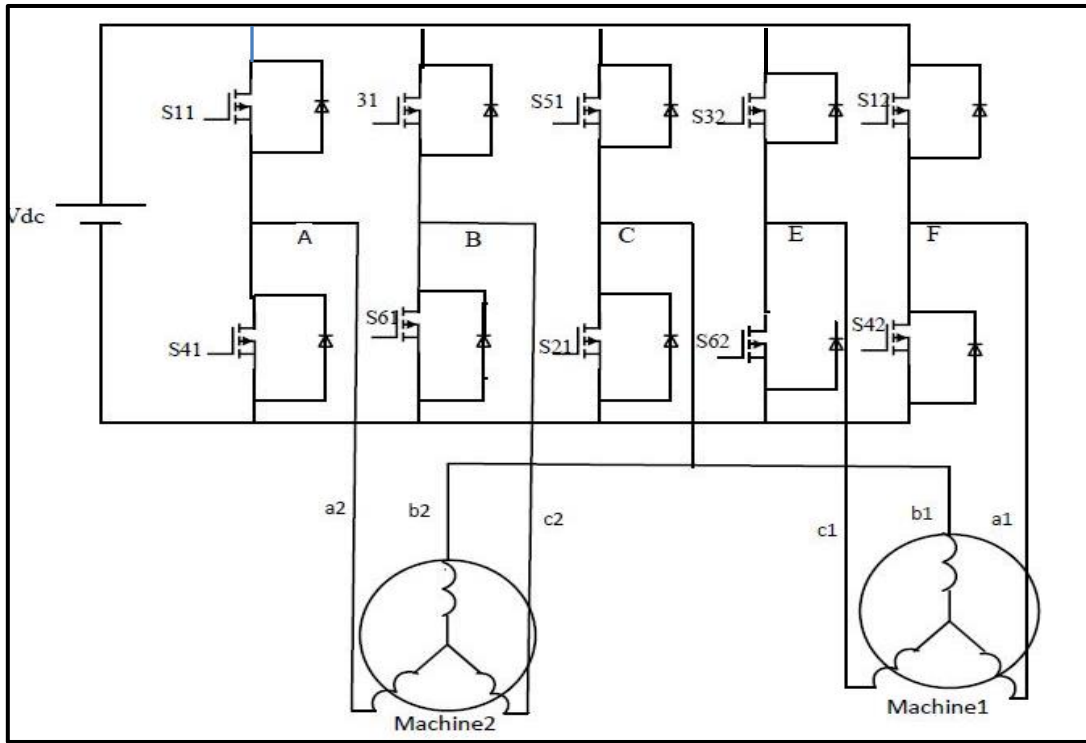


Fig. (3-1) FL VSI supplies dual three phase machine.

Table (3-1) Conduction period of Switching Conducting.

Period No.	Conduction Period	Switches
Step 1	$0 \leq \omega_t < \pi/5$	$S_{11} \cdot S_{62} \cdot S_{31} \cdot S_{42} \cdot S_{51}$
Step 2	$\pi/5 \leq \omega_t < 2\pi/5$	$S_{62} \cdot S_{31} \cdot S_{42} \cdot S_{51} \cdot S_{41}$
Step 3	$2\pi/5 \leq \omega_t < 3\pi/5$	$S_{31} \cdot S_{42} \cdot S_{51} \cdot S_{41} \cdot S_{32}$
Step 4	$3\pi/5 \leq \omega_t < 4\pi/5$	$S_{42} \cdot S_{51} \cdot S_{41} \cdot S_{32} \cdot S_{61}$
Step 5	$4\pi/5 \leq \omega_t < \pi$	$S_{51} \cdot S_{41} \cdot S_{32} \cdot S_{61} \cdot S_{12}$

Step 6	$\pi \leq \omega_t < 6\pi/5$	$S_{41} \cdot S_{32} \cdot S_{61} \cdot S_{12} \cdot S_{21}$
Step 7	$6\pi/5 \leq \omega_t < 7\pi/5$	$S_{32} \cdot S_{61} \cdot S_{12} \cdot S_{21} \cdot S_{11}$
Step 8	$7\pi/5 \leq \omega_t < 8\pi/5$	$S_{61} \cdot S_{12} \cdot S_{21} \cdot S_{11} \cdot S_{62}$
Step 9	$8\pi/5 \leq \omega_t < 9\pi/5$	$S_{62} \cdot S_{12} \cdot S_{11} \cdot S_{62} \cdot S_{31}$
Step 10	$9\pi/5 \leq \omega_t < 10\pi/5$	$S_{21} \cdot S_{11} \cdot S_{62} \cdot S_{31} \cdot S_{42}$

3.3 Topology of Five-Leg drive system

The topology of five-leg VSI supplies dual-three phase induction machine drive shown in Fig. (3-1), that will be saving two switches and lead to reduce in capital cost with respect to the standard configuration of dual three-phase voltage source inverter(VSI). In the five leg inverter topology, will be used one leg as the common leg, where this leg is shared by two motors leg C is chosen to share by two machines. Legs A and B of Inverter are connected to phases a_1 and b_1 directly, for machine 1. Legs F and E are connected to phases a_2 and b_2 , respectively, of machine 2. DC bus is of v_{dc} rated value [71-72].

3.4 Modulation methods of five leg voltage source inverter

There are several PWM techniques used for the five leg inverter(FLI)topology. Among these methods, [23-24] are

1. Dual Voltage Modulation (DVM).
2. The Modulation Bock Method (MBM).
3. The Inversion Table Method (IVM).
4. Double Zero Sequence Method (DZS).

The Double Zero Sequence is the best method where enables the DC link voltage to be an arbitrary distribution between two motors while its operation maintaining in constant switching frequency mode. Also, the DZS is easier to implement and show less complexity. This method is able to solve the drawbacks of previous PWMs such as the restriction voltage for one motor about 50% of the DC bus, sideband harmonics, underutilization of the switching state, asymmetrical switching frequency, high magnitude THD generation and their complexity problem [71]. the DZS method is using either carrier based or space vector PWM technique.

3.4.1 The Double Zero Sequence Modulation method

A space vector double zero sequence DZS is shown in Fig. (3-2). In this method, two standard identical SVPWM three- phase modulator are utilized to control each motor and it generating modulation signals for the five leg, where it is make able to assign either of the both machines any part of the DC bus voltage. For each machine respectively, voltage references become vector in d-q planes with complete arbitrary amplitude suitable to any the six sectors in d-q planes. Both modulators are operating in standard manner, where the total time of zero sequence is shared and equally among 111 and zero space vector, each reference space vector will have been realizing on average over the period of switching by adjusting two active space vector. Principally at first in the stationary frame setting is synthesized of the fundamental voltages in the 3-phase leg space vector modulator, then process will have repeated for setting modulator 2. The outputs of the SVPWM modulator is as assigned by duty cycle δ , to reduce the modulation signals from six to five will summed output signals of SVPWM machine1 and SVPWM machine 2 as an appropriate manner as shown in the block diagram configuration in Fig. (3-2). The output of five modulating signals for FLI are describe below [36-37,71].

$$\delta_A = \delta_{a_1} + \delta_{c_2} \quad \dots\dots (3.1)$$

$$\delta_B = \delta_{b_1} + \delta_{c_2} \quad \dots\dots (3.2)$$

$$\delta_C = \delta_{c_1} + \delta_{c_2} \quad \dots\dots (3.3)$$

$$\delta_D = \delta_{a_2} + \delta_{c_1} \quad \dots\dots (3.4)$$

$$\delta_E = \delta_{b_2} + \delta_{c_1} \quad \dots\dots (3.5)$$

Where the m_A, m_B, m_C, m_D and m_E denoted to the modulating signal which generated to FLI after compared with carrier signal. The placement of the zero Space Vector 111 will be in the middle of the switching pattern therefore the values of duty cycles will have equal to 0.5. After summation defined by Eqs. (3.1) to (3.5), the total duty cycles will be shifting between the rang 0.5 to 1.5 between two motors (motor '1' and motor "2") shifted into the range (0.5: 1.5), where does not fit with the value of the switching period. therefore, however, the value of 0.5 make be continuously subtracted from the duty cycles, which calculated by using Eqs. (3.1) to (3.5). The net effect of the duty cycle summation is there distribution of the application times of the zero space vectors. From the first three equations above ,it is visible that the addition of the value of the duty cycle δ_{c2} increases all three duty cycles, originally generated by the modulator1, in the same manner. Thus, the application time of the zero space vector 111 is effectively increased, and as a consequence application time of the zero space vector 000 is decreased (before shifting by 0.5), without affecting the application times of the two active space vectors. The same explanations apply to modulator2 on the basis of the last three equations above [23-24,36,71].

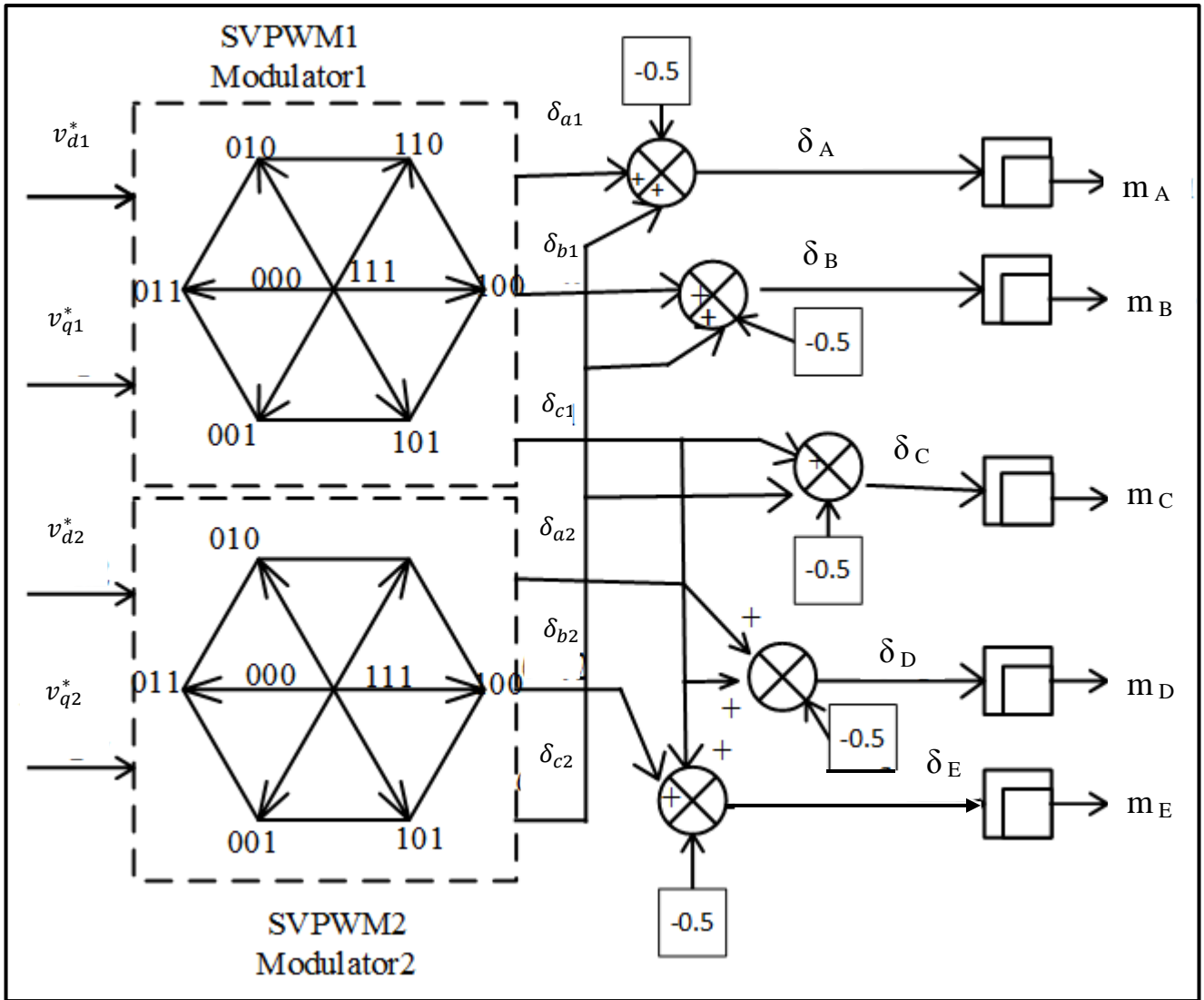


Figure (3-2) Space Vector Double Zero Sequence Method.

3.4.2 The Proposed Simulink model for Five –Leg Inverter Fed Two Induction Drive.

The Simulink model of five- leg voltage source inverter driving dual three phase induction motor and fed by sinusoidal voltage is shown in Fig. (3.3). The parameters of the symmetrical two induction machine are listed in appendix A and modeling of the machine is discussed in chapter two, the switching frequency is 10 KHZ, the modulation method is SVPWM double zero sequence can be use, each

three modulators is supplied from the reference voltage (V_{d1}^*, V_{q1}^*) for SVPWM modulator 1 and reference voltages (V_{d2}^*, V_{q2}^*) for SVPWM modulator2.

3.4.2.1 Simulink Model of Two SVPWM Modulator.

Two independent three – phase space vector modulators are utilized to control the dual machines (motor1 and motor2). The d–q rotating reference frame was as the voltage reference vector to dual motor, V_{d1}^* and V_{q1}^* reference voltages to SVPWM modulator1 and V_{d2}^* and V_{q2}^* to SVPWM modulator2 ,where the output is generated from the modulator1 used to determine the duty cycle (δ_{a1}, δ_{b1} and δ_{c1}) according to calculate SVPWM in Eqs. (2.33)to (2.35), and the output of modulator2 will be used to determine duty cycle (δ_{a2}, δ_{b2} and δ_{c2}). Two modulators are able to together satisfyingly need of both machines. Fig. (3.4) showing the simulink model of modulator1.

3.4.2.2 Simulink Model of five duty cycle $\delta_A, \delta_B, \delta_C, \delta_D$ and δ_E

To reduce the number of six modulating signal to five delta signal ($\delta_A, \delta_B, \delta_C, \delta_D$ and δ_E) and utilized for a FLI ,the duty cycles (δ_{a1}, δ_{b1} and δ_{c1}) generated from SVPWM modulator1and (δ_{a2}, δ_{b2} and δ_{c2})the output of SVPWM modulator2 are summing where the output of five switching delta signal proposed as below.

$$\delta_A = \delta_{a1} + \delta_{c2} \quad \dots\dots (3.6)$$

$$\delta_B = \delta_{b1} + \delta_{c2} \quad \dots\dots (3.7)$$

$$\delta_C = \delta_{c1} + \delta_{c2} \quad \dots\dots (3.8)$$

$$\delta_D = \delta_{a2} + \delta_{c1} \quad \dots\dots (3.9)$$

$$\delta_E = \delta_{b2} + \delta_{c1} \quad \dots\dots (3.10)$$

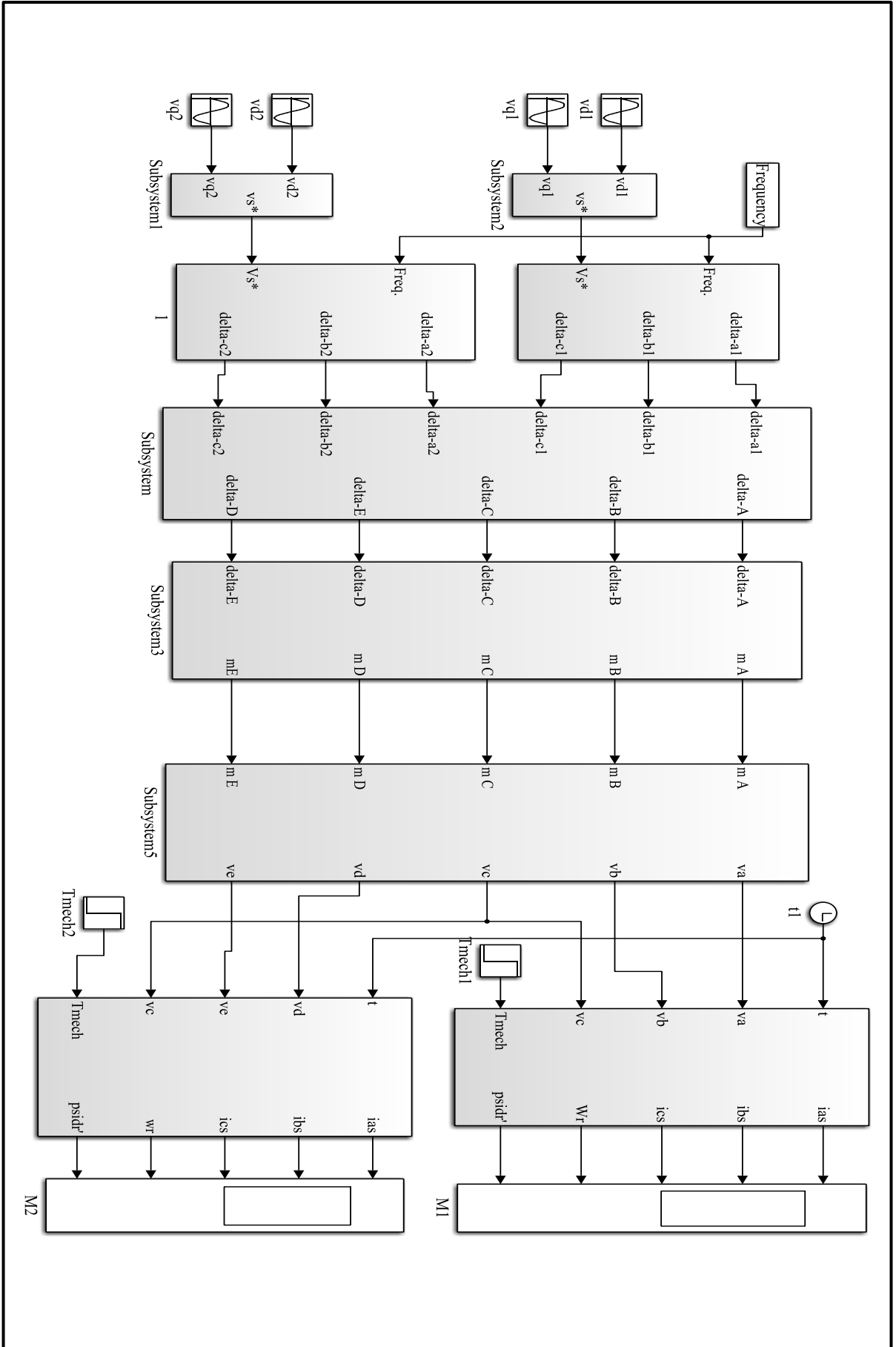


Fig. (3-3) Simulink of dual induction motor fed five phase inverter.

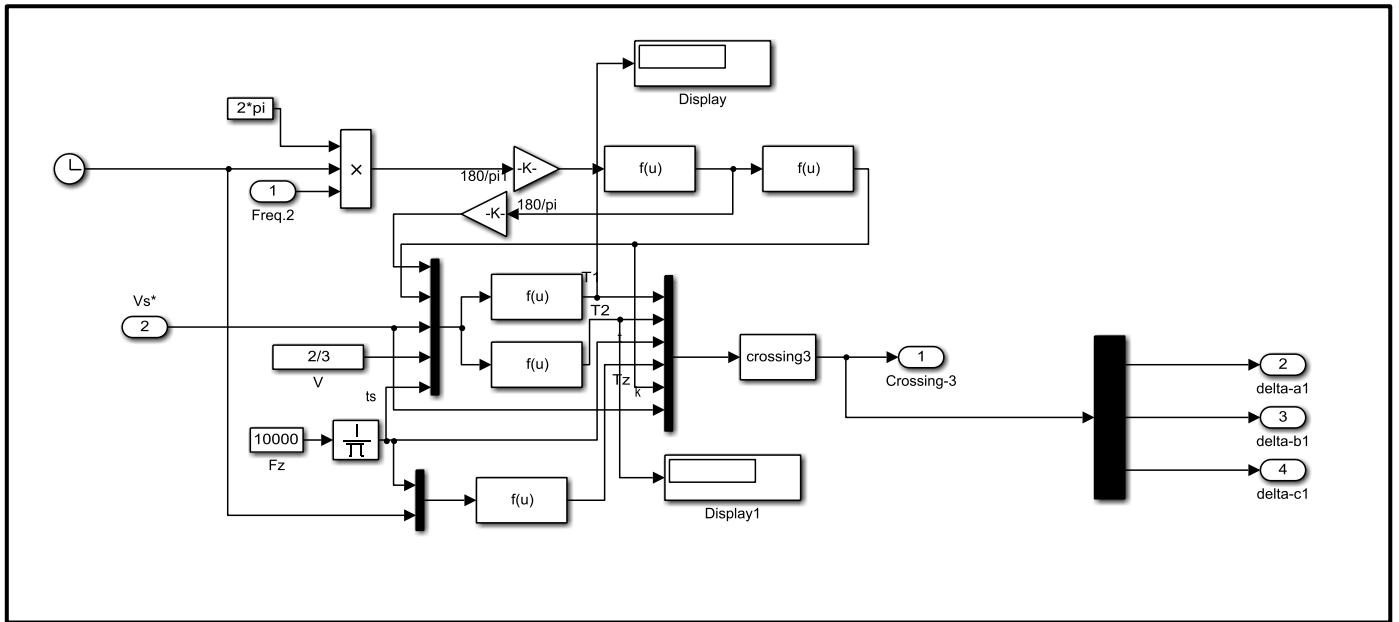


Fig. (3-4) Simulink model of the SVPWM Modulator.

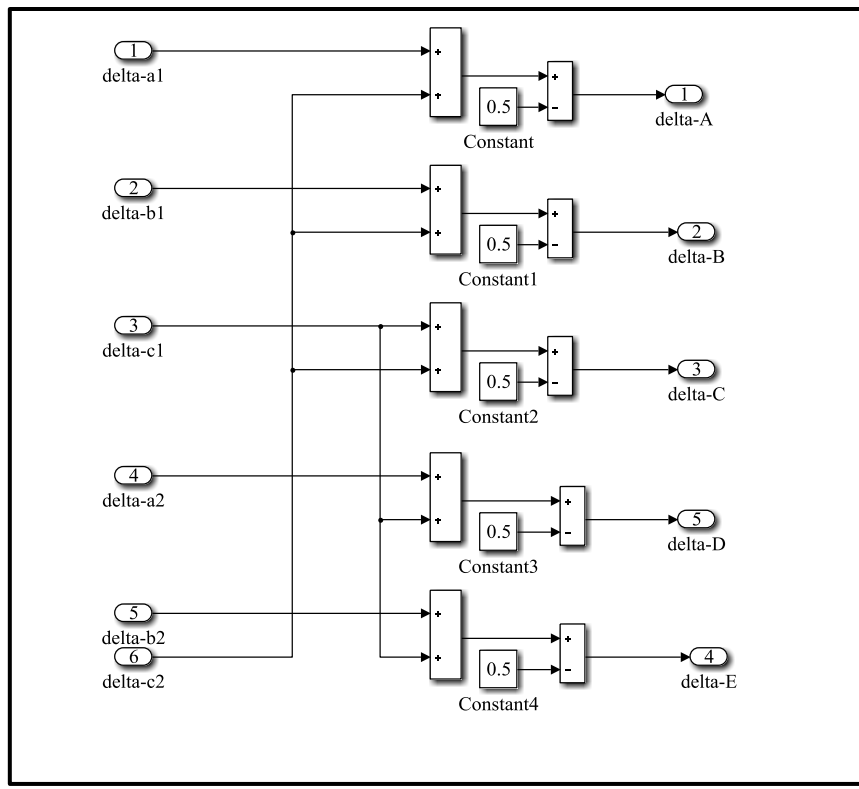


Fig. (3-5) Simulink model of calculation delta signals.

Where $(\delta_A \delta_B \delta_C \delta_D \delta_E)$ are the duty cycles of leg A,B,C,D and E respectively, and the subscripts "1" and "2 " is representing motor 1 and motor 2 respectively.

These total duty cycle will be shifted by rang 0.5 between two machines (M1 and M2) and these five switching duty cycle using as gating signal for the FLI as shown in Fig. (3-5)

3.4.2.3 Simulink Model of modulating signals (m_A, m_B, m_C, m_D and m_E)

To get the modulating signals m_A, m_B, m_C, m_D and m_E , the relay block is used. The relay block allows its output to switch between two specified values. When the relay is ON, it remains ON until the input drops below the value of the Switch OFF point parameter. When the relay is OFF, it remains off until the input exceeds the value of the Switch on point parameter, where the five duty cycle is the input to relay and the output the five signal to be gating signal to FLI. Fig. (3-6) shows the Simulink model of the modulating signals (m_A, m_b, m_c, m_D and m_E).

3.4.2.4 Simulink Model for five -leg VSI

Figure (3-7) represents the Simulink model of three phase five-leg VSI using (ten switching S_1 to S_{10}) with common Dc bus voltage. The five phase (V_a, V_b, V_c, V_d and V_e) are fed two identical induction motor where two phase fed to motor1 and other two phase fed motor2 ,the one leg will be shared by two machines as common leg.

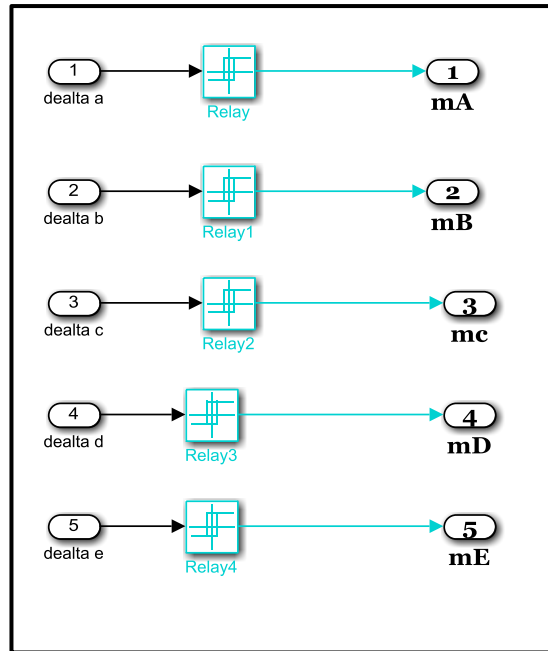


Figure (3-6) Simulink model the modulating signal m_A , m_{bB} , m_C , m_D and m_E .

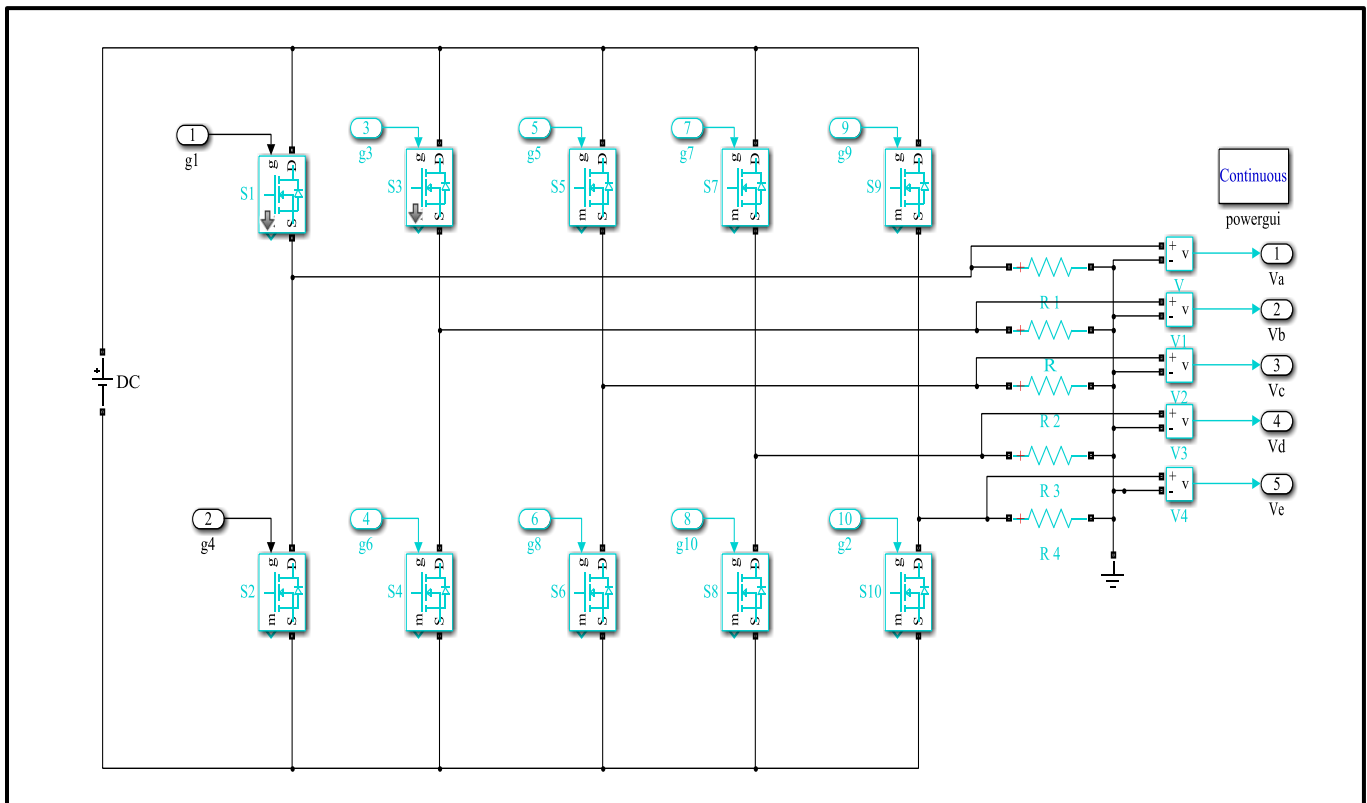
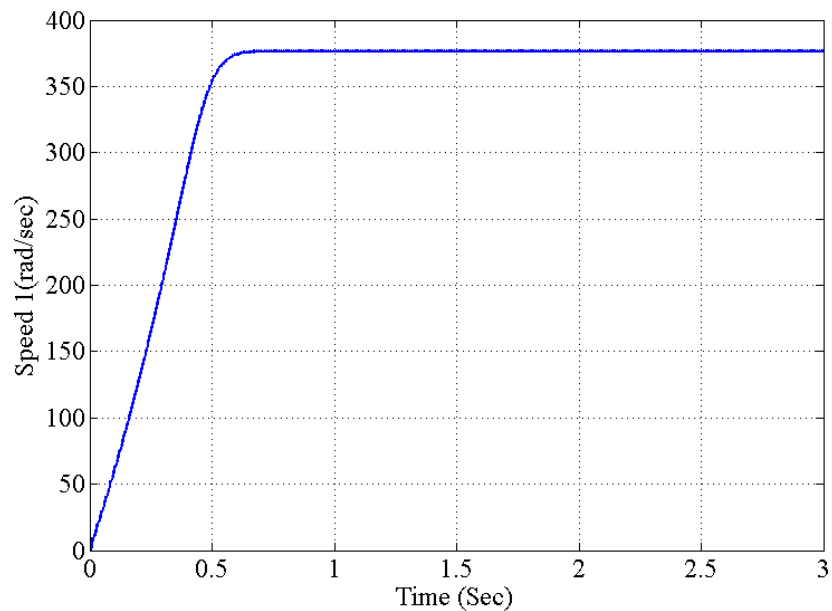


Figure (3-7) Simulink model of five –leg inverter.

3.4.3 Simulation Result of five -leg VSI

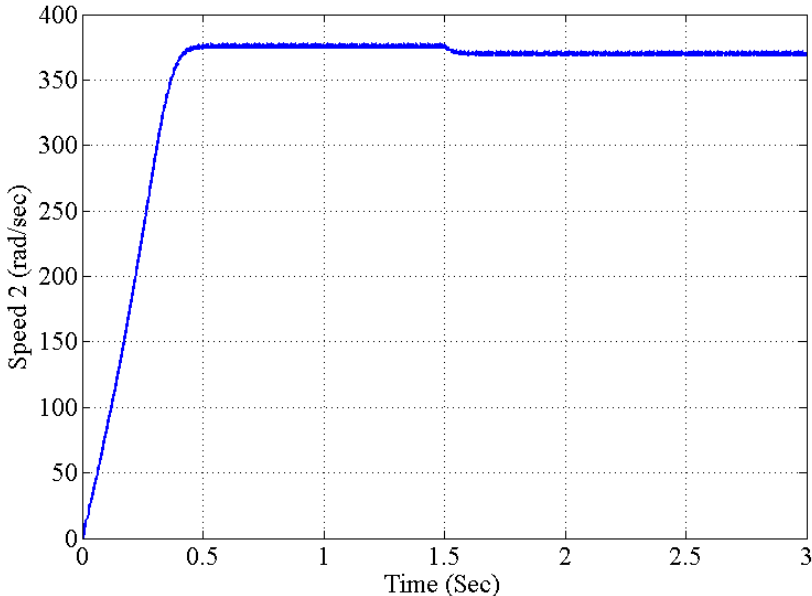
The dynamic simulation of two identical induction motor fed by five leg VSI as shown in Fig. (3-3), the two motors operate with the same time and reference speed. The speed for motor1 is shown in Fig. (3-8a), where motor 1 operates at no load and the motor 2 is operated with a load 2N.m is applied on it at 1.5 Sec, the speed ω_{r2} shown in Fig. (3-8b). The characteristic of torque for motor1 and motor2 shown in Figs. (3-8c) and (3-8d). The direct axis current of motor1 is shown in Fig. (3-9e), the quadratic axis current i_{qs2} of motor2 is shown in fig. (3-8f).



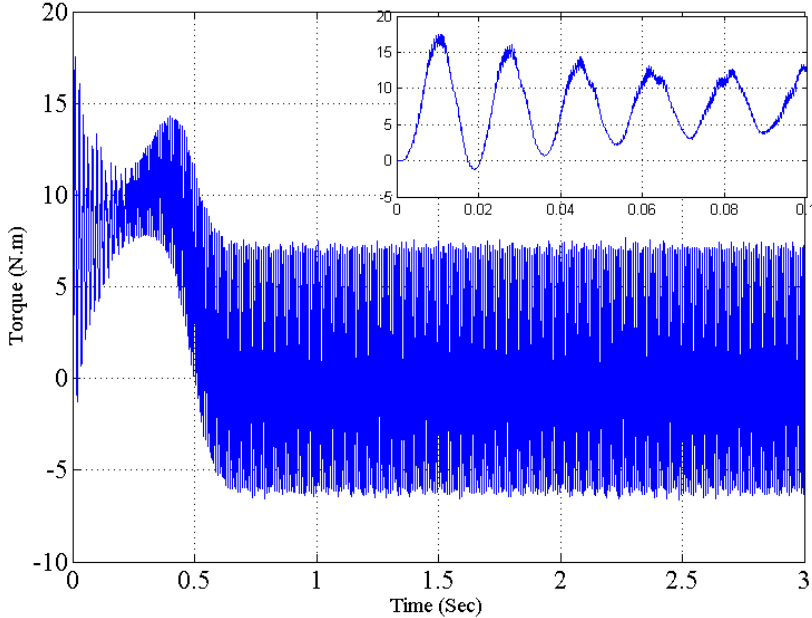
(a)

Figure (3-8) Dynamic Response of Dual IMs fed SVPWM FLI inverter

(a)Speed, of motor1 (b)Speed of motor2, (c)Torque of motor1, (d) Torque of motor2, (e)iqd1, (f) iqs2

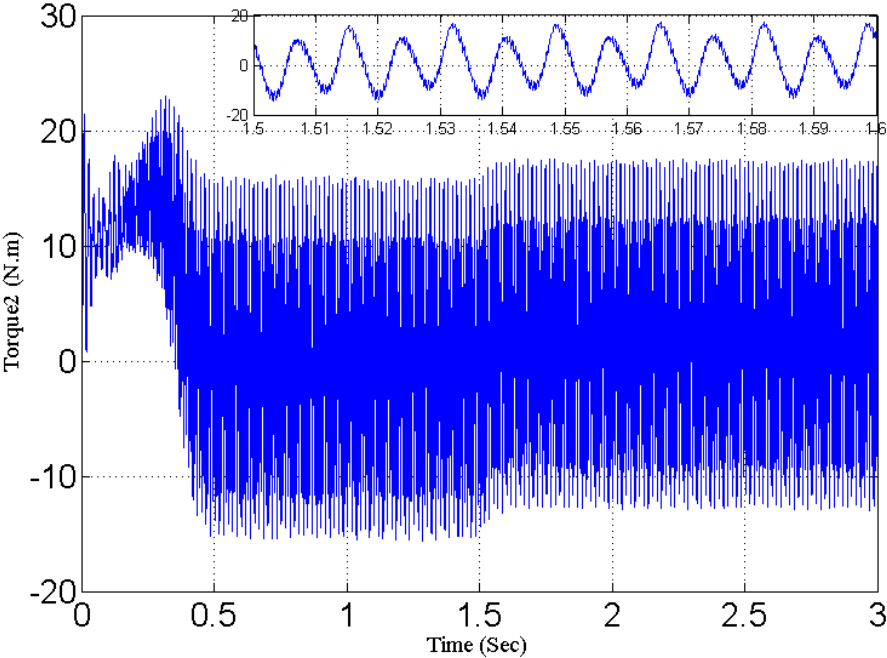


(b)

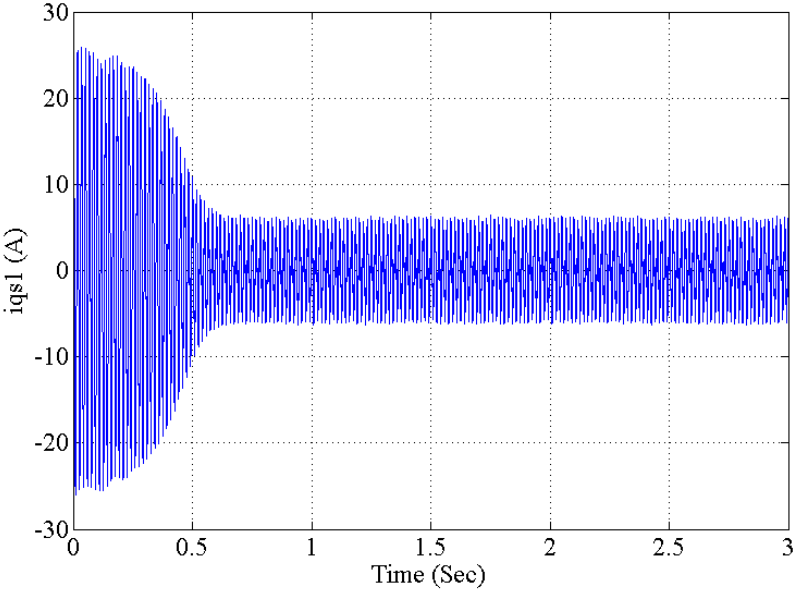


(c)

Figure (3-8) continued.



(d)



(e)

Figure (3-8) continued.

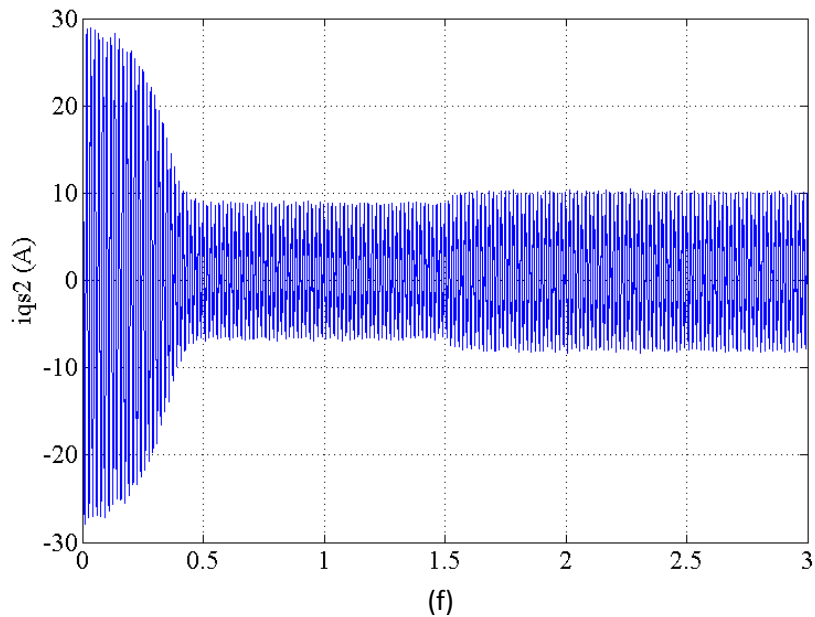


Figure (3-8) continued.

3.5 Control Method of Three Phase Induction Motor

In general, the control and estimation of AC drives are very complex compare with DC drives [73]. In order to have better controllability and high performance, vector control is used where advanced control of IM is required an independent control of torque and magnetic flux like as Dc machine and special control for IM [30,74].

By decoupled control for flux and torque of machine, the vector control techniques consider faster transient response of the machine and ensures improved performance. Vector control is classified into two types depending on the way of calculating the field angle: direct oriented field FOC and indirect field oriented vector control IFOC. In direct vector control, the field angle is obtained from current and terminal voltage while in indirect field control the field angle is get using rotor position calculating [35,75].

The IFOC of IM drive is the widespread used in high performance of IM drive because of its advantages like high efficiency, extremely rugged, good power factor, very simple, easy implementation, low cost and it does not require starting. The IFOC motor drive is gaining greatly attention because of reduced machine parameter dependence and its less calculation complexity, it allows the decoupling of electromagnetic torque and rotor flux variables by means of nonlinear coordinate transformation and manipulating the field oriented quantities by using the vector components of direct and quadrature axis current by utilizing the unit vector [8]. The vector control methods enable the induction motor to be operated with good dynamic performance that is comparable with the characteristics of a separately excited DC motor.

3.5.1 Principle of Indirect Field Oriented Vector Control Method

In the IFOC method, there is no needed to find the position of the rotor flux as in other type of vector control method (direct vector control), where a suitable value is applying to the slip frequency to adjusted appropriate position to the stator current of machine. After the estimation of the slip frequency, it will have summed with the actual rotor speed to obtain the stator angular frequency and integrated to obtain the electrical angular position [31]. Figure (3-9) shows the block diagram of an indirect field orient control induction motor drive. In IFOC ,the decoupling control is achieved one the component of stator flux represent by current i_{dS} and other torque component represent by current i_{qS} ,both component may be controlled separately therefore the induction motor can be controlled as separately excited DC motor[76-79].

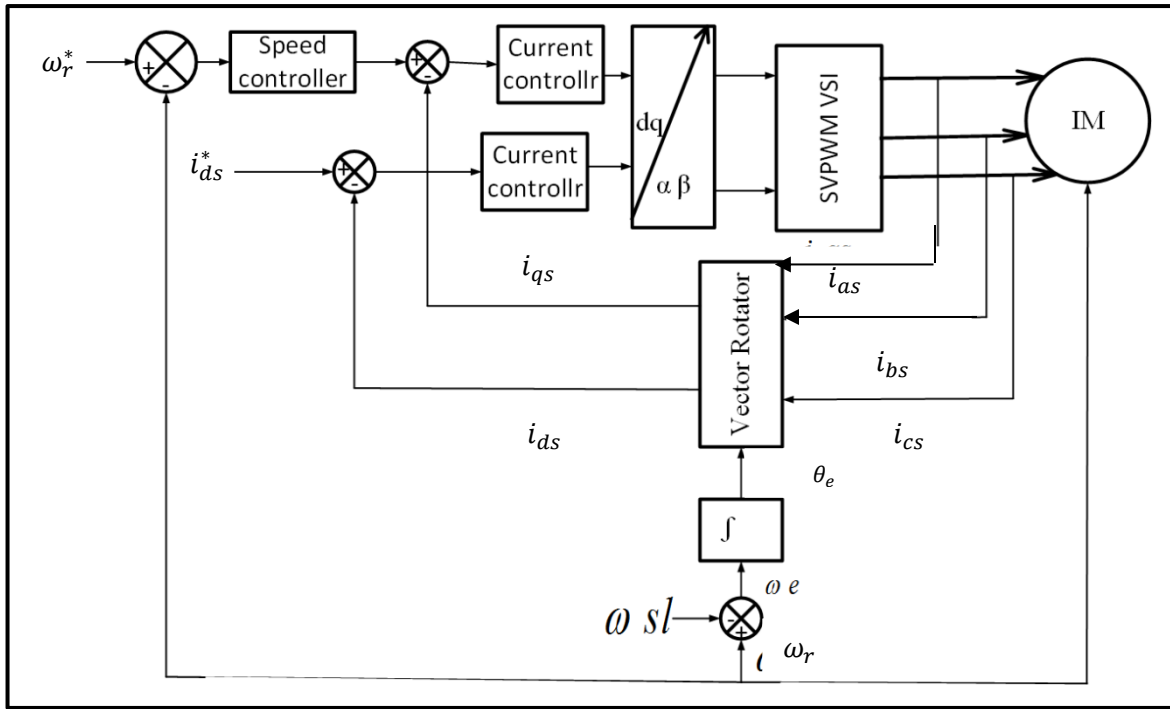


Figure (3-9) Indirect Field Oriented Controlled Induction Motor Drive.

3.5.2 Implementation of Indirect Field Vector Control Method

The component of stator current i_{qs} and i_{ds} consider constant in the rotor reference frame. The indirect vector control method is essentially same as the direct vector control except the unit vector is generated in an indirect manner using the measured speed ω_r and slip speed ω_{sl} . [79-80].

The induction motor (IM) is fed by a SVPWM inverter, which operates in voltage control mode where the actual speed of motor ω_r is compared with the reference speed ω_r^* and will produced the error, which is fed to (PI or any intelligent controller) the speed controller. The output of the speed controller is electromagnetic torque T_e^* [32,80].

$$T_e^* = \frac{3}{2} \frac{p}{2} \frac{L_m}{L_r} (\hat{\psi}_r i_{qs}^*) \quad \dots (3-11)$$

The electromagnetic torque reference T_e^* is used to calculate the quadrature -axis stator current reference i_{qs}^* is calculated from[80]

$$i_{qs}^* = \left(\frac{2}{3}\right) \left(\frac{2}{p}\right) \left(\frac{L_r}{L_m}\right) \left(\frac{T_e^*}{\hat{\psi}_r}\right) \dots (3-12)$$

Where

$$\hat{\psi}_r = \frac{L_m i_{ds}}{1 + \tau_r s} \dots (3-13)$$

and

$$\tau_r = \frac{L_r}{R_r} \text{ is the time constant of rotor.} \dots (3-14)$$

The direct-axis current reference of stator i_{ds}^* is obtained from reference rotor flux input ψ_r^*

$$i_{ds}^* = \frac{\varphi r^*}{L_m} \dots (3-15)$$

The rotor flux position θ_e is obtained by added the feedback rotor speed to slip speed frequency ω_{sl} , then the slip speed together with the speed of rotor is integrated[81].

$$\theta_e = \int \omega_e dt = \int (\omega_r + \omega_{sl}) \dots (3-16)$$

The slip frequency ω_{sl} is generated by the stator reference current i_{qs}^* and the parameters of motor.

$$\omega_{sl} = \frac{L_m R_r}{\hat{\psi} L_r} i_{qs}^* \dots (3-17)$$

3.5.3.1 Simulink Model of i_{ds}^* and i_{qs}^*

The references current of stators current component i_{ds}^* and i_{qs}^* are obtaining from torque and rotor flux ,which is estimated according to equation (3-12), (3-15), Figure (3-11) shows calculated the d-axis reference of stator current.

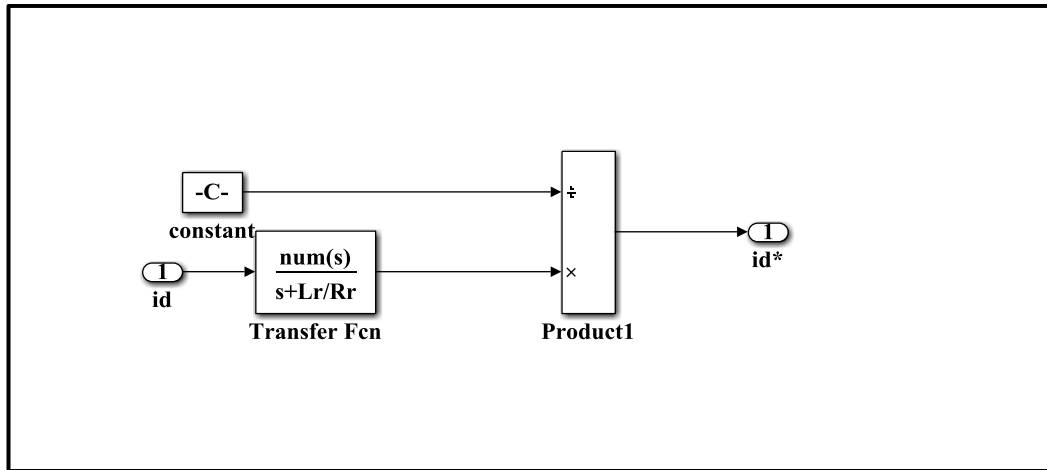


Figure (3-11) d-axis reference of stator current.

3.5.3.2 Simulink Model of PI controllers.

In IFOC method three feedbacks are used, one of them to actual rotor speed and others for stator current component (i_{ds} and i_{qs}). The deviation between the reference speed ω_r^* and speed of feedback ω_r is determine through PI controller, the output of PI speed is q-reference of stator current to control to the torque .The deviation between i_{qs} of the motor obtained by park transformation and the reference current i_q^* is obtained through PI1 current controller where output it the command voltage to SVPWM inverter v_q . Other current loop used PI3 to compared the i_{ds} actual component of stator current of motor with i_{ds}^* to produced v_d command voltage to SVPWM inverter. In both decomposed of stator current obtained the separately control for torque and flux so may getting the control as DC motor. The K_p and K_I gain values of the controllers is tuning using trial and error.

3.5.3.3 Simulink Model of Slip Frequency

In IFOC method needed the frequency of the rotor flux vector ω_e from the summed the actual rotor speed with slip frequency ω_{sl} . Fig. (3-12) shows the calculated slip frequency according to equation (3-17).

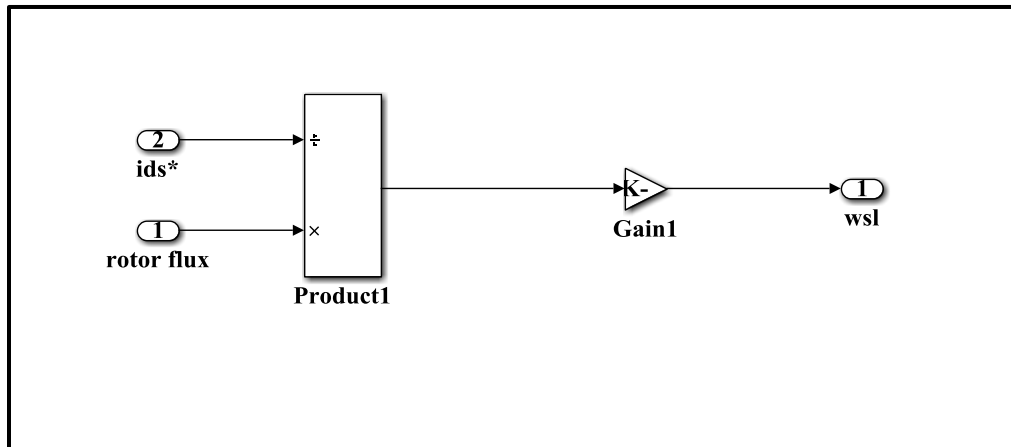


Figure (3-12) Simulink model of slip frequency.

3.5.3.4 Simulink Model of Determination Rotor position θ_e

The main distinguish between IFOC and FOC method that how to determine the rotor position where in IFOC method evaluated by summed the slip frequency in Fig. (3-13) with speed of feedback and taking integral of the summing according to Eq. (3-16). Figure (3-13) shows the Simulink model of determine position of rotor θ_e .

3.5.3.5 Simulink Model of Electromagnetic torque

The torque is proportional to the product of the stator q axis current and the rotor flux linkages, this expression of torque is similar to Dc motor, which is proportional to the product of the armature current and field flux linkages, the torque equation given in Eq. (3-11). Figure (3-14) shows Simulink model of electromagnetic torque.

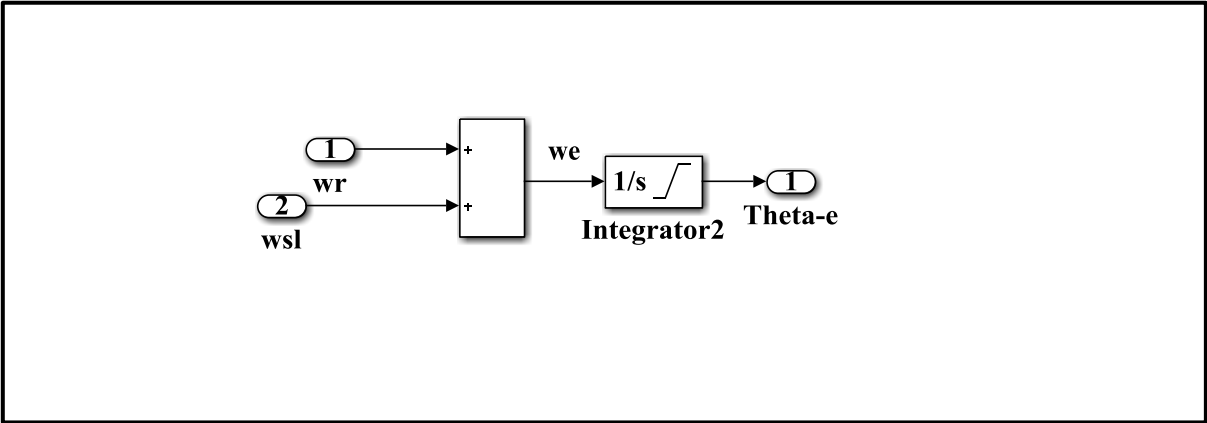


Fig. (3-13) Simulink model of determine rotor position.

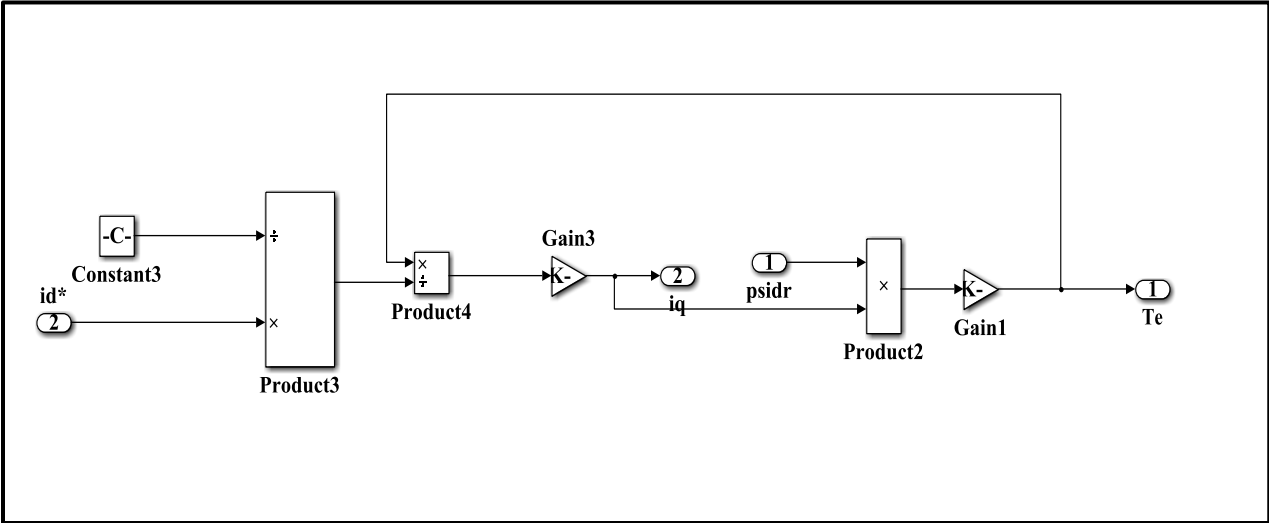
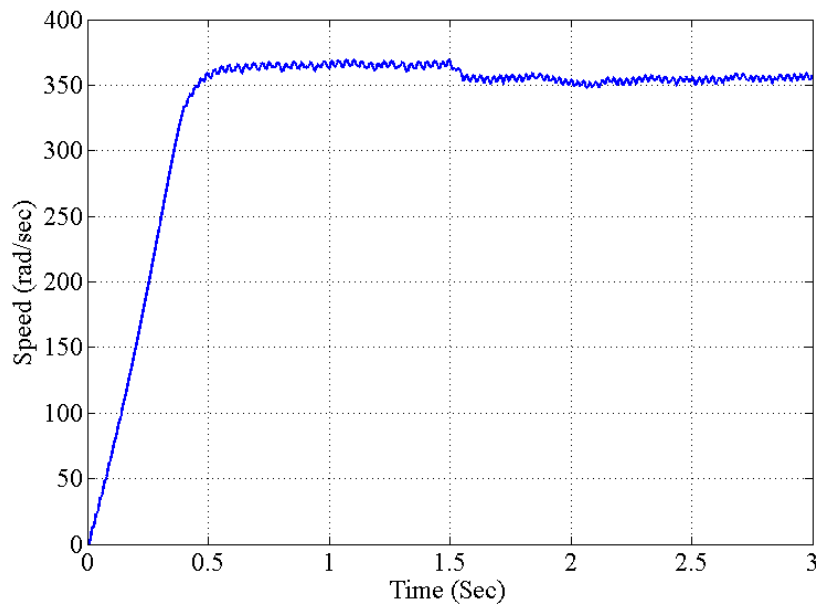


Figure (3-14) Simulink model of determine electromagnetic torque.

3.5.4 Simulation Results of IFOC Method for IM fed SVPWM inverter

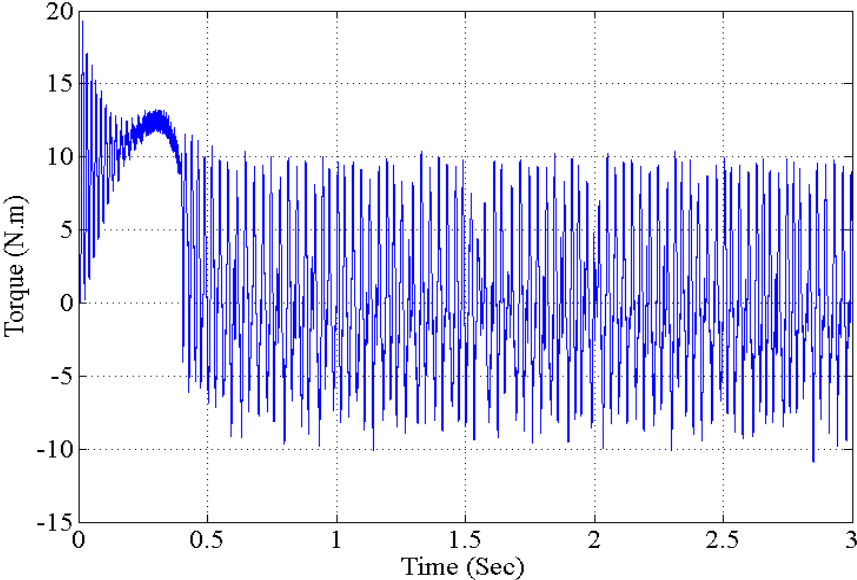
An IFOC pulse width modulated voltage source inverter which gives superior field orientation and decoupling performance with the addition of two current PI controllers has been introduced. The Figure (3-15) shows the performance of motor. Fig. (3-15a) shows the rotor speed at the reference speed for PI controller at no load, Fig.(3-15b) shown the electromagnetic torque. The 2 N.m load is applied at time 1.5Sec, the motor starting and arrives steady state at reference speed with time 0.6Sec.



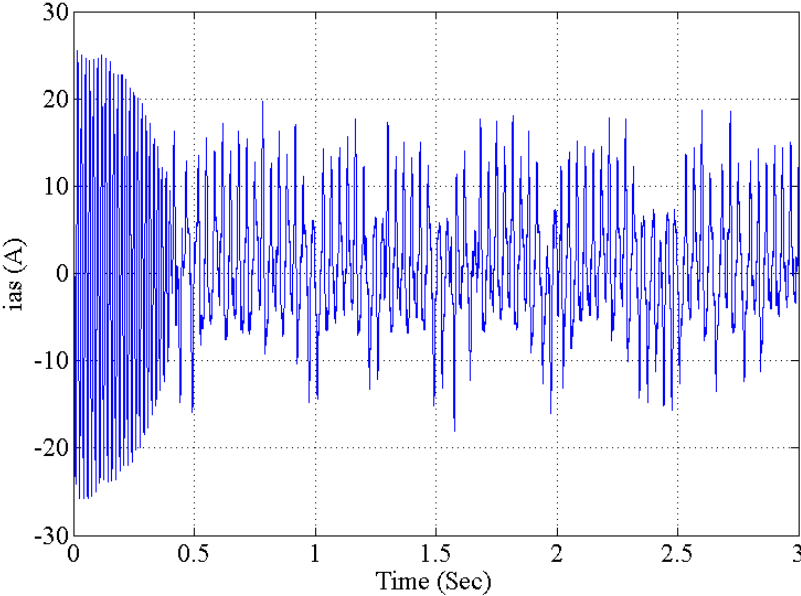
(a)

Figure (3-15) Dynamic Response of IM based on IFOC with a load 2N.m.

(a) Speed,(b) Torque,(c)Stator phase current,(d) i_{ds} ,(e) i_{qs}

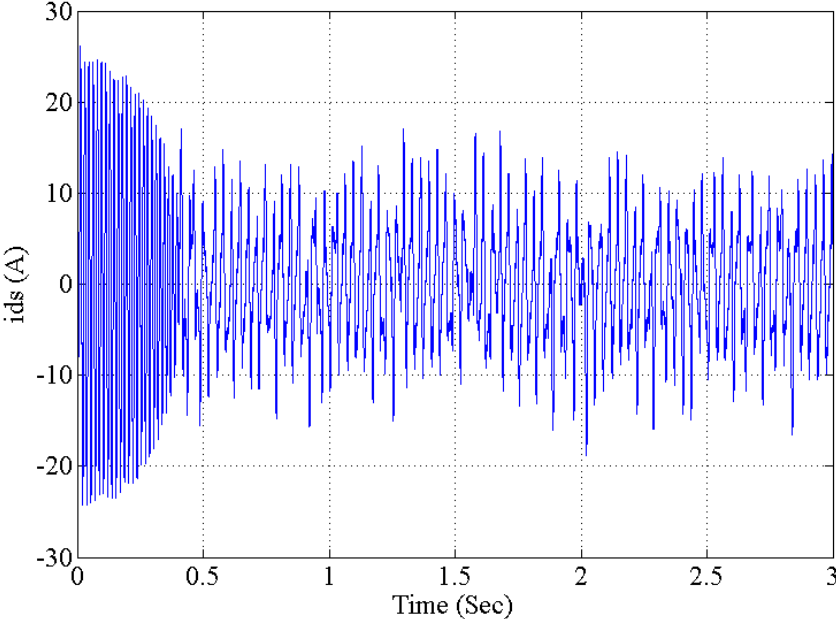


(b)

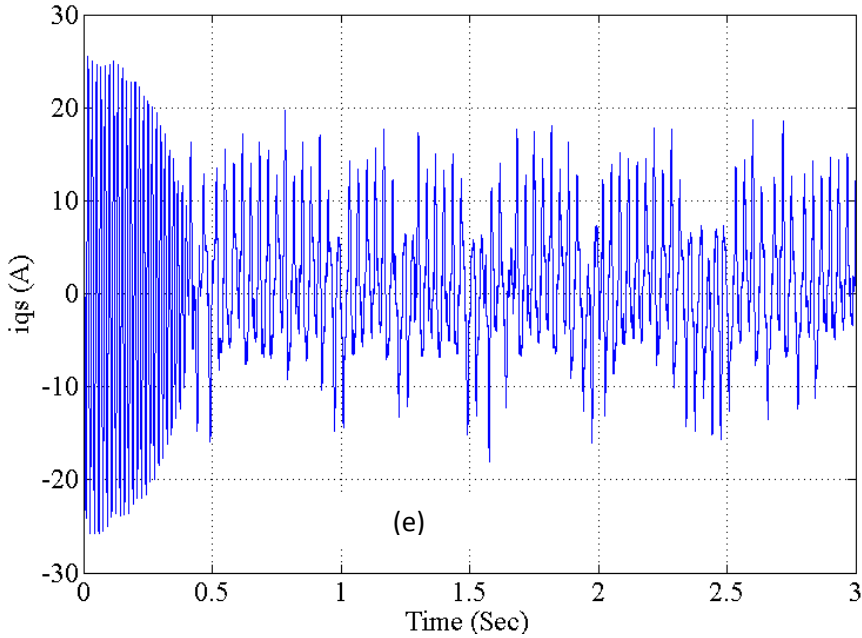


(c)

Figure (3-15) Continued.



(d)



(e)

(e)

Figure (3-15) Continued.

3.6 Indirect Vector Control of Dual IM Drive by Five Leg Inverter(FLI)

The control strategy of vector control for dual independent three phase induction motor drive fed by five leg inverter is shown in Fig. (3-16). The control strategy is based on two classical indirect field oriented vector. This achieved by oriented the flux on the d-axis in the d-q frame [66]. The control system consists of two machines (IM1 and IM2), voltage source FLI, IFOC 1 for motor1, IFOC 2 for motor2 and the double zero sequence modulation(DZS) as shown in Fig. (3-16). Where two speed controllers PI and four current controllers PI are using. In the IFOC of motor1 IM1, the flux component and torque component of the stator current is going through coordinated transformation to supply the voltage amplitude, phase, and frequency. The speed demand is given as the speed reference ω_{r1}^* or ω_{r2}^* for motor M1 and motorM2, respectively. The speed demands are compared with the actual rotor speeds ω_{r1} and ω_{r2} , the deviation is amplified in the speed control PI controller and the output of the speed controller serves as the reference input to the torque current loop. The reference torque current i_{qs1}^* is compared with the actual torque current component, i_{qs1} and result of the error is processed to generating the reference voltage torque component V_{qs1}^* . On the other hand, the current flux component, i_{ds1}^* which was earlier set to a constant value is compared with the actual values of the d axis- stator current of motor i_{ds1} . The error signal is applied to the PI controller to generate the command values of the flux voltage component, V_{ds1}^* . The inverse Park transformation reference is using to transform the reference voltage to the stationary reference frame ($\alpha\beta$ frame) coordinate. A similar principle is applied to the IFOC of IM2. Both signals after that synthesized using the DZS modulation to control the voltage supply required for the motors [59,71].

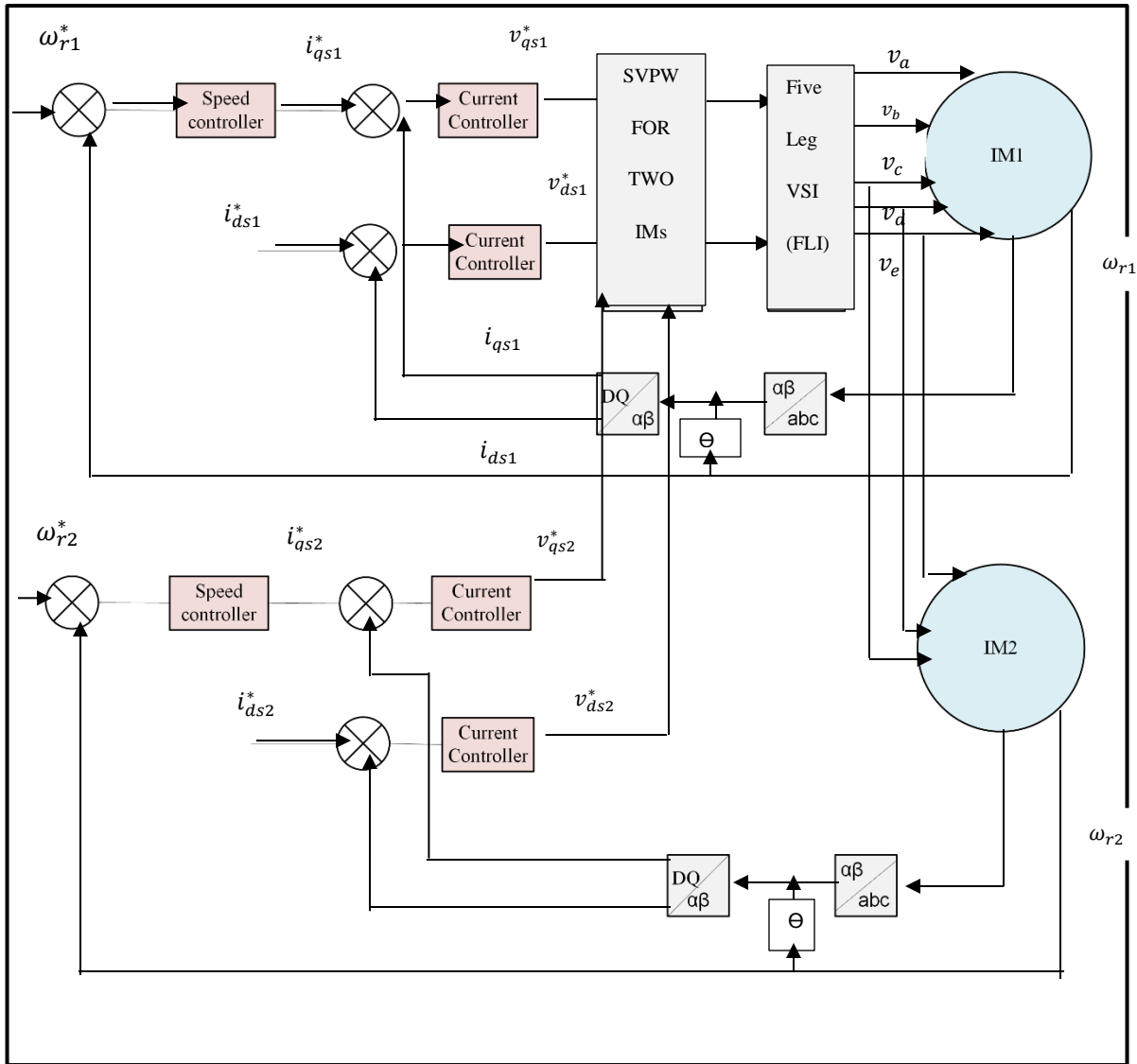


Figure (3-16) Block diagram of dual IM fed by SVPWM FLI.

3.7 Simulink model of the IFOC for Dual IM

Figure (3-17) shows the simulation of IFOC method of dual IM using Matlab/Simulink program. The configuration of dual IMs feed SVPWM FLI with its control circuit shown in Fig. (3-18). The Simulink model consist of two identical three phase induction motor both parameters are identical and listed in appendix A, two independent IFOC method for each motor using, single FLI which circuit

consist of five MOSFET modules (2-packs) and Dc bus voltage, will used one leg as the common leg, where this leg is shared by two motors leg C is chosen to share by two machines. Legs A and B of Inverter are connected to phases A1 and B1 directly, for machine 1. Legs D and E are connected to phases A2 and B2, respectively.

3.7.1 Simulink model of Two IFOC Method

Two independent vector control is used to control of two induction motor, each IFOC1 loop is independent on IFOC2 loop, where first to control the M1 and second control to M2. In IFOC1 loop using three PI controllers loop, rotor position loop, slip frequency loop and torque loop respectively. These PI controller loop is used conventional PI controllers, one for rotor speed of M1 compared between the reference speed and actual speed then the output of it produce the reference torque where will be the input to second PI current controller which error between stator current i_q and reference i_q^* product v_q^* and other PI current controller is error between i_d current of machine with the i_d^* to product v_d^* . v_q^* and v_d^* are the outputs of two PI controllers to the reference vector voltage of SVPWM1 modulator that used in DZS modulation of five leg inverter . The slip frequency(ω_{sl}) is determined according to equations (3-16) and Figs.(3-12). The rotor position (θ_{e1}) of M1 is calculated according to equation (3-16) and fig. (3-13). IFOC2 loop is same the principle of IFOC1 to control the M2. The inverse Park transformation is utilizing to transform to three stator current of M1($i_{as1}, i_{bs1}, i_{cs1}$).The gains (K_i and K_p) of PI controllers the same in two control for each machine and same in the case of one IM derived by SVPWM voltage source inverter.

3.7.2 Simulink model of Two IM fed by FLI

To achieve high performance independent control IFOC with two induction motor is used both identical and the same parameters, the mathematical module of IM is discussed in chapter two, the modulation of FLI is DZS which is better modulation, the two SVPWM modulators used to get the five signal to five leg inverter which fed M1 and M2 with leg shared between them. Figure (3-19) shows two identical IM fed by FLI.

3.8 Simulation Results of Two IFOC for Dual IM fed by FLI

The performance of control system for FLI VSI fed identical two IMs is tested by MATLAB/SIMULINK. The results show independent control for two motors. Both motors have same parameter and specification. The two motors operate at the reference speed, the motor1 is operate at no load. The performance of the system is obtained by two test. First test is shown in Fig. (3-20). The motor1 is operated at no load condition. Fig.(3-20a) shows the rotor speed of Motor1 which is stable with steady state at time 0.6 sec, while the motor2 operate at time the same time of motor1 and sudden load 2 N.m is applied at time 1.5 Sec, the rotor speed of motor2 is shown in Fig. (3-20b), the torque for both motors is shown at Figs. (3-20c) and (3-20d). Figures(3-20e) and (3-20f) are show the stator current of two motors. The next test illustrated in Figs. (3-21), the motor1 stay at no load and the motor2 is applied sequence load, full load, half load from full load and quarter load from full load. The two motors motor is driven at the reference speed. Figure(3-21a) shows the speed response of the motor1 at during no load and Fig. (3-21b) shows the speed of motor2. The developed torque during no load and load condition is shown in Figs. (3-21c) (3-21d). The direct current of stator component given in Figs.(3-21e) and (3-21f) respectively. From the results, it shown that the rotor speed of motor1 is steady state

with time 0.6sec and the rotor speed of motor2 is steady with time 0.4sec and noted when motor1 is run in no load and the motor2 is loaded the two motor are independent control. The independent control for two motors drive by FLI.

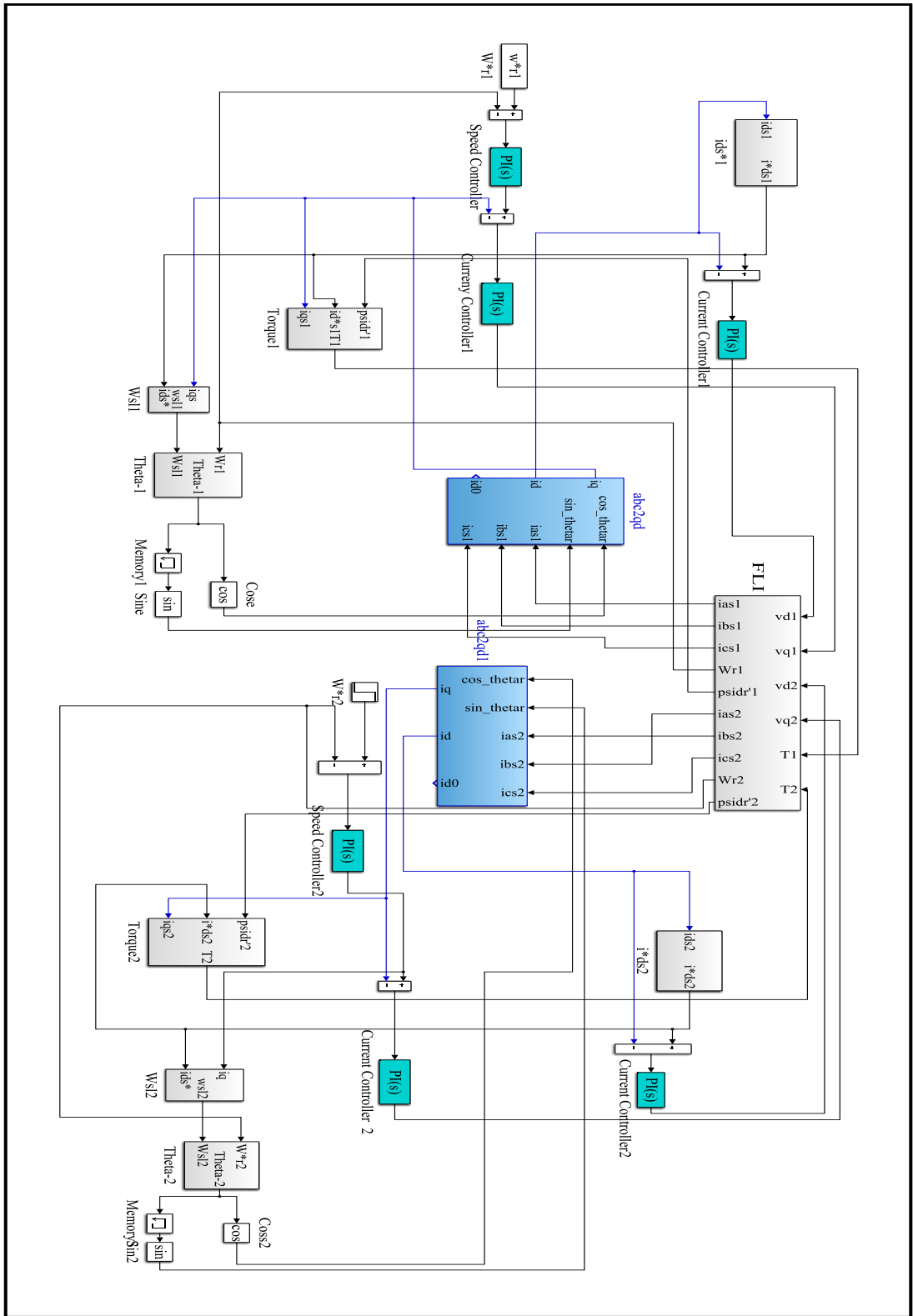


Figure (3-17) Simulink model of dual independent IFOC two IM.

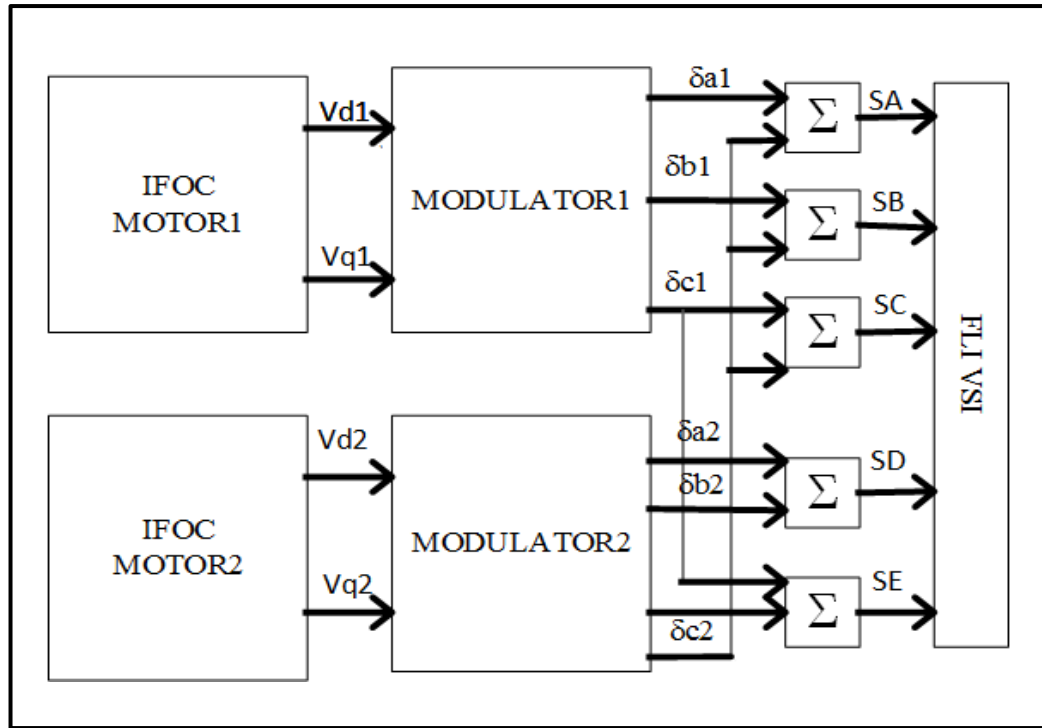


Figure (3-18) Two IFOC of two motors.

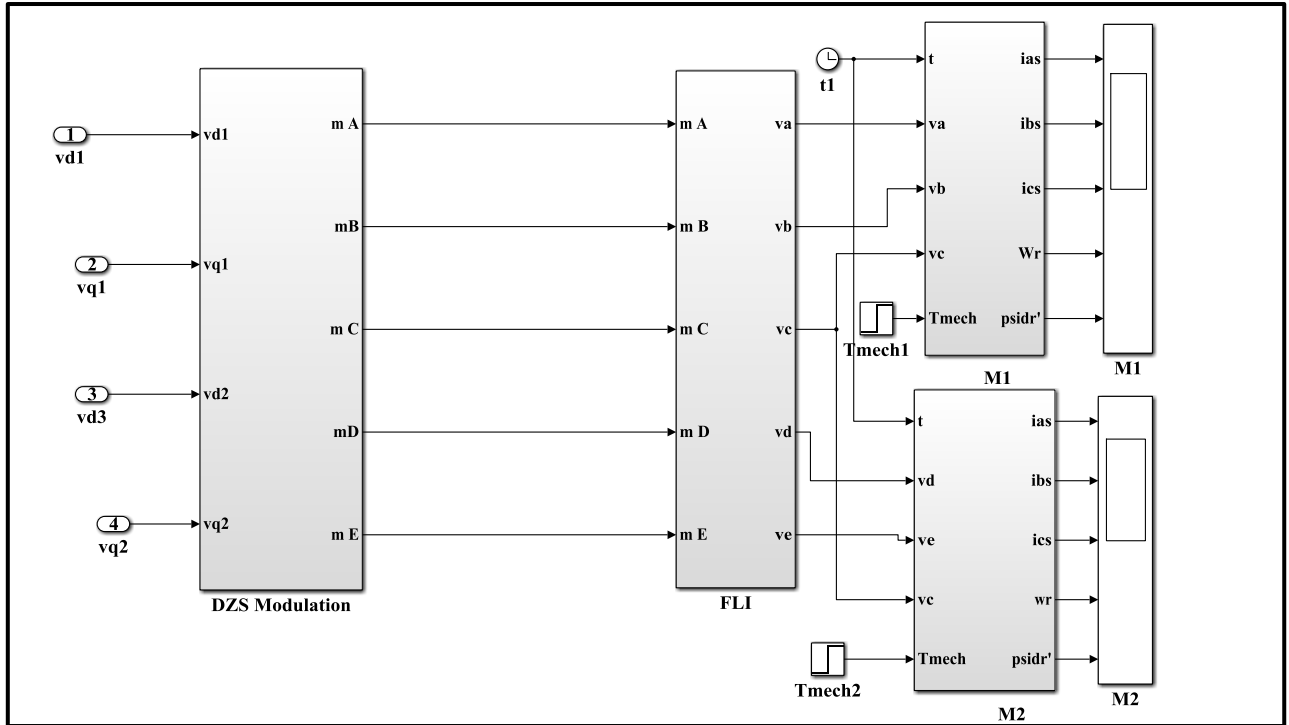
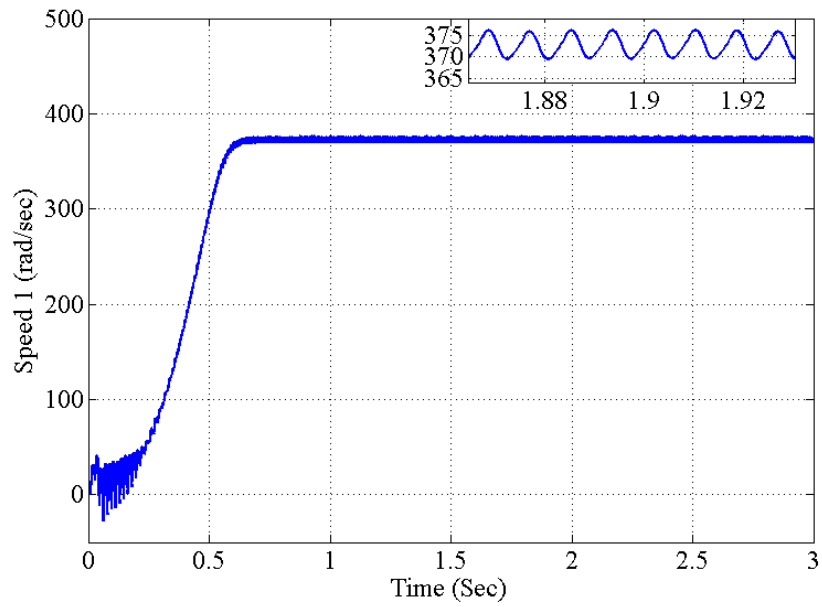
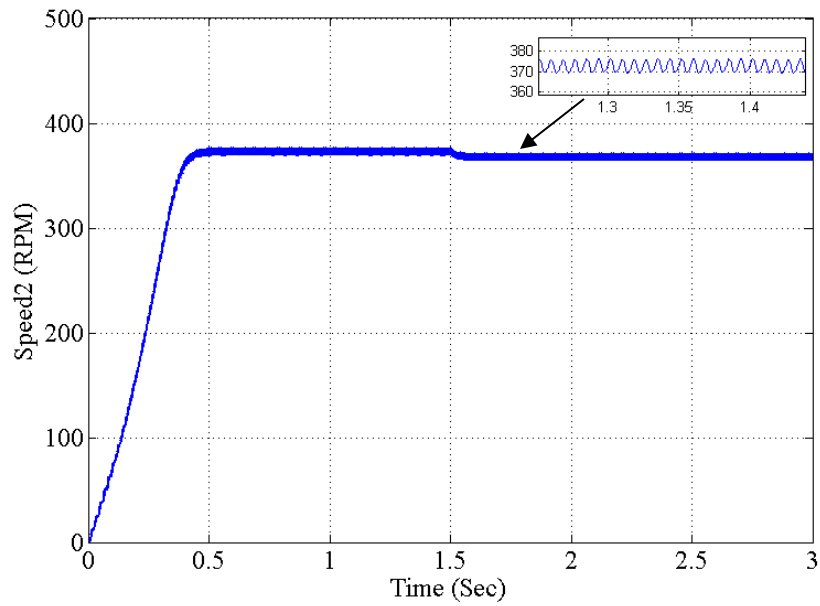


Figure (3-19) Simulink Model of two IMs fed by FLI.



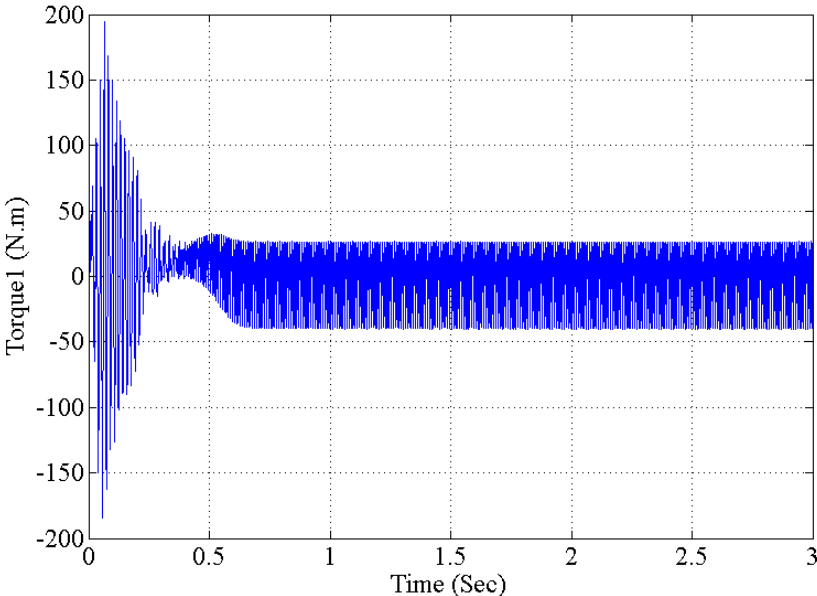
(a)



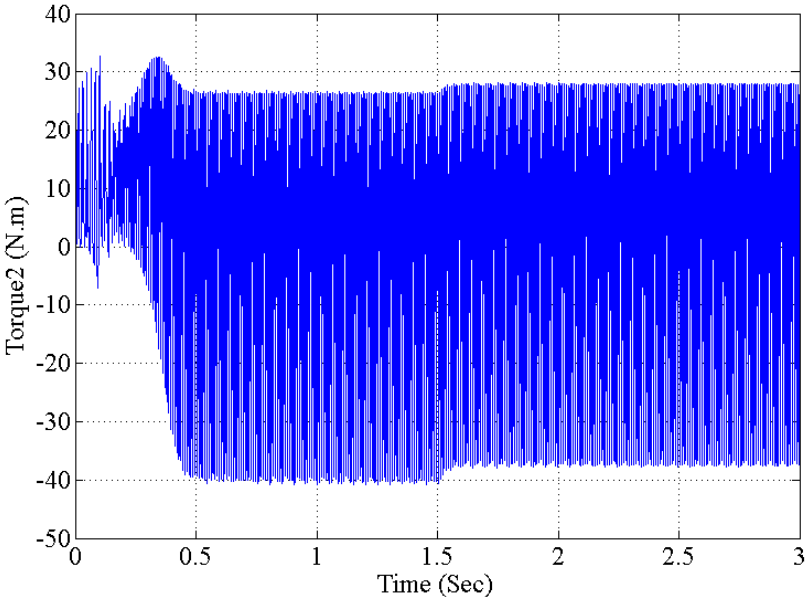
(b)

Figure (3-20) Dynamic Response of Dual IMs fed SVPWM FLI inverter

(a)Speed, of motor1 (b)Speed of motor2, (c)Torque of motor1, (d) Torque of motor2, (e) i_{qs1} , (f)
 i_{qs2}

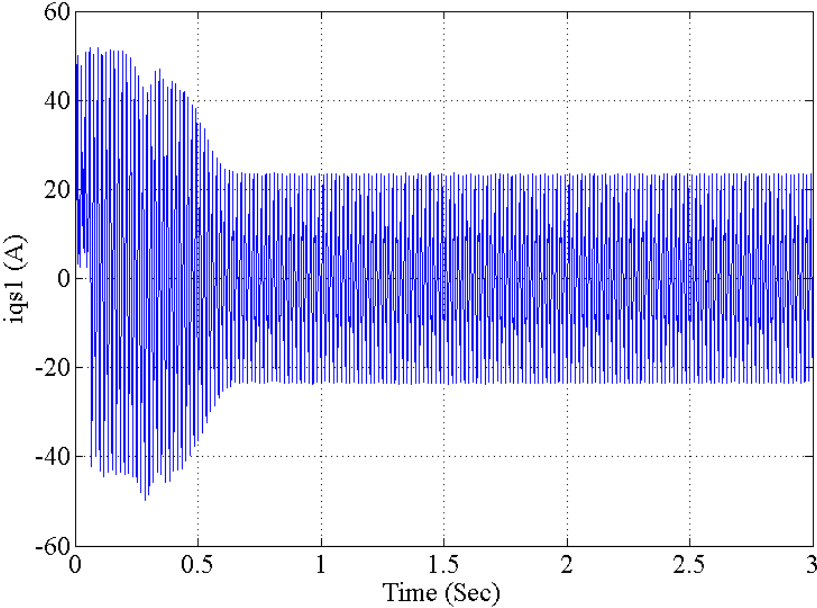


(c)

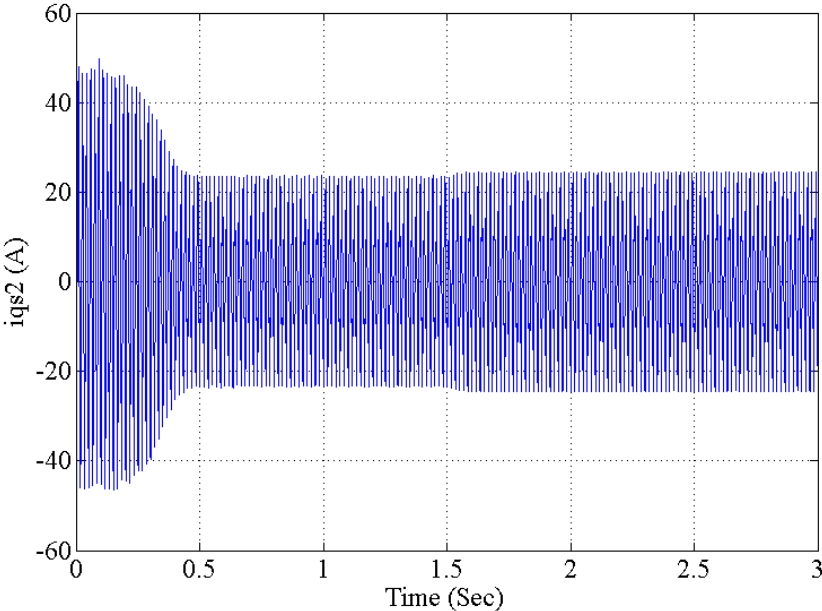


(d)

Figure. (3-20) continued.

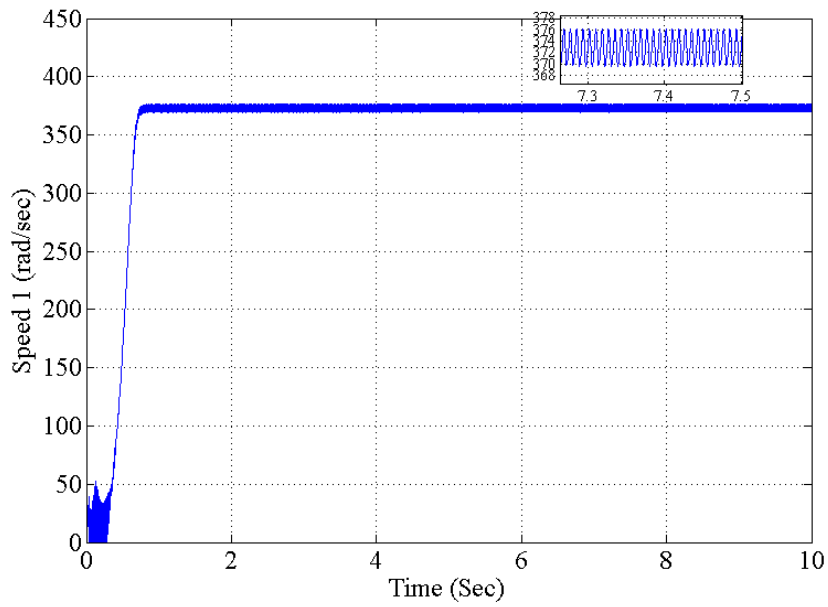


(e)

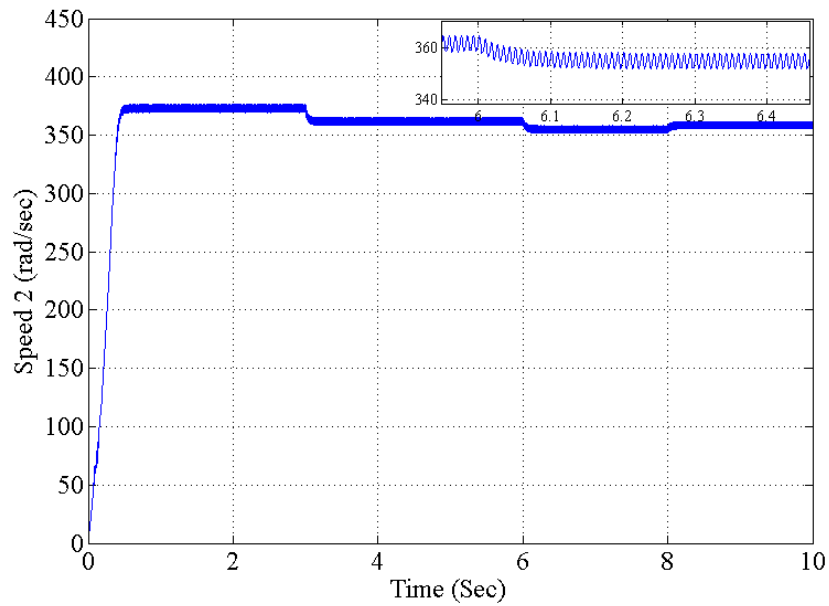


(f)

Figure. (3-20) continued.



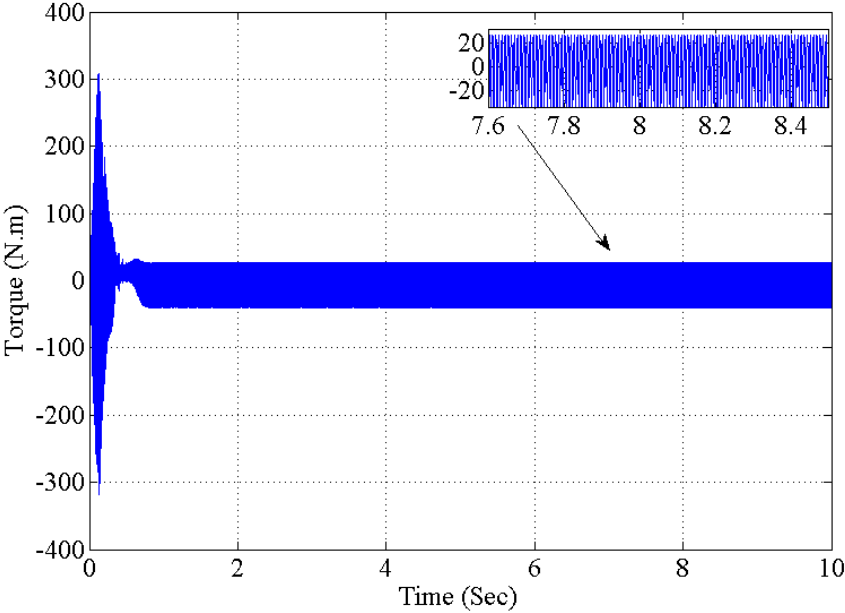
(a)



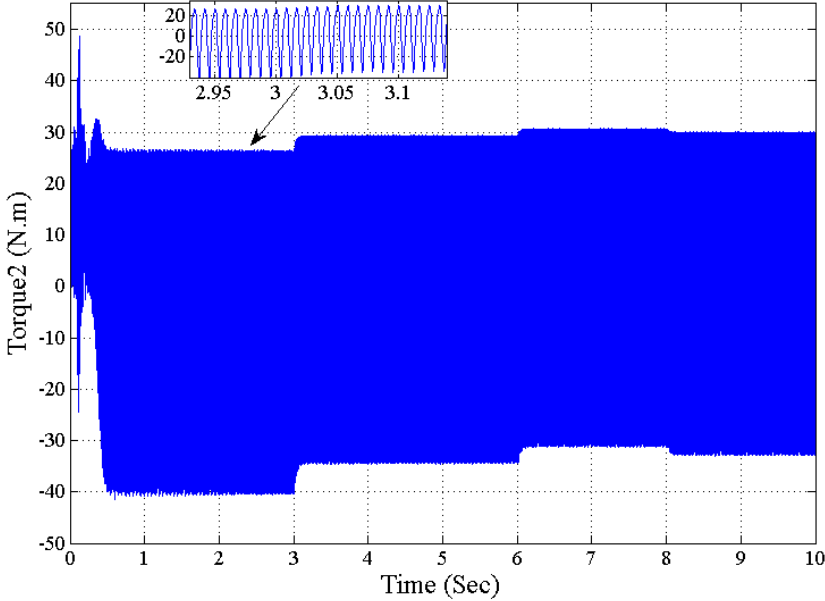
(b)

Figure (3-21) Dynamic Response of Dual IMs fed SVPWM FLI inverter at second test.

(a)Speed, of motor1 (b)Speed of motor2, (c)Torque of motor1, (d) Torque of motor2, (e) id_{s1} , (f)
 id_{s2}

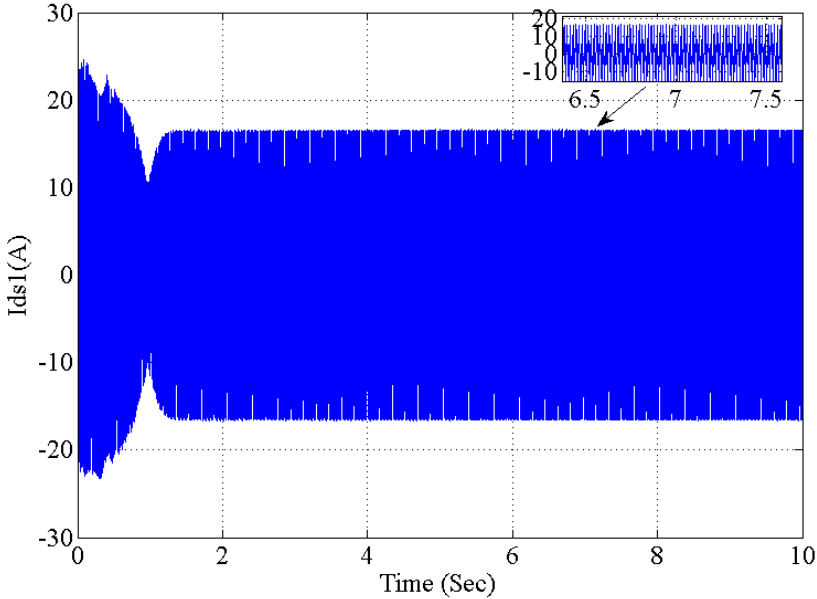


(c)

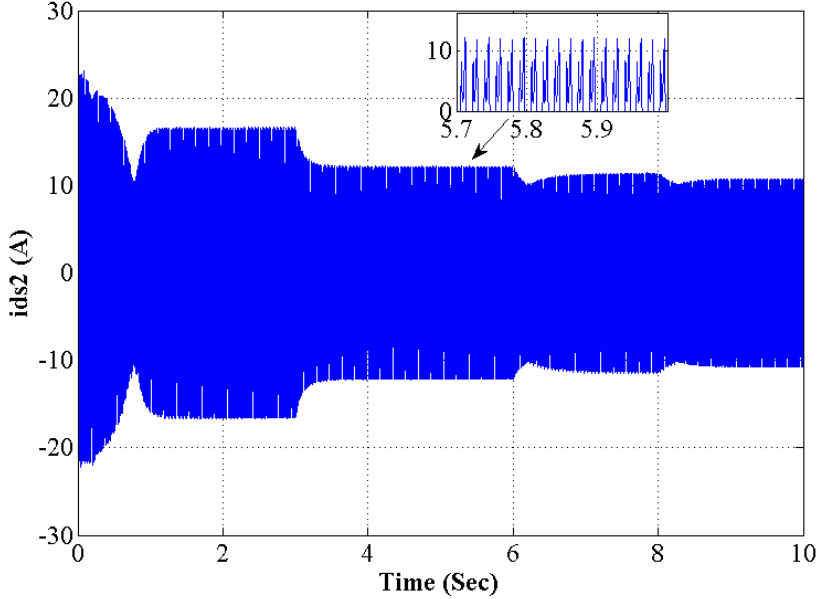


(d)

Figure (3-21) continued



(e)



(f)

Figure (3-21) continued

3.9 Particle Swarm Optimization (PSO)

Particle swarm optimization (PSO) is a population depend on computational technique inspired from the simulation of social attitude (social-psychological methods) fish schooling, bird flocking and swarm theory. Firstly PSO was designed and evolved by Eberhard and Kennedy [82]. TO thee powerful in solving problems exhibiting the non-linearity and the non-differentiability this theory had been made. The schema is developed from research on swarm such as bird flocking and fish schooling. Instead of utilizing the evolutionary processes such as crossover and mutation that have been used for algorithms manipulation, in the PSO algorithm none of these processes are used, the dynamics of the population simulates a "bird flocks" attitude, where sociably sharing of information takes the main part of work and individuals can profit for discovering and former experience of all the other escorts during the food searching process [83]. Each particle represents a perfect solution to the optimization problem. The best position visited by the particle has effect on the particle position it-self, so that i.e. the particle experience and the best particle position in the particle neighborhood (neighboring particles experience). When the neighborhood of a particle is the entire swarm, the best position in the neighborhood is referred to as the global best position of the particle and the resulting algorithm is referred to as the global best position PSO. Local best position (lbest) is called to any particle that gives the best quondam position (which give the minimum fitness value). The global best position (gbest) name is called to the best particle index of all particles in a population. Based on the optimization problem each particle performance can be measured by updating its corresponding's fitness function. The PSO algorithm is given according to flow chart which is shown in Fig. (3-22). [82].

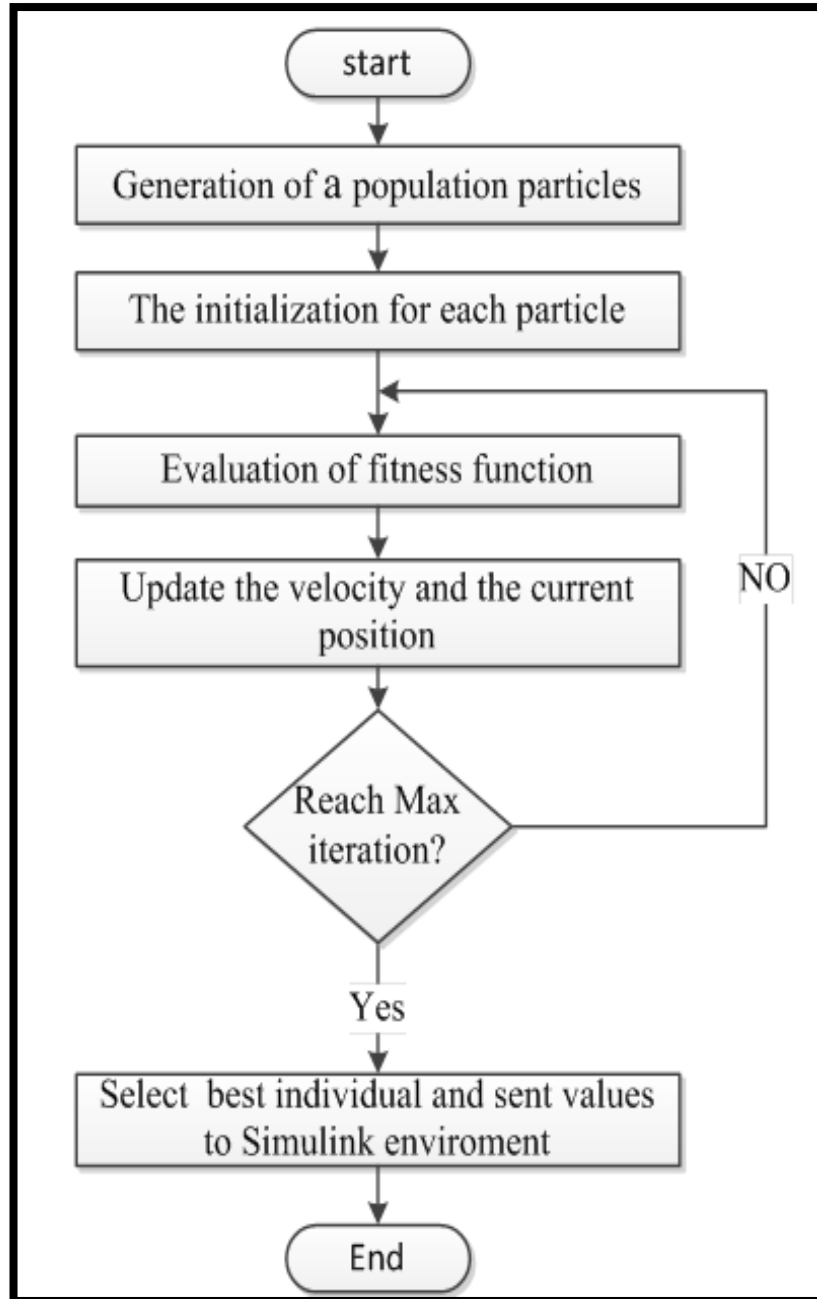


Figure (3-22) Flow Chart algorithm of PSO[82].

3.9.1 Simulation and results of PSO

The Simulink model of the motor based on IFOC by using PSO algorithm is obtained. The controller has been implemented as shown in Fig. (3-23). The results show that the PSO algorithm gives optimal value for the PI controller parameters and enhance the system performance, where the steady state time and smoothing with PSO is better with respect to PI controller. The PSO parameters is shown in Table (3-3). Figs (3-24a-b) show the motor speed and torque due to the PSO tuned parameters of the IFOC for motor fed by SVPWM VSI when the no. of birds is 50 bird and no. of iteration is 50 iterations. Figs.(3-25a-d) show the motor speed and torque due to the PSO tuned parameters of the IFOC of two IM fed by FLI. The results show independent control for two motors and the steady state time is better with respect to the PI controller in trial and error method.

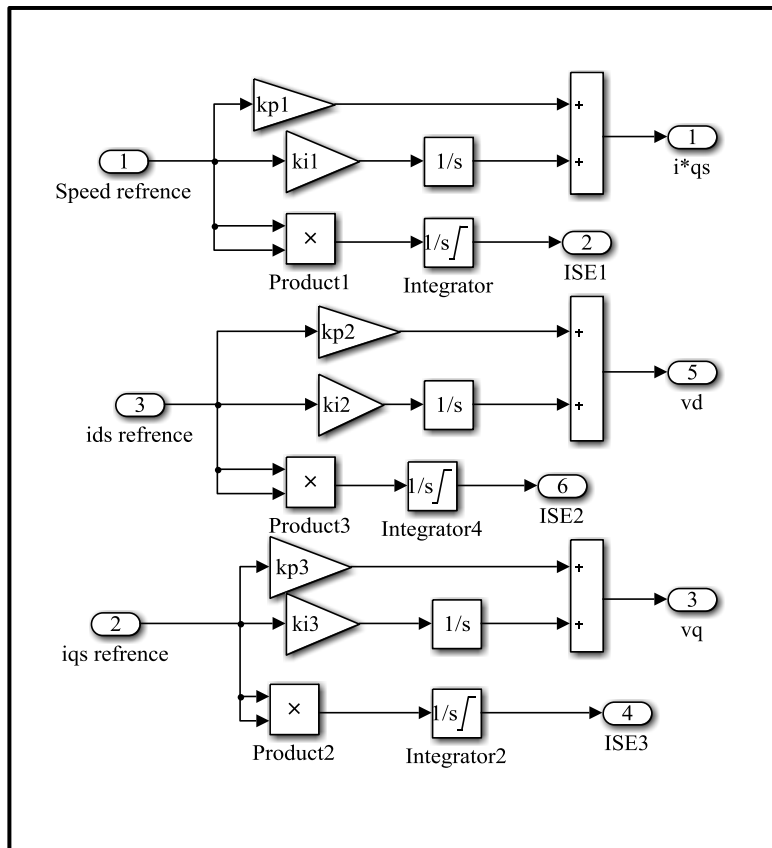
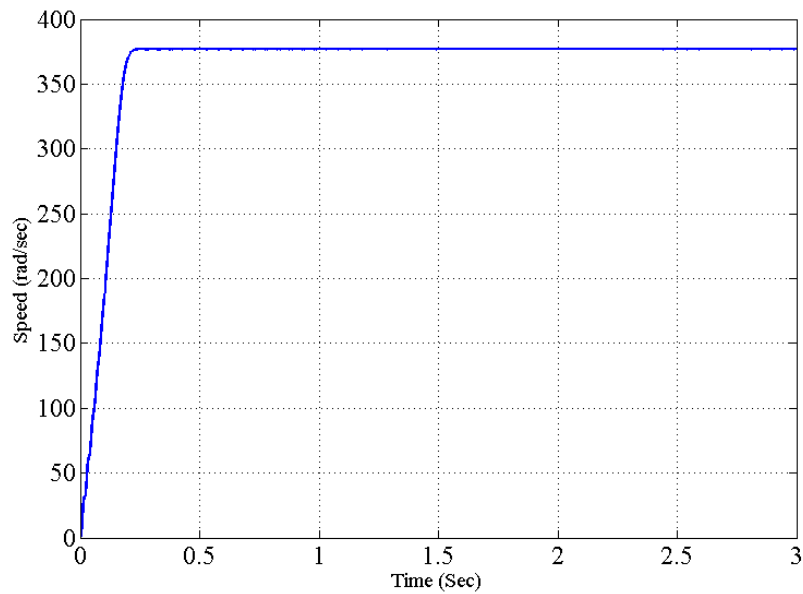


Figure (3-23) Simulink model for the PSO fitness function calculation.

Table (3-3): PSO parameter values

PSO Parameters	Value
Size of the swarm " no of birds "	200
Maximum iteration number	50
Dimension	6
PSO parameter c_1	1.2
PSO parameter c_2	1
Wmax	0.8
Wmin	0.2



(a)

Figure (3-24) Dynamic Response of IM fed SVPWM TLI inverter with PSO.

(a)Speed, of motor (b) Torque of motor.

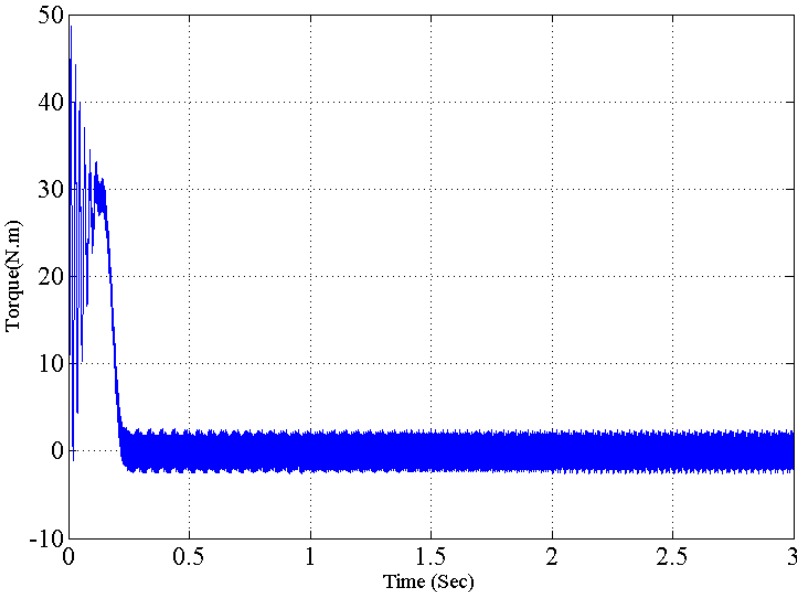
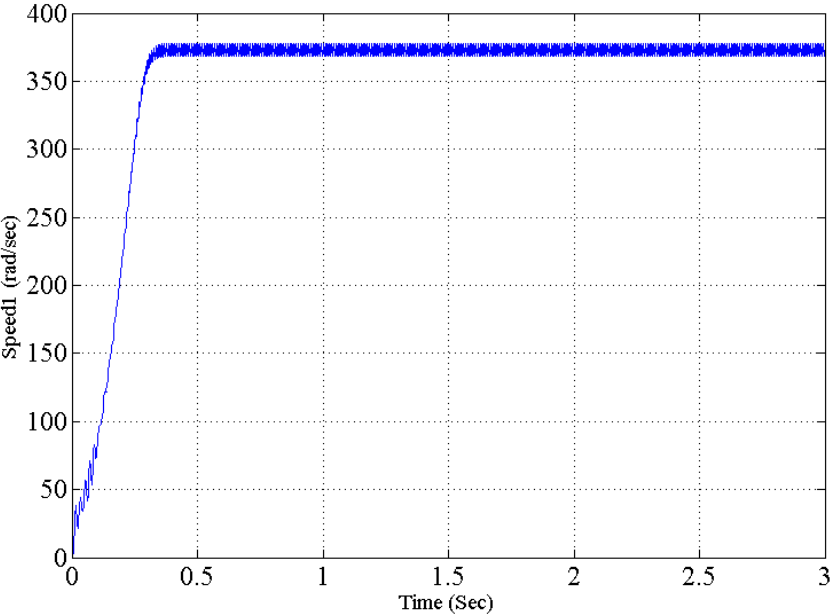


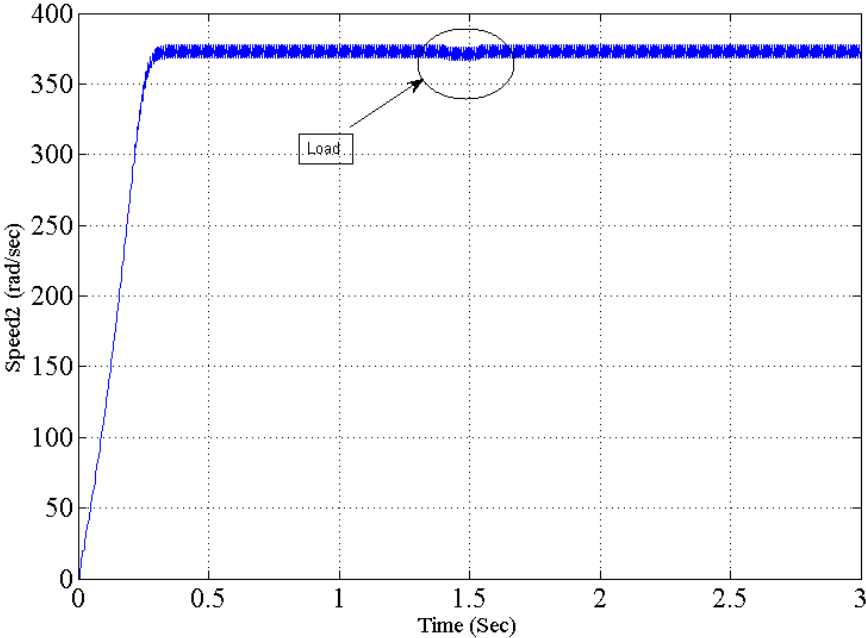
Figure (3-24) continued.



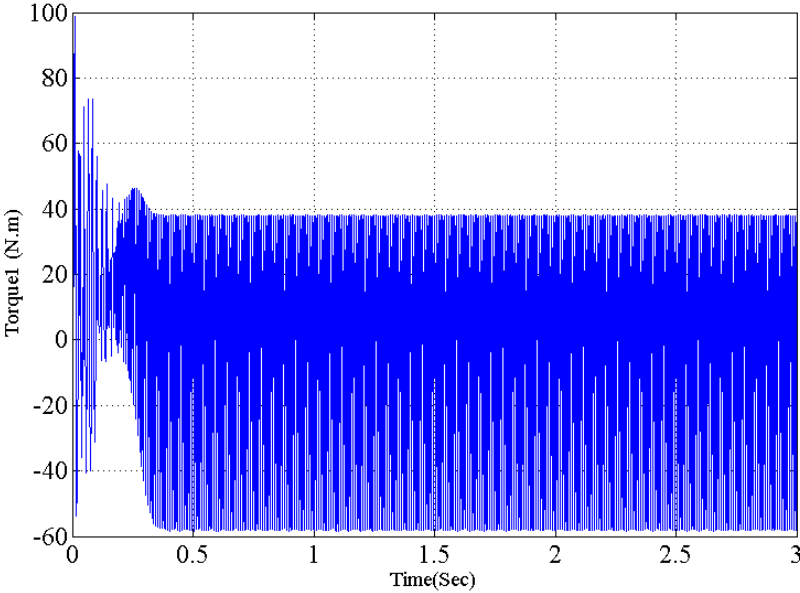
(a)

Figure (3-25) Dynamic Response of Two IMs fed SVPWM FLI inverter with PSO.

(a)Speed1, (b) Speed2, (c) Torque1, (d)Torque2.

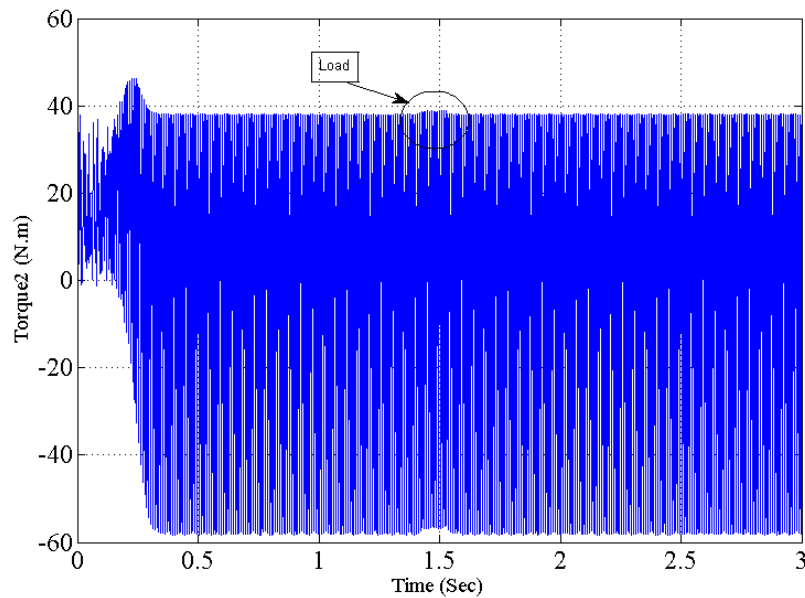


(b)



(c)

Figure (3-25) continued



(d)

Figure (3-25) continued

3.10 Conclusion

In this chapter two identical induction motors are controlled independently using IFOC method for both motors. At first section is studied the configuration of five leg inverter FLI and its modulation method by using space vector DZS modulation. The best performance is offered by the DZM method, which is also simple to implement. It enables each machine to fully utilize the available DC bus voltage. After that the three section is discussed performance of one IM modulated by SVPWM VSI and controlled by IFOC where used PI classical controller to study the performance both speed, torque and currents. The steady state time of torque and speed is suitable. The second section in this chapter discussed the performance of dual vector control used to know control applied to both IMs with same parameters. The dual motors are fed by FLI where DZS modulation is used to generate five signal of FLI. The Simulink model of the two IMs with its control circuit consist of, two pulse generators of the

standard three-phase inverter and two IFOC vector controls for both motors are used. The PSO in the final section is discussed where the comparison between it and PI controller give better performance. The simulated results show a robustness and stable of system, and prove that the topology of FLI is applicable to drive dual IM independently. The term independently refers to each motor that can be operated at different operating conditions such as different direction, speed and load torque. Here motor1 and motor2 work at different operation (here take with respect to load where one motor operates at no load and other motor at different load). It is showed that the five-leg VSI supplied two-motor drive is well suited to constant power applications, such as center-driven winders, where the motors are independently control.

Chapter Four

DUAL INDIRECT VECTOR CONTROL OF TWO IMs USING FUZZY LOGIC CONTROLLER (FLC)

4.1 Introduction

The extensively used of AC motor drives in industrial application are requiring high performance, the speed of motor should be close following the specified reference trajectory regardless to any disturbance of load, model uncertainties and parameter variations at high performance system. To achieve high performance, field-oriented vector control of IM drive is employed. However, the control design of such a system is playing a role in performance of system. The decoupling characteristics of vector-controlled IM are affected adversely on the parameter changes in the IM [31].

The speed control of IM is conventionally handled using fixed gain PID and PI controllers, these controllers are extremely sensitive to load disturbances and parameter variations. This controller parameter may to be continuously adapted and many control techniques is used to solve the problem. The design of the entire controller depends on the exact system mathematical model and from difficulty to develop an accurate mathematical model because of unavoidable parameter variations and unknown load variation [32].

The above problems can have solved by Fuzzy Logic Controller(FLC). The FLC can replace the conventional controller, it has some advantages such as more simplicity, stability in design, improvement the response in transient, and dose not demand mathematical model of system, it is based on linguistic rules within IF-THEN general structure, which is the basic of the human logic [84-85].

FLC allows a simpler and more robust control solution whose performance can only be matched by a classical controller with adaptive characteristics [86]. In this chapter the two stage discussed: one stage study the performance IM fed SVPWM three phase VSI utilizing IFOC fuzzy controller, and other stage study performance IFOC of dual IMs fed by FLI double zero sequence modulation is accomplished by a Mamdani type fuzzy controller. To obtain the better performance of motor with respect to setting time, over shoot, rise time from the classical controller PI which discussed in chapter three.

4.2 Fuzzy Logic Controller(FLC)

Ever after the implementation of the PI controller of off-line tuning is difficult according to variation of continuous parametric in the IM as well as the presenting of non-linearity in the entire system, it becomes of interest to go for intelligent controller. It is well-known that the resistances of stator and rotor of IM may be changed with the temperature up to 50% and the inductance of motor varies with the magnetic operating point. Further, the changing of the load torque due to mechanical disturbances is change [87].

This problem can be solved by several control techniques such as sliding mode control, model reference adaptive control, self-tuning PI controllers and variable structure control etc. Fuzzy logic bases intelligent controller is used instead of the conventional PI controller, this controller is achieved excellent control performance in the presence of drive non-linearity and parameter variation [33].

The fuzzy logic has the following advantages: (1) The linguistic, not numerical, variables make the process similar to the human think process. (2) It is related output to input, without all the variables are understanding, the design of system is permitting stable and more accurate than the conventional control system. (3) Simplicity allows

the solution of previously unsolved problems. (4) It is possible to rapid prototyping because, a system designer doesn't have to know everything about the system before starting work. (5) Robustness has been increased. (6) A great complexity is encompassing to few rules [87]. FLC provides a standing framework to achieve simple solutions and robust among different access of Intelligent computation. Fuzzy model is a combination of IF - THEN rules and variables having degree of membership from -1 to 1 with indistinguishable predicates that utilize a fuzzy interface such as Sagano and Mamdani models. When output of membership functions either constant or linear, Sagano type systems is using to model any inference system whereas if the output either linear or nonlinear, Mamdani type produces is used [35]. In general, FLC contains four main parts, Fig (4-1) explained the block diagram of structure of the FLC, and consist of four main parts [88]:

1. Fuzzification measures the values of input variable and converts input data into suitable linguistic values.
2. Knowledge base consist a database and provides necessary definitions, which are used to define linguistic control rules.
3. Fuzzy inference engine is the process that relates input fuzzy sets to output fuzzy sets using IF-THEN rules and fuzzy mechanism to derive reasonable output form crisp or fuzzy inputs. This rule base characterized the control goals and control policy of the domain experts by means of a set of linguistic control rules. Decision-making logic or inference mechanism is main part of a FLC. It has the capability of simulating human decision-making based on fuzzy concepts and of inferring fuzzy control actions employing fuzzy implication and the rules of inference in fuzzy logic.

4. Defuzzification is a scale mapping, which converts the range of values of output variables into corresponding universe of discourse and also yields a non-fuzzy control action from an inferred fuzzy control action

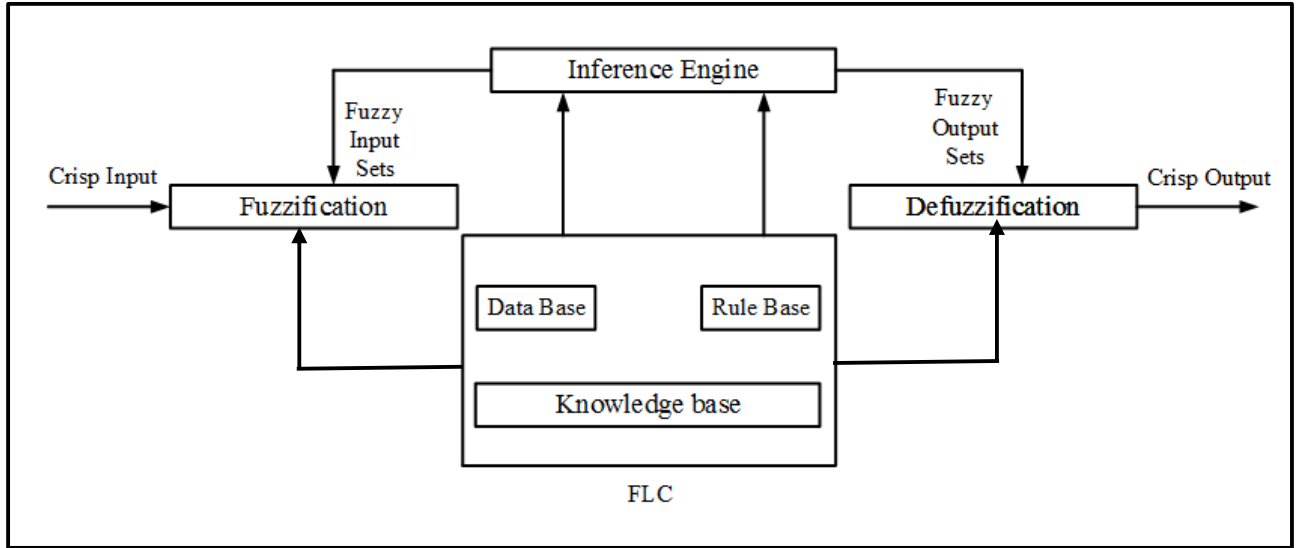


Figure (4-1) General Block Diagram of FLC.

4.3 Design and Principle of Fuzzy Logic Controller for IM Drive

In operation of drive, the speed can be controlled by controlling the torque indirectly, which is proportional directly to the current for the normal operating region. FLC has proven effective for complex, non-linear and imprecisely defined processes for which standard model based control techniques are impractical. Fuzzy Logic, unlike Boolean or crisp logic, deals with problems that have vagueness, uncertainty and use membership functions with values varying between -1 and 1 [89-90]. Figure (4-2) shows the fuzzy logic control of IM drive with IFOC method [91].

The performance of drive SVPWM is improved by employing one fuzzy logic controller. For the proposed FLC, the speed error (e) and rate of change of the speed error (ce) are considered as the input linguistic variables and the output linguistic

variable is considering as torque-producing current component [92,93]. Therefore, the functional relation of the FLC can be expressed as[85].

$$i_q(n) = \int \Delta i_q(n) = f(\Delta e(n), \Delta \omega_r(n)) \quad \dots (4-1)$$

Where

$\Delta e(n) = \Delta \omega_r(n) - \Delta \omega_r(n - 1)$ the change of speed error,

$\Delta \omega_r(n) = \omega_r^*(n) - \omega_r(n)$ the past sample of speed error,

$\Delta \omega_r(n - 1)$ the sample of speed error,

$\omega_r(n)$ the present sample of actual speed,

$\omega_r^*(n)$ the present sample of reference speed.

The main role of the control system is to path the command speed to provide the appropriate torque-producing current component i_q depending upon the operating conditions. In real time, the motor position information and output of the FLC, which is considered as the command q-axis current i_q^* as well as the command d -axis current , are used to get the command phase currents.

4.3.1 Implementation of FLC for IM

The implementation of FLC based speed controller of IFOC drive system is showing in Fig. (4-3). The FLC is observing the pattern of the speed error and the current error and correspondingly updates the output Δi_{dS}^* and Δi_{qS}^* . The advantage of utilizing fuzzy controller, it improves the performance of the IM, where no oscillations and overshoot occurs in flux and torque value, and the response of speed is faster and smother. The design and implementation of FLC does not required the mathematical modeling of the system and

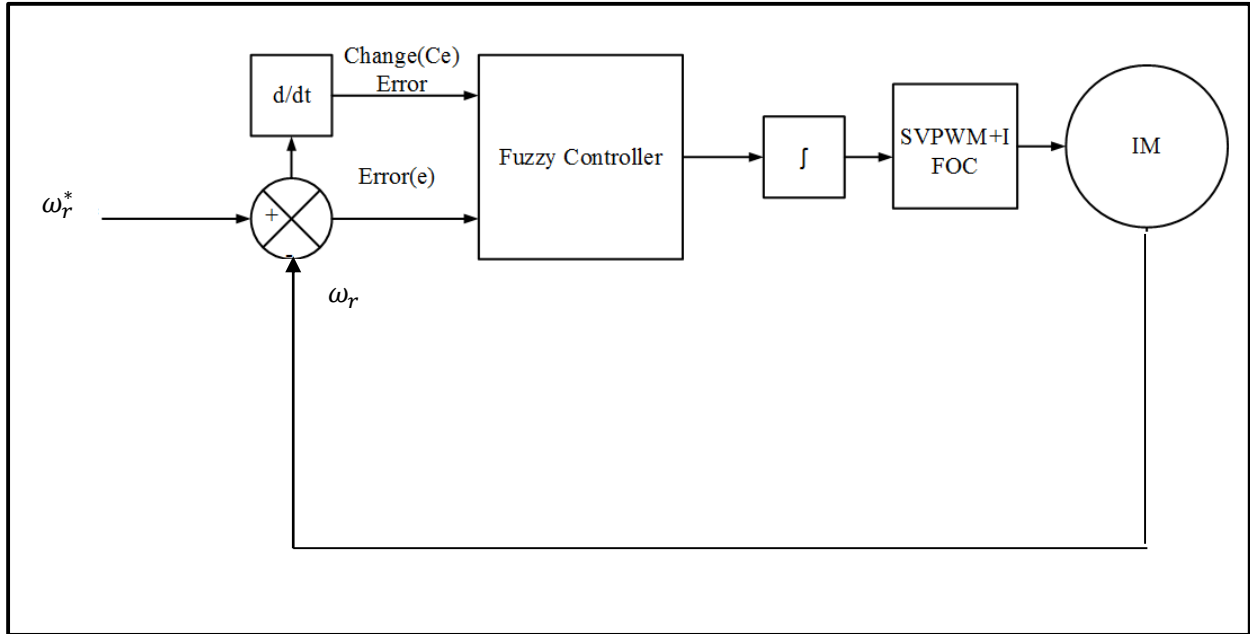


Figure (4-2) Fuzzy logic controller with IM derive.

obtains performance is robust even in the presence of the changing in unexpected load and variation of motor parameter [81]. The four stage of fuzzy logic controller FLC as following:

1.The fuzzification:

In this stage the crisp input variables are converted to fuzzy variables , two inputs and output are converted into linguistics variables Here the first input variable is the speed error 'e' and second input is the change of speed error 'ce' and the output variable i_q^* . The calculation of error and change in error is expressed as below.

$$e(t_s) = \omega_r^*(t_s) - \omega_r(t_s) \quad \dots (4-2)$$

$$ce(t_s) = e(t_s) - e(t_s - 1) \quad \dots (4-3)$$

where ω_r^* the reference speed of rotor.

ω_r the rotor speed.

After the linguistic labels of fuzzy sets of the fuzzification maps is selected as error, change of error and output. Membership function is choosing where was takes the triangular shape for both. The proposed controller uses following linguistic labels NB is Negative Big, NM is Negative Medium, NS is Negative Small, ZE is ZERO, PS is Positive Small, PM is Positive Medium, PB is Positive Big.

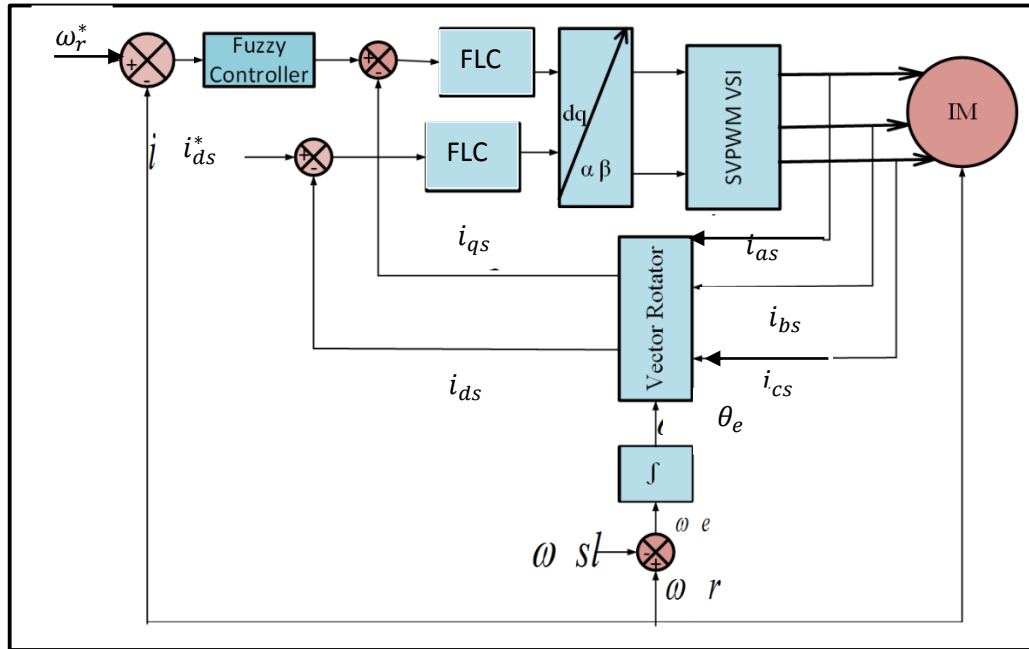


Figure (4-3) Fuzzy logic controller with IFOC of IM

2. The Knowledge base and inference stage:

Here the rules are representing as IF-THEN by giving the relationship between input (error and change of error) and output variables in expression of membership function where there are five member ships for both input and seven for output explained in Figs. (4-4) and (4-5). In this stage the input variables e and ce are processed by the inference mechanism that executes 5×5 rules shown in Table (4-1). Where will consider the first rule, as IF change in speed error is NB and change in speed is NB, THEN the output will be NB. Here for inference mechanism Mamdani algorithm is used.

3-Defuzzification:

After the inputs are processing by knowledge base and inferencing mechanism the defuzzification is the next stage, where the variables of fuzzy are converted into a crisp variable. In this stage will obtained the output fuzzy variable i_q^* . Here, the centroid method is used to determine the final fuzzy value i_q^* . The output function is expressed as[94]:

$$i_q^* = \frac{\sum_{k=1}^n i_{q(k)} \mu(i_{q(k)})}{\sum_{k=1}^n \mu(i_{q(k)})} \dots\dots (4-2)$$

Table (4-1) Fuzzy controller Rule Base [95].

Ce e	NB	NS	ZE	PS	PB
NB	NB	NB	NB	NM	ZE
NS	NB	NM	NS	ZE	PS
ZE	NB	NS	ZE	PS	PB
PS	NS	ZE	PS	PM	PB
PB	ZE	PM	PB	PM	PB

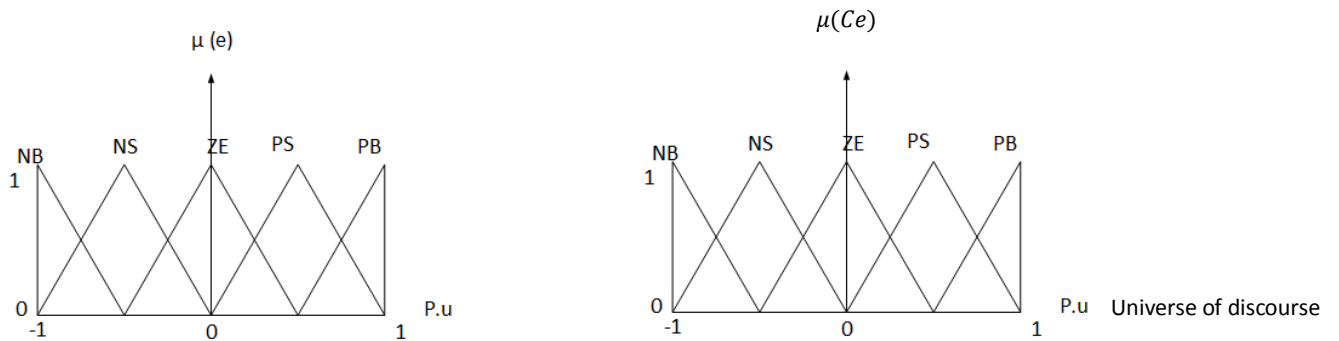
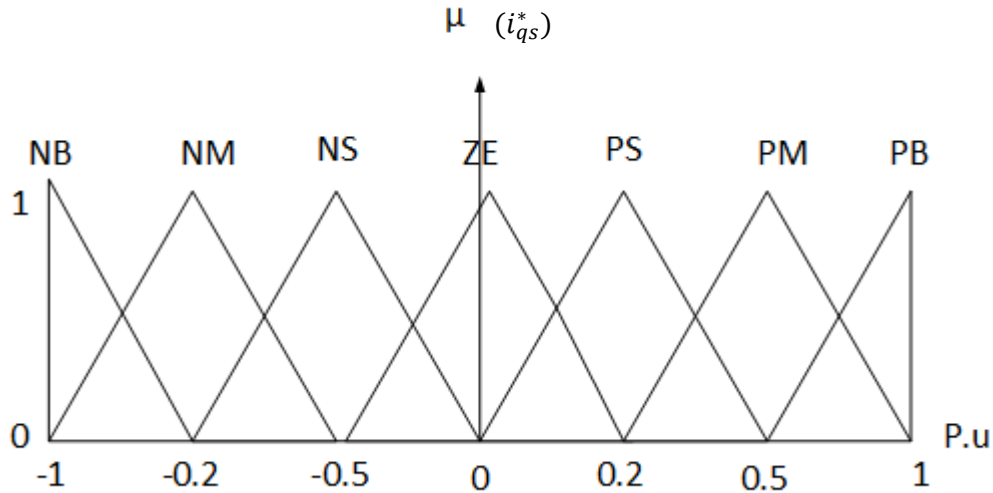


Figure (4-4) Membership for speed error and change of speed error

Figure (4-5) Membership for command current i_{qs}^*

4.4 Simulink Model of IFOC with FLC for Speed

Simulink Model of IM with its control circuit IFOC and FLC is shown in Fig (4-6). The speed PI Controller in Fig (3-12) in chapter three is replaced by FLC. The block of fuzzy controller with two inputs are error and change of error and one output is i_q^* , the error is determine by subtracted actual speed of rotor from reference speed. The FLC designed through the FIS editor.

4.4.1 Simulation Results of FLC

The proposed IM fed by SVPWM VSI with FLC is tested under no load operation condition using Matlab/Simulink software. Comparisons are made with the results previously obtained in chapter three. The results of motor testing at no load. The Fig. (4-7a) shows the rotor speed, where the rotor speed with FLC comes out to be almost smooth and no overshoot, and less steady state error compared with PI controller. Fig (4-7b) shows the mechanical torque for the motor. It can be seen that with FLC there is no overshoot in the torque and peak to peak ripple is less.

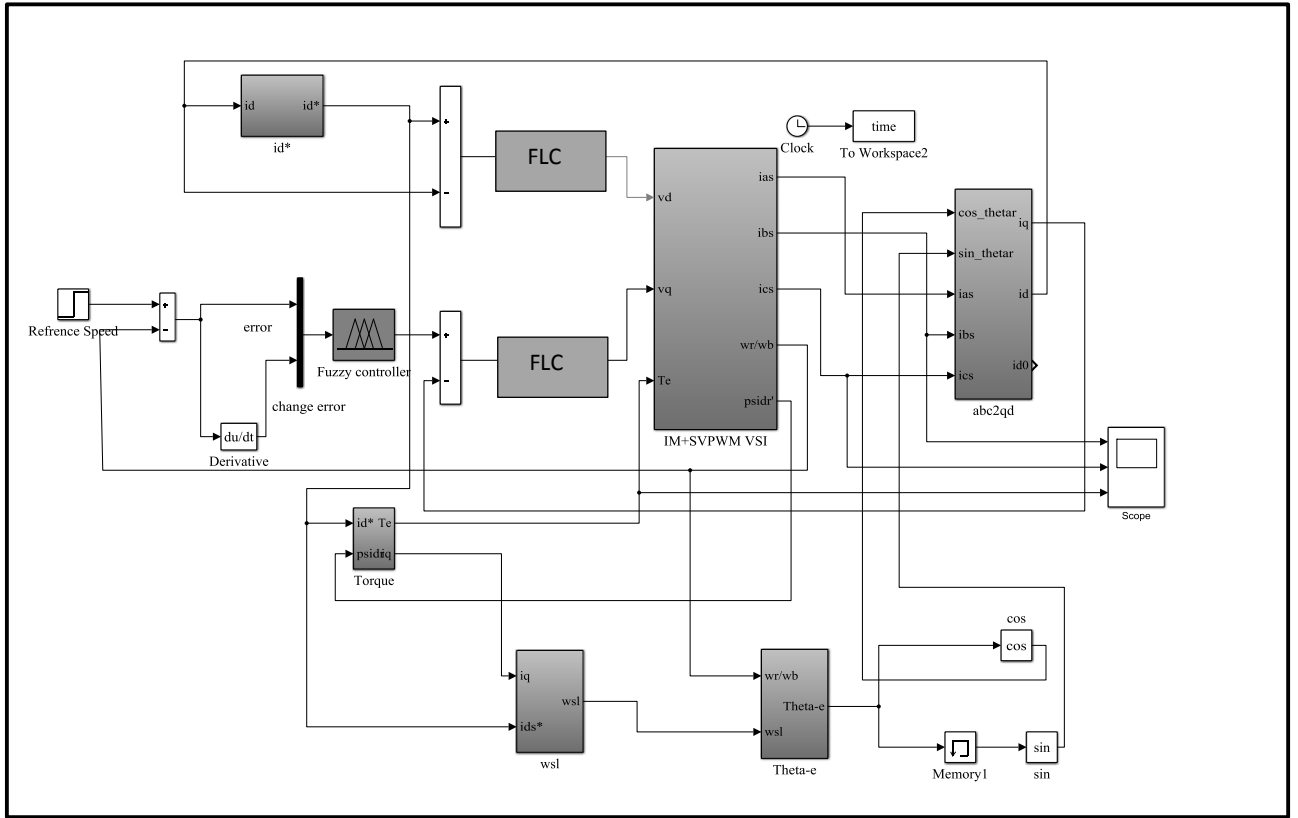
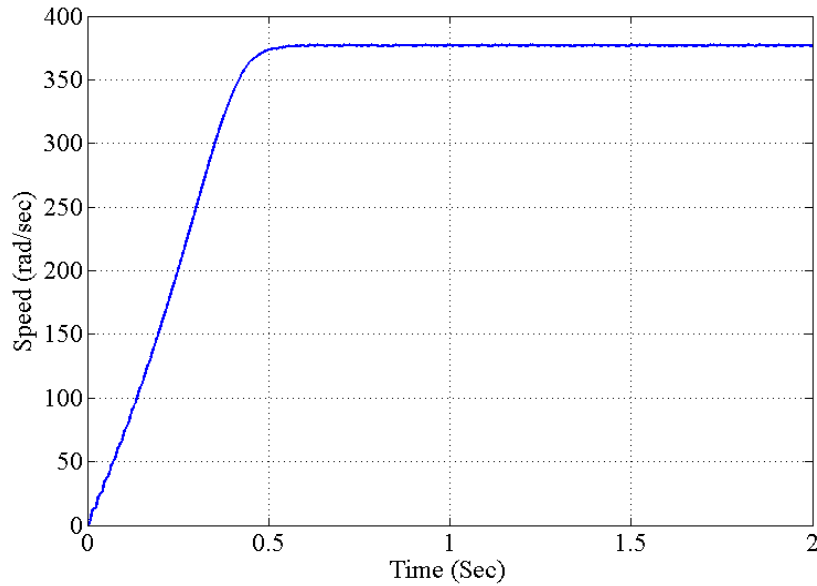
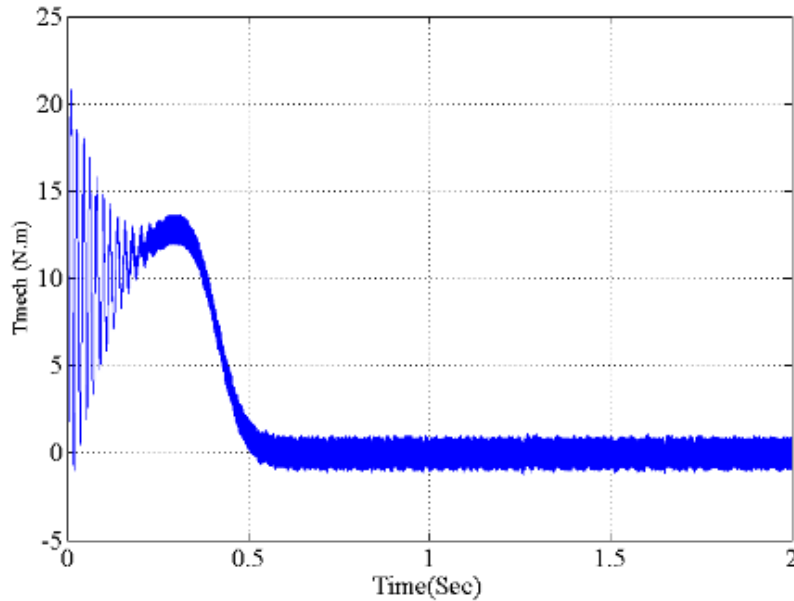


Figure (4-6) Simulink model of FLC based on IFOC.



(a)

Figure (4-7) Dynamic response of IFOC with FLC: (a) Speed ω_r , (b) Torque.



(b)

Figure (4-7) continued.

4.5 Simulink Model of IFOC with Three FLC

The proposed FLC-based vector control of IM is shown in Fig (4-8) by replacing all PI controller in Fig (3-12) in chapter three by FLC. Two FLC is used instead of PI controller of currents one for i_{qs} current to adjusted torque and other i_{ds} current to adjust flux. Also here there are five member functions (MFs) for inputs e and ce signals for both controller, these five MFs with overlap, and triangular shape are used for each input variables, and there are seven MFs for the output. The membership functions of linguistic variable are shown in Figs (4-4) and (4-5). All the MFs are symmetrical for positive and negative values of the variables. Depending on these input variable values, the output variable value is to be decided from the experience encoded in the form of rules. Table (4-1) shows the corresponding rule table for the speed and both current controller.

4.5.1 Simulation and Results of IFOC with Three FLC

To evaluate the dynamic performance of the IFOC shown in Fig.(4-8). The performances of control technique is implemented with a FLC to control of speed and currents of motor. The simulation tests for IFCO vector control of IM were carried out utilizing FLC. The speed responses under different operating conditions such as step change in reference speed or sudden change in load were observed. Fig. (4-9a) shows response of speed with FLC at no load, and, the performance of FLC is better with respect to steady state errors and ripple. Fig. (4-9b) shows the torque at no load. Figures (4-10a-d) shows the performance of machine with load 2N.m applied at time 1.5Sec. The load disturbance doesn't have any effect on speed response by using both controllers but FLC has better transient response. It is evident from the results that the fuzzy controller gives better responses in terms of overshoot, steady-state error and fast response.

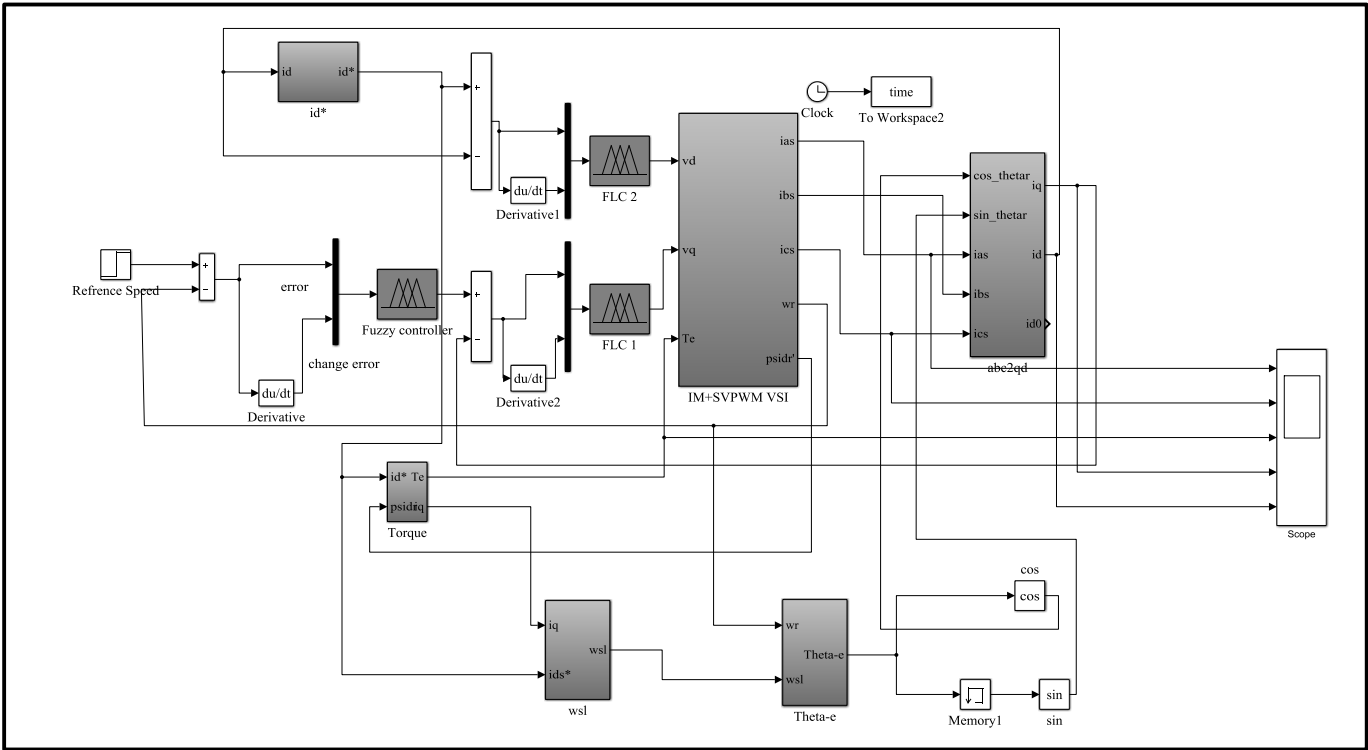
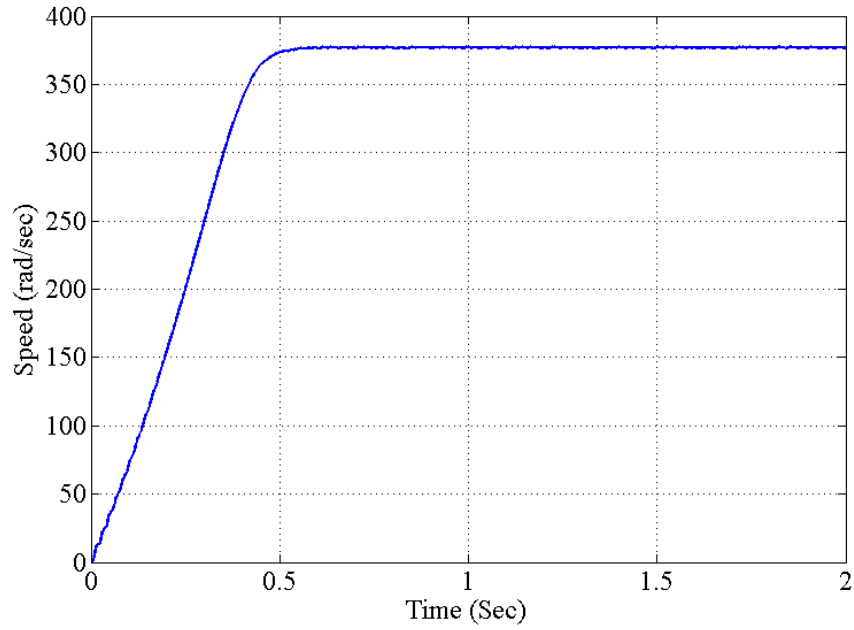
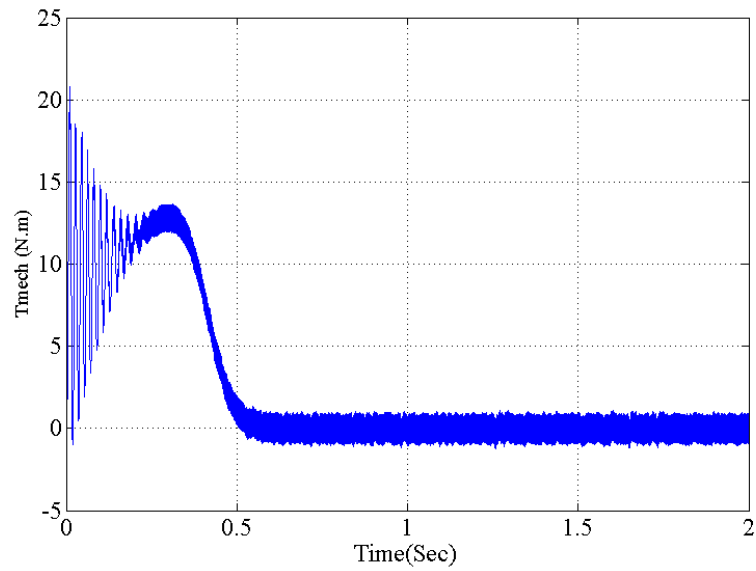


Figure (4-8) Simulink model IFOC with Three FLC.



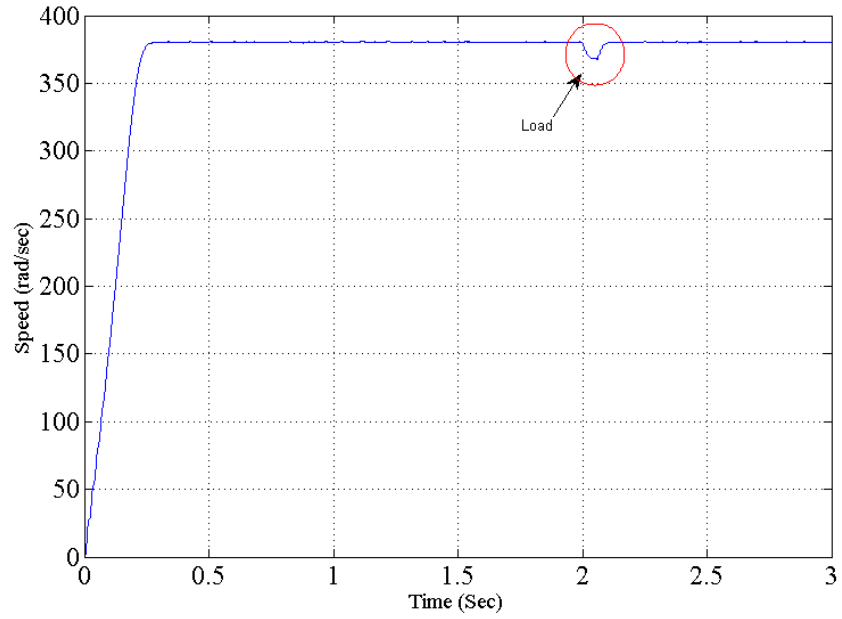
(a)

Figure(4-9) Dynamic Response of IFOC with FLC,(a)Speed,(b) Torque.



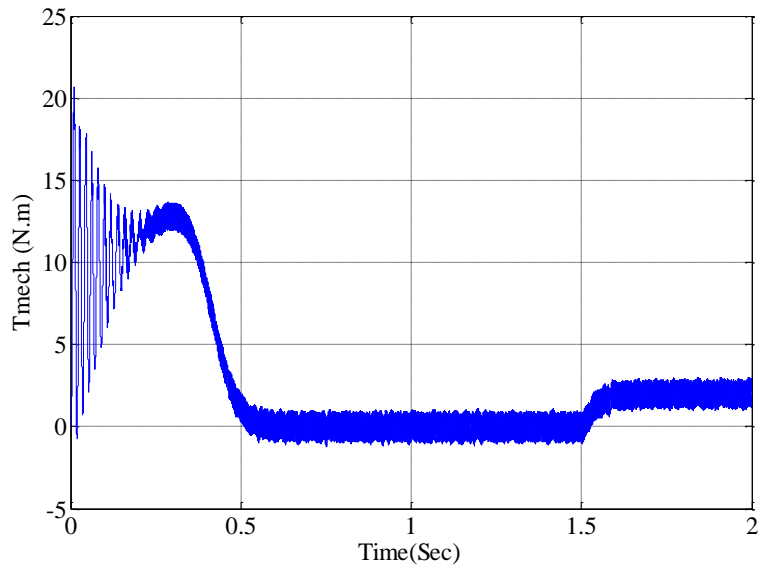
(b)

Figure (4-9) continued

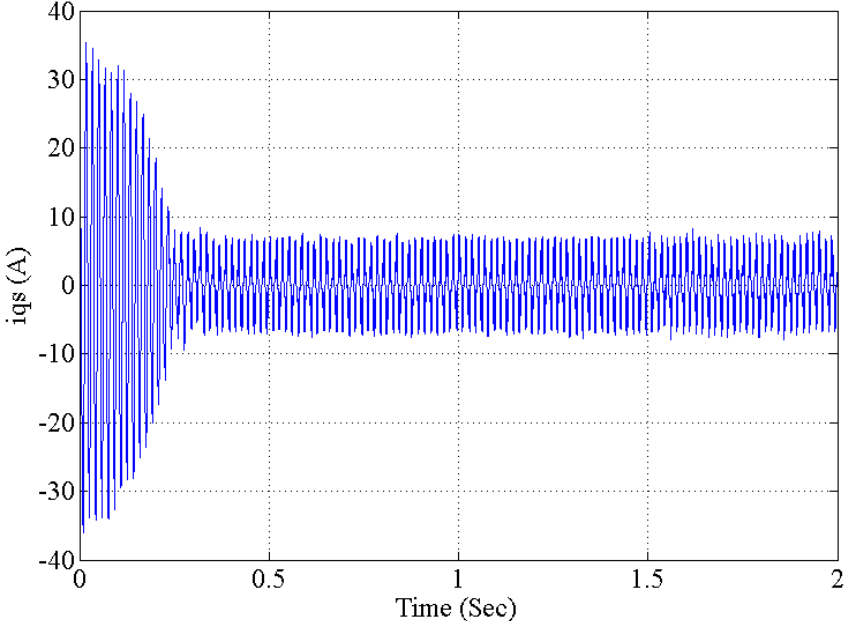


(a)

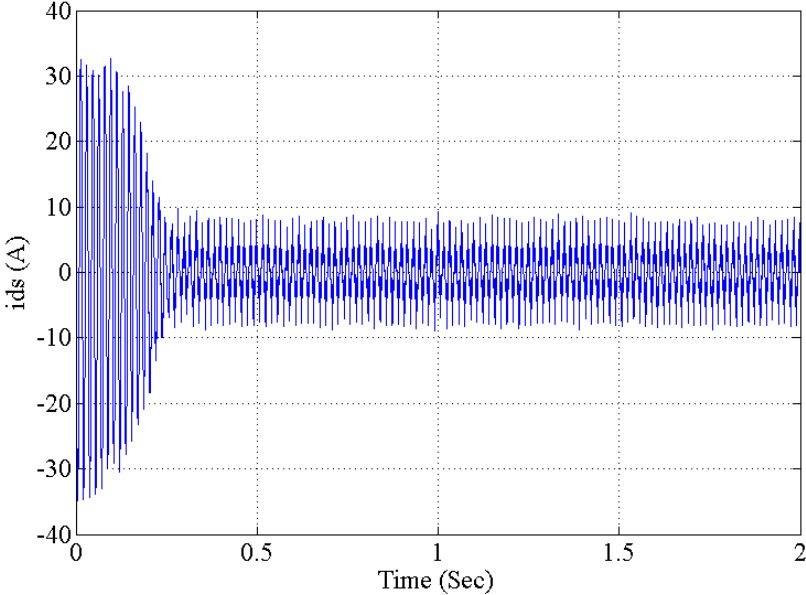
Figure (4-10) Dynamic response of IFOC with FLC at step load 2 N.m.(a)Speed, (b)Torque, (c) i_{qs} (d) i_{ds}



(b)



(c)



(d)

Figure (4-10) continued.

4.6. Fuzzy logic Controller of Two IMs fed by SVPWM FLI

The double IFOC for two IMs fed by FLI is explained in chapter three and now replaced PI speed controller of each motor with FLC. Figure (4-11) shows the block diagram of IFOC of two IMs fed SVPWM FLI implements FLC for the speed of dual motor. Here Mamdani algorithm is utilized as an inference strategy and for defuzzification, center of gravity is used. The FLC operation is depend on the same rules was using in one IM. The membership functions associated to the control variables have been chosen with triangular shapes as shown Figs. (4-4) for input variables and (4-5) for output. The universe of discourse of all the input and output variables are established as [-1, 1].

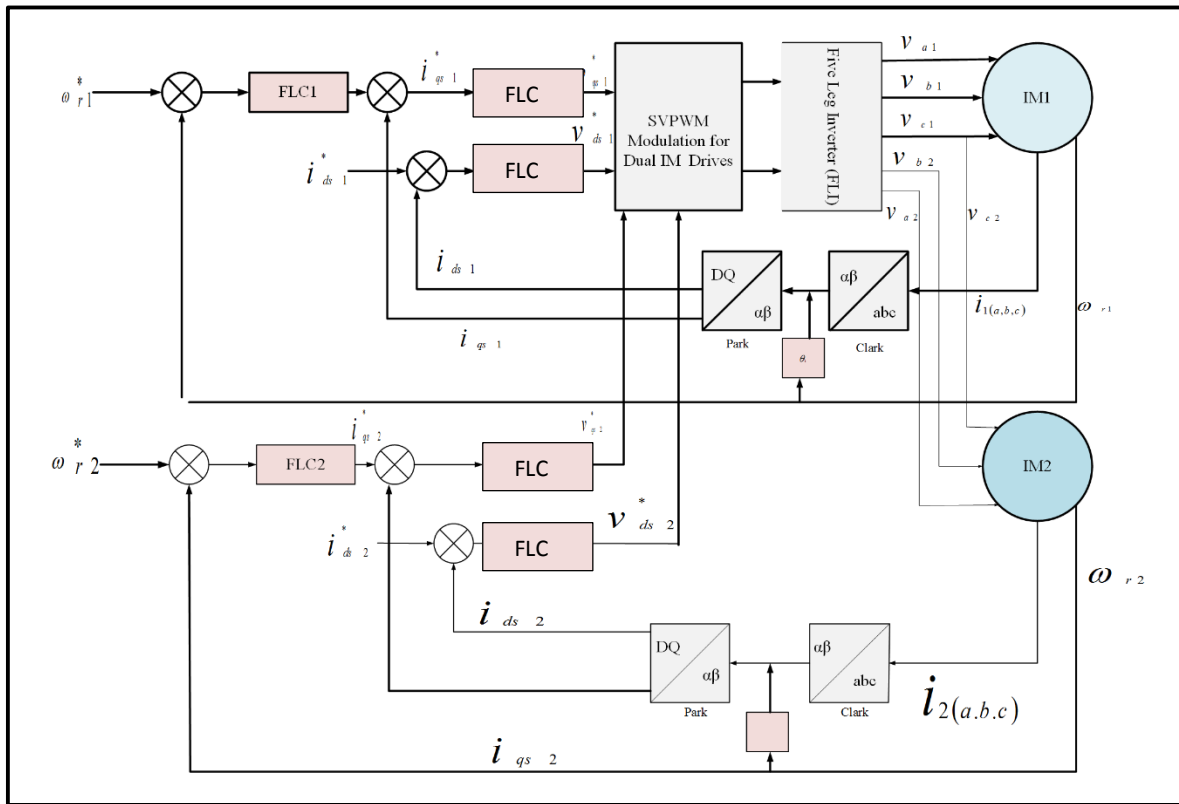


Figure (4-11) Block Diagram of IFOC of two IMs fed by SVPWM FLI implements FLC.

4.6.1 Simulation and Results

Simulation of two identical IM with FLC for each speed of motor is shown in Fig. (4-12). The performance of no load test is obtained for motor1 and motor2 with the same reference speed for both two speed FLC. The speed of motor1 and motor2 at no load shown in Figs (4-13a) and (4-13b). Torque for two motors (Torque1 and Torque2) also shown at Figs. (4-13c) and (4-13d). The next test is done where two motors are operating at the same time, one machine operates at no load condition, other machine is operating at same reference speed of motor1 and step load for full load 4N.m, half of the full load 2 N.m and 1N.m one fourth the full load. Figs. (4-14a) and (4-14b) shows the speed of motor1 and motor2 respectably. Figures (4-14c) and (4-14d) shows torque for both machines. Figures(4-14e), (4-14g) and (4-14f) show the direct and quadrature component of stator current. From the result is noticed when the motor2 is loaded, the motor1 no effected that mean the two motor independently control with FLC. Also the performance of two motors is better with respect to speed, torque and current in chapter three according to rise time and steady state. FLC is better from PI controller.

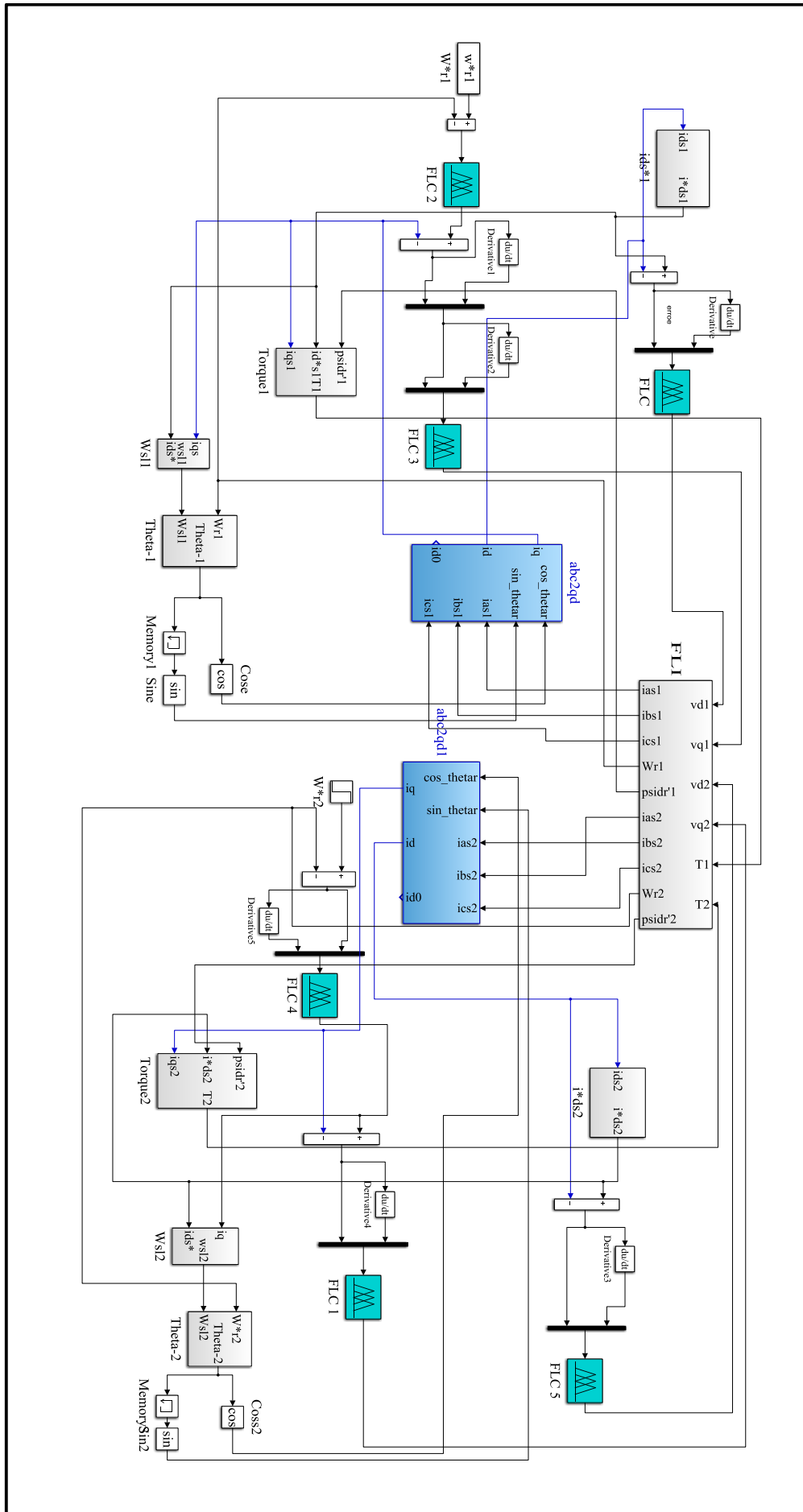
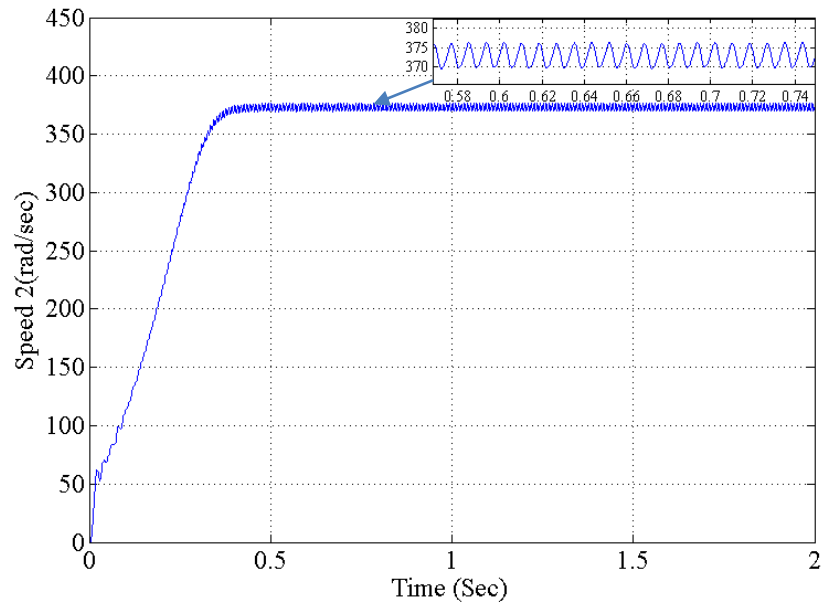
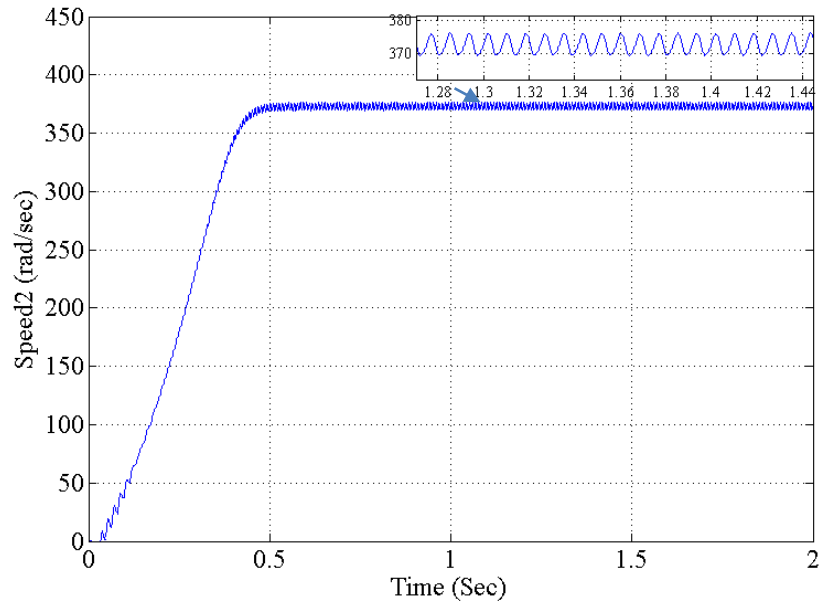


Figure (4-12) Simulink Model of FOC of two IMs fed by SVPWM FLI implements FLC.



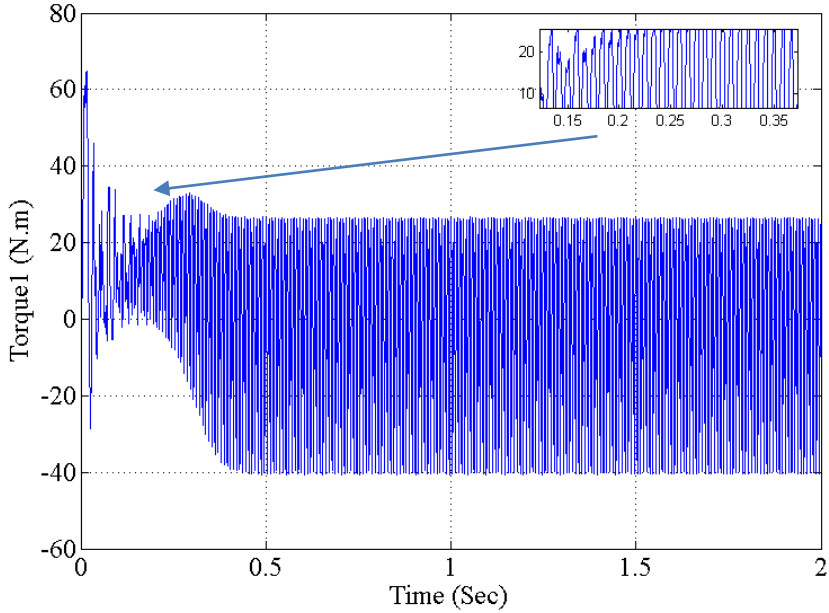
(a)



(b)

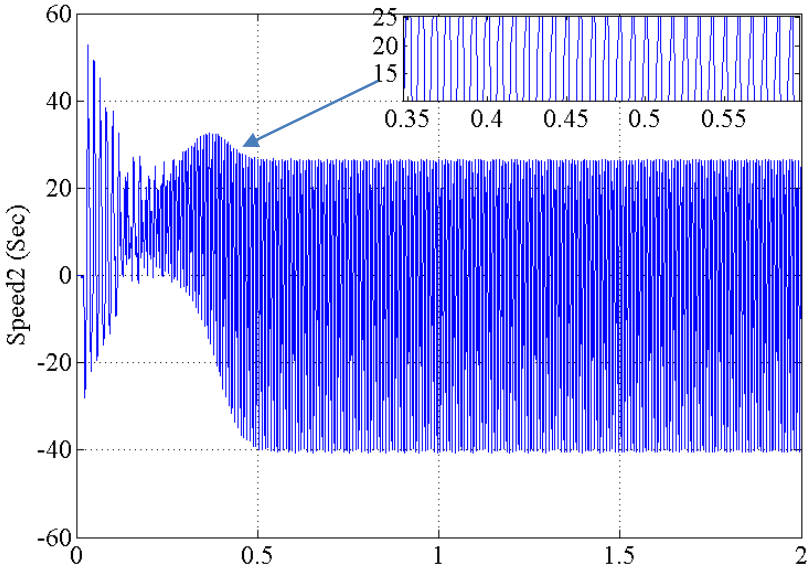
Figure (4-13) Dynamic response of IM1 and IM2 at no load with FLC

(a)Speed 1, (b) Speed 2, (c) Torque 1, (d) Torque2.



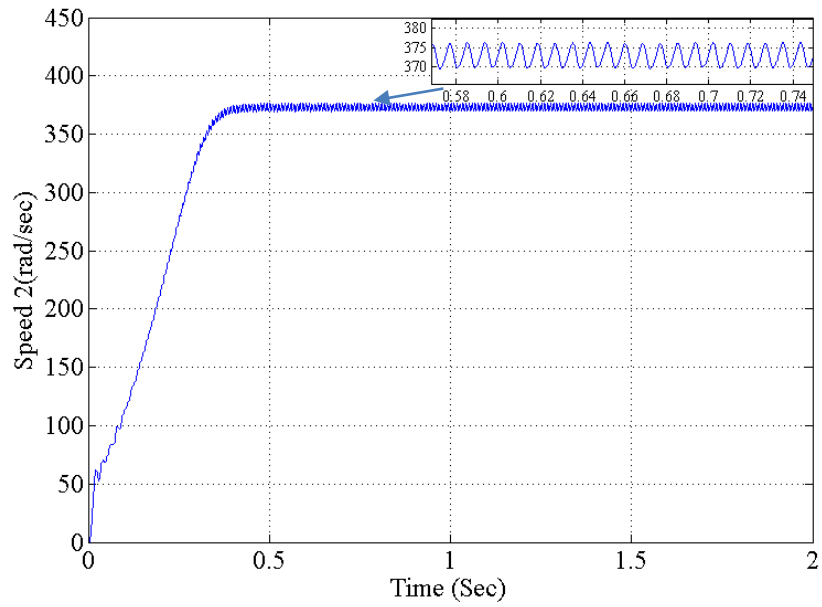
(c)

Figure (4-13) continued

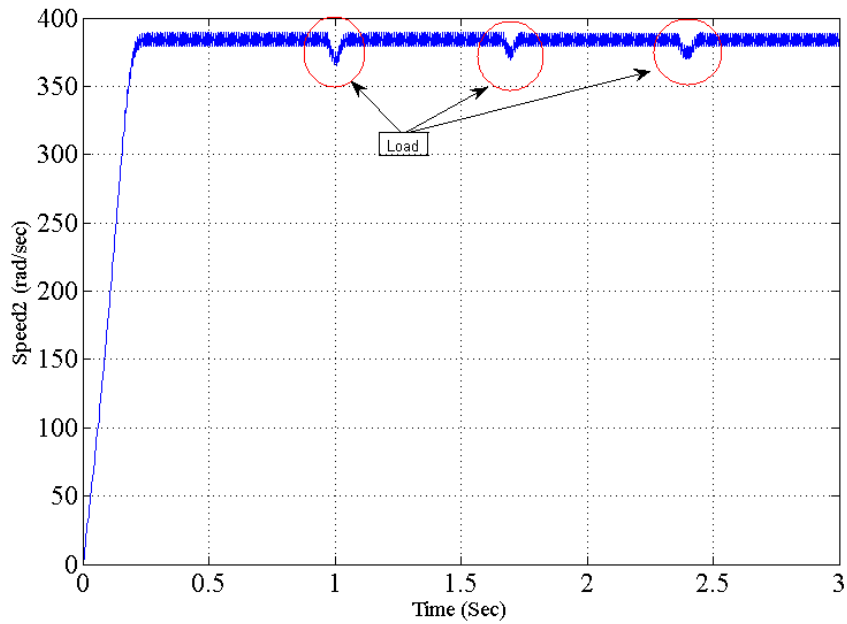


(d)

Figure (4-13) continued

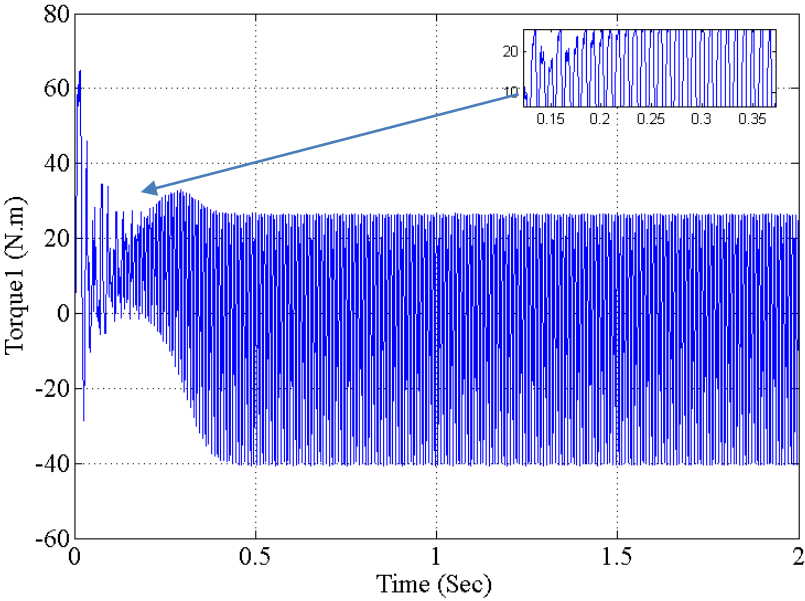


(a)

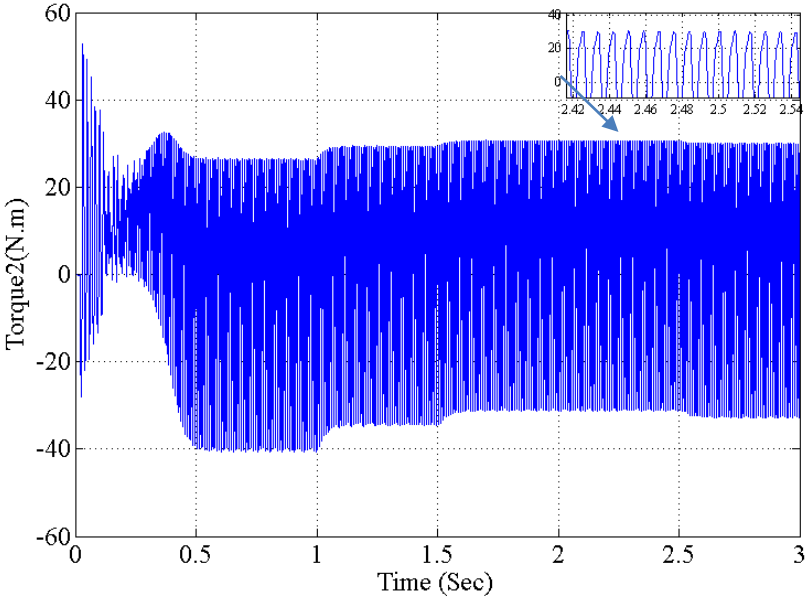


(b)

Figure (4-14) Dynamic response of IM1 and IM2 at no load for IM1 and step load IM2 with FLC(a)Speed 1, (b) Speed 2, (c) Torque1, (d) Torque 2,(e) i_{qs1} , (f) i_{qs2} , (g) i_{ds1} , (h) i_{ds2}

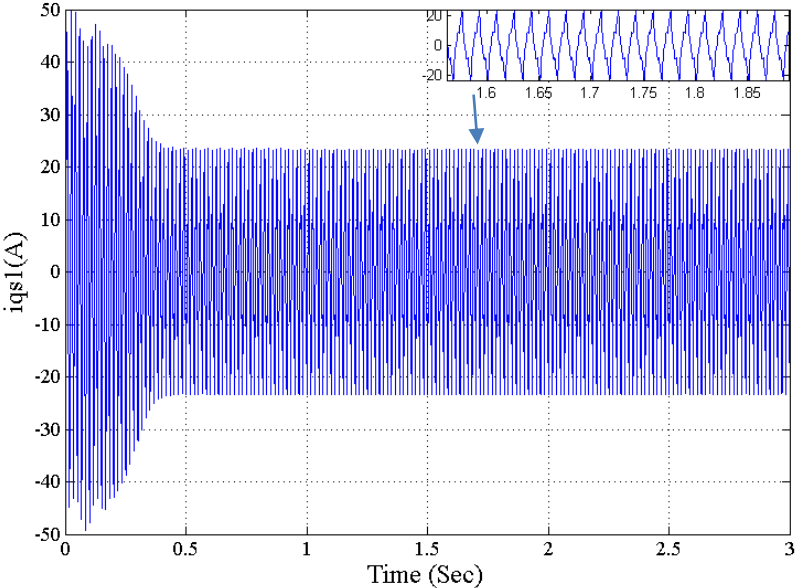


(c)

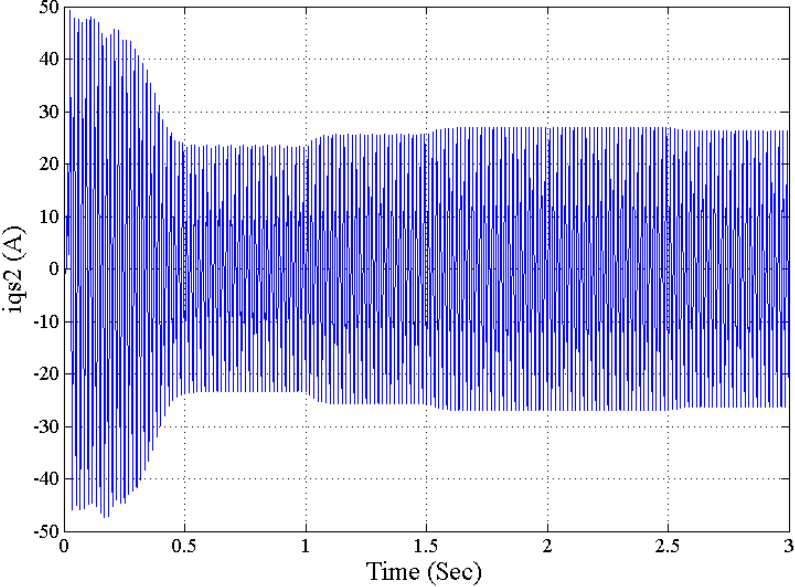


(d)

Figure (4-14) continued

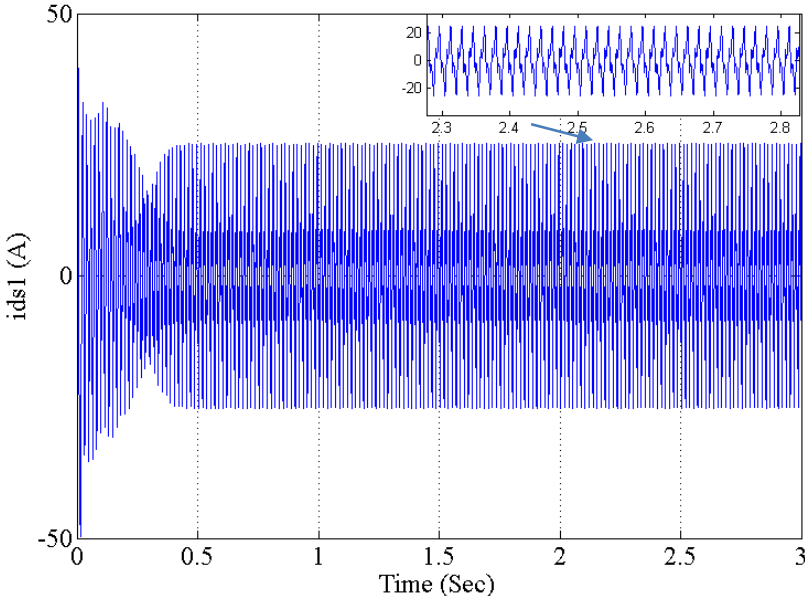


(e)



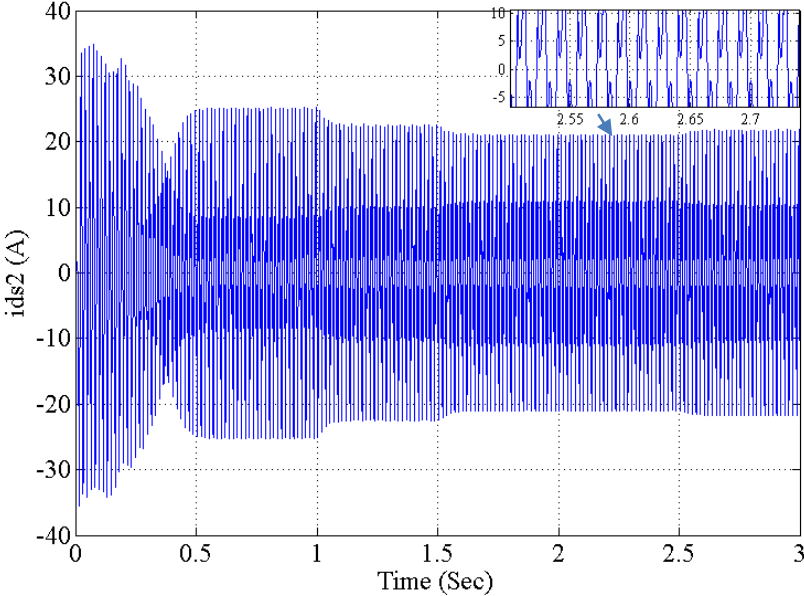
(f)

Figure (4-14) continued



(g)

Figure (4-14) continued



(h)

Figure (4-14) continued

4.7 Conclusion

In this chapter an indirect vector controlled induction motor drive system has been introduced by using two identical IMs are controlled independently using dual IFOC fuzzy logic controller, where the performance of FLC tested in two stage and compare the performance with PI conventional controller. Many tests were performed to evaluate the performance of the FLC based IFOC of the IM drive system. It is concluded that the proposed FLC has shown superior performances over the PI controller. Based on the study of indirect field oriented control of three phase induction motor a simulation model using Matlab/Simulink. The model smoothly works over the FLC. FLC to be more robust as compared with PI. FLC Simulation results showed that the fuzzy logic controller is more robust during load changes and eliminates the transients during sudden changes in speed . Overall simulation results showed that the fuzzy controller has higher performance than the PI controller and two motor are independent control.